2011

Attenuation of Acid Mine Drainage Enhanced by Organic Carbon and Limestone Addition: A Process Characterization

Anna M. Gillmor
University of Massachusetts Amherst

ATTENUATION OF ACID MINE DRAINAGE ENHANCED BY ORGANIC CARBON AND LIMESTONE ADDITION: A PROCESS CHARACTERIZATION

A Thesis Presented

by

ANNA MARGARET GILLMOR

Submitted to the Graduate School of the
University of Massachusetts Amherst in partial fulfillment
of the requirements for the degree of

MASTER OF SCIENCE

May 2011

Geosciences

ATTENUATION OF ACID MINE DRAINAGE ENHANCED BY ORGANIC CARBON AND LIMESTONE ADDITION: A PROCESS CHARACTERIZATION

A Thesis Presented
by
ANNA MARGARET GILLMOR

Approved as to style and content by:

_____
Richard F. Yuretich, Chair

_____
David F. Boutt, Member

_____
Steven T. Petsch, Member

_____
R. Mark Leckie, Department Head
Geosciences

ACKNOWLEDGEMENTS

I would like to express my appreciation to Dr. Richard Yuretich for his keen and insightful eye for interpretation, years of patient guidance, utmost reasonableness and good humor. This appreciation extends next to the committee; Drs. David Boutt and Steven Petsch for their know-how, practical experience, encouragement and excellent instruction. Thank you.

I would also like to express my appreciation to the members of the Davis Mine Research Group; professors Nüsslein, Ergas, Ahlfeld and Feldman and the Nüsslein (Microbiology) and Ergas (Environmental Engineering) Labs. Thanks also to the Reckhow Lab for DOC analyses.

Thanks to Erika Lopez-Luna for early help in the lab and the first opportunity to assist in the field. Thanks to Caryl-Ann Becerra for wisely pointing out that sulfate and iron stories can never really be told separately. Thanks to Ashmita Sengupta for helping me with my inner-sphere complex and for her steadfast friendship.

Thanks to Carrie Petrik and Karen Miller for courageous and unflappable field assistance as well as fruitful discussion upon returning.

Finally, thanks to the Geosciences Department as a whole, to graduate student friends and colleagues and to my family.

ABSTRACT

ATTENUATION OF ACID MINE DRAINAGE ENHANCED BY ORGANIC CARBON AND LIMESTONE ADDITION: A PROCESS CHARACTERIZATION

MAY 2011

ANNA MARGARET GILLMOR, B.S., VALPARAISO UNIVERSITY

MASTER OF SCIENCE, UNIVERSITY OF MASSACHUSETTS AMHERST

Directed by: Professor Richard Yuretich

Surface and groundwaters in contact with mining-exposed pyritic materials have the capacity to generate acid mine drainage (AMD), an acidic, sulfate-rich, metals-laden effluent. The Davis Mine located in northwestern Massachusetts offers a model site to study the processes of natural attenuation of acid mine drainage. These include physico-chemical processes such as dilution and sorption, geochemical processes such as aluminosilicate weathering and biological processes such as transformation and cycling of sulfate, iron and acidity by bacterial metabolism. A focus of recent research undertaken at the site has been characterizing the presence and activity of these bacteria with an aim to stimulate their capacity to attenuate the severity of acidic conditions. To further this investigation, a pilot-scale treatment system was installed, composed of a modified permeable reactive barrier containing organic carbon and limestone. Down-gradient groundwater was sampled over a sixteen-month period for concentrations of dissolved metals, major cations and sulfate, along with pH and redox measurements. The results showed a decrease in dissolved metals, a possible increase in calcium and

decrease in sulfate, and measurable increase in pH and corresponding decrease in oxidation-reduction potential. Major decreases in dissolved iron and aluminum were observed, a change which is not entirely consistent with metals removal by combination with biogenic sulfide alone. The additional influence of hydrolysis was proposed and the anticipated action of this alternate process found to bear resemblance to the observed changes. Groundwater composition from the experimental period was compared to previous measurements and significant changes described in pH, Fe^{tot}, Al^{3+}, Cu^{2+} and Zn^{2+} and to a lesser extent in Ca^{2+} and SO_4^{2-}. Comparisons were also made with concurrent surface water compositions and findings of analogous studies. Conclusions that can be drawn include: the pH and redox environment into which a treatment system is placed can greatly influence the reactions which take place, side-reactions which occur in reducing and alkalinity-generating amendments may also have an attenuating effect, and variable processes influence groundwater composition in these biogeochemically complex environments.

CONTENTS

Page

LIST OF TABLES

LIST OF FIGURES

Figure **Page**

CHAPTER 1

INTRODUCTION AND PREVIOUS WORK

Acid Mine Drainage (AMD) is a common and pervasive environmental concern, one that can occur anytime pyrite (FeS_2) or other sulfide minerals are excavated, exposing them to surficial oxygen, water and bacteria. It is characterized by acidic (pH<5), sulfate (SO_4^{2-}) rich water with high concentrations of dissolved metals. The presence of these metals and metalloids can significantly impair biological functions in the receiving streams, with even small amounts (100-200μg/L) of dissolved inorganic Al^{3+} capable of fish kills (Baker *et al*., 1996). The process can also occur where sulfide minerals are exposed by subsidence or other non-mining activities (Acid Rock Drainage, ARD). In the Eastern US, the largest impact spatially comes from the mining of coal, in which the associated sulfide minerals are present at low weight percents (<5%), but the extent of mining distributes the effect over large regions. The severity of the impact is exacerbated by mining practices such as mountain-top removal, which backfills tailings and crushed rock into local valleys, encouraging the passage of oxygenated waters through the tailings or waste rock.

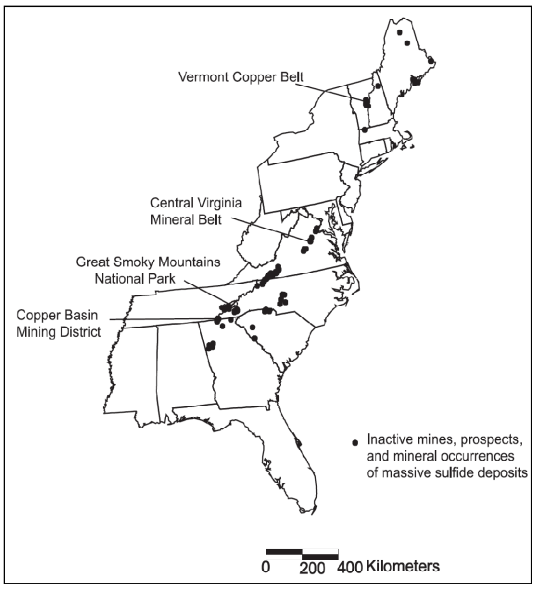

Figure 1: Inactive Sulfide Mines of the Eastern US (Hammarstrom *et al.*, 2005)

Less extensive spatially but often more severe locally is the mining of massive sulfide and base metal deposits, in which the concentrated metal sulfide minerals themselves are of economic interest. Base metal and massive sulfide deposits may not share a syngenetic relationship with carbonate minerals as coal may, instead they may be hosted in formations whose mineralogy offers little buffering capacity. The most severe acid mine drainage generated has come from these

types of deposits, such as extremely low pH (<0.5) measured at the Richmond Mine at Iron Mountain in California (Robbins *et al*., 2000), or the widespread pH 2 conditions measured in the Iberian Pyrite Belt (Bond *et al.*, 2000, Sánchez España *et al*., 2005). Within the Eastern US, a series of inactive sulfide mines runs roughly along the Appalachian Mountains, as shown in Figure 1 (from Hammarstrom *et al.*, 2005). The locality of this study is the Davis Pyrite Mine located in northwestern Massachusetts.

1.1 Acid Mine Drainage Generation Chemistry

Acid drainage forms when the sulfide minerals (Pyrite FeS_2, Pyrrhotite Fe_7S_8 , Chalcopyrite $FeCuS_2$, etc.) are oxidized to form sulfuric acid (H_2SO_4).

Once pyrite is exposed to O_2, water, and bacteria by mining activities, the generation of acidic effluent begins. The processes by which the pyrite sulfide is converted to aqueous sulfate are variable, but the principal process is a four step sequence.

In the initiation step, FeS_2 is oxidized abiotically by O_2 and H_2O (EQ 1).

$$FeS_2 + 7/2\ O_2 + H_2O \rightarrow Fe^{2+} + 2\ SO_4^{2-} + 2\ H^+ \qquad \text{(EQ 1)}$$

As the system becomes more acidic and oxidizing, the ferrous iron (Fe^{2+}) generated in this first step may be then oxidized to ferric (Fe^{3+}) iron (EQ 2).

$$Fe^{2+} + ¼\ O_2 + H^+ \leftrightarrows Fe^{3+} + ½\ H_2O \qquad \text{(EQ 2)}$$

At this juncture, the Fe^{3+} generated may then proceed down either of two paths; it may precipitate from the effluent as an iron hydroxide (EQ 3) or iron hydroxysulfate, or it may oxidize pyrite (EQ 4). Both the Fe^{3+} hydrolysis path and the FeS_2 oxidation by Fe^{3+} path are acidity producing. It has been shown that once Fe^{3+} is generated, it becomes the preferred oxidant of pyrite, and the concentrations of O_2 available to oxidize dissolved Fe^{2+} increases.

As acidity generation proceeds, the rate of abiotic Fe^{2+} oxidation (EQ 2) slows as pH declines past 5. At this pH range, Fe^{2+} oxidation is taken over by acidophilic bacteria such as *Acidothiobacillus ferrooxidans* and at further lower pH, *Leptospirulum spp.*. These iron and sulfur oxidizing bacteria are autotrophic and live in oxic environments, deriving their energy from

oxidizing dissolved or solid phase Fe^{2+} (with O_2) and fixing dissolved CO_2 for biomass. Although not represented in EQ 4 below, biotic iron oxidation requires CO_2 and O_2 and is therefore most active in moist, surficial environments. These bacteria have been shown to mediate a $Fe^{2+} \rightarrow Fe^{3+}$ oxidation (EQ 2) which is ~10^6 times faster than the abiotic mechanism (Singer and Stumm, 1970).

$$Fe^{3+} + 2H_2O \leftrightarrows FeOOH + 3H^+ \quad \text{(EQ 3)}$$

$$FeS_2 + 14\ Fe^{3+} + 8H_2O \leftrightarrows 15\ Fe^{2+} + 2SO_4^{2-} + 16H^+ \quad \text{(EQ 4)}$$

This last equation (EQ 4) in which pyrite is oxidized by Fe^{3+} can be thought of as a comprehensive reaction of sulfide oxidation under biotic conditions. Notice that for each mole of pyrite oxidized 16 moles of proton acidity and one excess ferrous ion (available to sustain the reaction) are generated.

Although acid drainage is formed within tunnels during active mining, it is limited by continuous water removal. Once abandoned, the severity of acidity generated within the flooded mine workings is influenced both by the sulfide geochemistry and by the hydrogeology; the volume and recharge of oxygenated water. After discharging to oxic surface water systems, the dissolved Fe^{2+} may oxidize and undergoes hydrolysis (EQ 3 above), further decreasing pH at distance from the mine shaft.

Acidity is also generated from traces of unrecoverable sulfide minerals within the large volumes of rock milled during the beneficiation process and deposited in nearby tailings impoundments. Acidity generation begins in these tailings shortly after they are deposited, moving in an oxidation front from the air contact downward. Once the saturated zone is reached, oxidation can be slowed by low aqueous solubility of the gases; of O_2 needed to oxidize pyrite abiotically and of O_2 and CO_2 needed to biotically oxidize pyrite.

1.2 Acid Mine Drainage Attenuation Chemistry

1.2.1 Geochemical Neutralization

Geochemical neutralization is one of a few processes that attenuate the severity of acid mine drainage. The progression of pore-water or groundwater geochemical neutralization reactions within tailings-piles has been described extensively by Blowes *et al.* (2003 and 2005). In their conceptual model, the groundwater pH is controlled by a sequence of dissolution reactions with different mineral classes; first the carbonates, then the hydroxides and lastly the aluminosilicates.

Table 1: Mineral Buffering Ranges for Soil H_2O (Blowes *et al.*, 2005)

Mineral	pH Range
$CaCO_3$	6.5-7.5
$FeCO_3$	4.8-6.3
$Al(OH)_3$	4.0-4.3
$Fe(OH)_3$	2.5<3.5
aluminosilicates	<3.0

The pH of metals-laden groundwater may be near neutral in cases where the gangue material contains sufficient carbonate minerals. Carbonate minerals include calcite ($CaCO_3$), dolomite ($CaMg(CO_3)_2$), and primary or secondary siderite ($FeCO_3$). Reactions with carbonates are considered kinetically fast relative to groundwater velocity and near equilibrium conditions can be achieved. At mildly acid pH (~5-7), carbonate dissolution occurs via:

$$Ca(CO_3)_2 + 2H^+ \rightarrow Ca^{2+} + 2HCO_3^- \quad \text{(EQ 5)}$$

And at moderately acid pH (<5):

$$Ca(CO_3)_2 + 2H^+ \rightarrow Ca^{2+} + H_2CO_3 \quad \text{(EQ 6)}$$

Once carbonate minerals are consumed, buffering reactions with Al^{3+} and Fe^{3+} hydroxides control the pH of ground and pore-waters in the acidic range of 2.5 to 5.0. As acidification and weathering proceeds, the dissolved concentrations of Fe^{3+} and Al^{3+} increase. As acid waters containing Fe^{3+} and Al^{3+} encounter more neutral waters, hydrolysis occurs, leading to deposition of solid phase Al^{3+} and Fe^{3+} hydroxides. These deposits are then available for mineral buffering. The common iron hydroxides are Ferrihydrite (nominally $Fe_5HO{\bullet}4H_2O$, sometimes represented as $Fe(OH)_3$) and goethite (α-FeOOH), with amorphous varieties

frequently found. Similarly, the common aluminum oxides include crystalline gibbsite ($Al(OH)_3$) and amorphous $Al(OH)_3$. The precipitation and dissolution of these hydroxides is pH sensitive (as in EQ 3 and EQ 7); their dissolution consumes acidity and their precipitation releases it. Because of this interplay, iron and aluminum chemistry is recognized as the mechanism responsible for buffering acidic soils (Sparks 1995, Chapter 9). The precipitation and dissolution of these minerals is again kinetically fast and expected to be in near equilibrium with the groundwater.

$$Al^{3+} + 3H_2O \leftrightarrows Al(OH)_3 + 3H^+ \qquad \text{(EQ 7)}$$

Lastly, the acid pH of waters will be attenuated by the dissolution of aluminosilicate minerals in the lowest pH range (<3.0) where carbonate and hydroxide minerals are absent. Though they are less reactive than the other mineral classes mentioned, aluminosilicates are more common, comprising the majority of rock forming minerals. Their dissolution is a major influence on groundwater chemistry at the Davis Mine site. The low pH (2-3) effluent with large concentrations of dissolved Si, Al^{3+} and other major cations was previously recognized as resulting from this mechanism (Gál 2000, Bloom 2005). This idea was further supported when clay minerals including illite and chlorite were found in the tailings-pile area, presumably formed via aluminosilicate weathering (Cerato 2004). An example of aluminosilicate weathering showing albite weathering to kaolinite is given (EQ 8).

$$2NaAlSi_3O_8 + 2H_2SO_4 + 9H_2O \rightarrow Al_2Si_2O_5(OH)_4 + 2Na^+ + 2HSO_4^- + 4\,H_4SiO_4 \qquad \text{(EQ 8)}$$

Unlike the previous reactions, aluminosilicate dissolution may be kinetically slow with respect to groundwater velocity, and is less likely to approach equilibrium. Even aluminosilicates with high neutralization potential will not necessarily have a chance to react before ground water moves on.

If allowed to react under no-flow conditions, the acid neutralization capacity of aluminosilicate minerals is fairly low relative to that of carbonate minerals. Common minerals described in Davis Mine's Hawley Formation Amphibolite (by *Helm 1982) are shown below in

Table 2. Also shown are representative neutralization potentials for these minerals, determined in a static conditions weathering study (by **Jambor *et al.*, 2002) standardized to surface area of 1 m^2/g. These minerals have neutralization potentials which are 2-3 orders of magnitude lower than that of calcium carbonate.

Table 2: Neutralization Potentials of Selected Host Rock Minerals

Hawley Formation Amphibolite*	**Neutralization Potential**** kg $CaCO_3$ eq / 1000 kg rock S.A. = 1 m^2/g)
Hornblende (Actinolite) $Na(Ca,Fe)_5(SiAl)_8O_{22}(OH)_2$	3.3 – 8.2
Plagioclase (Ab*) $NaAlSi_3O_8$	--
(An) $CaAl_2Si_2O_8$	9.5 – 68.5
Chlorite $(Mg,Al)_3[Si_4OH_{10}(OH)_2(Mg,Fe)_3(OH)_6]$	0.5 – 8.5
Garnet $Mg_3Al_2[Si_3O_{12}]$	5.5 – 98.1

The bulk of the Davis Mine's host rock amphibolite is made up of albite, actinolite hornblende, and chlorite; these minerals represent aluminosilicate weathering at the site and they are likely to be the source of the major cations in solution.

1.2.2 Bacterial Fe^{3+} and SO_4^{2-} Reduction

Bacterial iron and sulfate-reduction are other processes which contribute to the attenuation of acidity. Whereas activity by iron and sulfur oxidizing bacteria contributes to the generation of acidity, activity by iron- and sulfate-reducing bacteria contributes to the attenuation of acidity. These heterotrophic reducing bacteria live in suboxic environments, using oxidized iron or sulfur species and reduced carbon for their metabolism. The iron reducing bacteria attenuate acidity by reducing the Fe^{3+} (in either dissolved or solid phase) otherwise available for pyrite oxidation and oxidizing organic carbon to bicarbonate. The reaction with solid-phase Fe^{3+} is shown in EQ 9. The sulfate reducing bacteria attenuate acidity by reducing sulfate to sulfide and by oxidizing organic carbon to bicarbonate (EQ 10).

$$4FeOOH + CH_2O + H_2O \rightarrow HCO_3^- + 4Fe^{2+} + 7OH^- \quad \text{(EQ 9)}$$

$$SO_4^{2-} + 2CH_2O \rightarrow 2HCO_3^- + H_2S \quad \text{(EQ 10)}$$

The sulfate-reducing bacteria are a phylogenetically and metabolically diverse group of organisms most often found living in consortia with other microbes such as fermenters, from which they derive labile carbon; in this case low molecular weight organic acids. Though traditionally thought of as active in reducing, circumneutral environments, in recent years some evidence of bacterial sulfate reduction has been found in oxidizing, acidic environments (Fortin *et al.*, 2002, Praharaj and Fortin, 2004).

Tuttle *et al*. (1969) first observed increased pH and decreased SO_4^{2-} concentrations in a pond of coal-related acidic effluent which had previously flowed through a wood dust dam, then sampled sediment from the dam drain and pond, and found the bacteria present capable of reducing sulfate in laboratory conditions such as culture in Postgate's B medium. More recently, Praharaj and Fortin (2004) sampled the acidic and oxidizing upper 15 cm (pH ~3, E_H 600 mV) of Cu-Zn sulfide tailings from the Kamkotia mine-site (Ontario), where the tailings seem to have been deposited over organic rich, moist forest soil. Cells recovered from the sediment were capable of reducing sulfate in laboratory conditions. However, evidence of sulfate reducing activity was stronger at other mine sampling sites when sediment samples were taken from a depth where pH had risen and E_H declined.

Bioremediation can also be performed by Fe^{3+} reducing bacteria, another phylogenetically diverse group of heterotrophic microorganisms, which can limit the amount of ferric iron available to oxidize pyrite. The Fe^{3+} reducers are capable of reducing both dissolved and solid phase Fe^{3+}. The Gibbs free energy yield ($\Delta G°$) for iron reduction is greater than that of sulfate reduction, at -0.79 G per kJ/mol glucose vs. -0.45 G per kJ/mol glucose (Stumm and Morgan 1996), leading to some discussion regarding whether iron reducers might out-compete sulfate reducers. In instances where bacteria are capable of either mechanism, Fe^{3+} reduction can inhibit SO_4^{2-} reduction (Weber *et al*., 2006).

By either reducing mechanism, each equivalent of organic carbon consumed is transformed to a molecule of bicarbonate (HCO_3^-), increasing the alkalinity of the solution.

When bacterial sulfate reduction proceeds, the now reduced sulfur species (HS^-, H_2S) will then react with other dissolved components or exsolve. The produced H_2S, together with high concentrations of divalent metals present at AMD sites (i.e. Fe^{2+}, Cu^{2+}), may precipitate secondary sulfide minerals. Sulfidogenesis thereby decreases the dissolved concentration of metal and sulfur species, lessening their aqueous toxicity. An example with Cu^{2+} is shown below (EQ 11).

$$Cu^{2+} + H_2S \rightarrow CuS + 2H^+ \qquad \text{(EQ 11)}$$

1.3 Davis Mine: Previous Remediation Experiments

Davis Mine, located near the town of Rowe in Western Massachusetts, was once the largest pyrite (FeS_2) mine in the state. Operating from 1882 until 1911, the mine then collapsed due to poor mining techniques (McCarthy, 1977). Subsequently abandoned, the collapsed shaft has since flooded, and now discharges ~ $0.002 m^3/s$ of affected water (Adams *et al.*, 2007a).

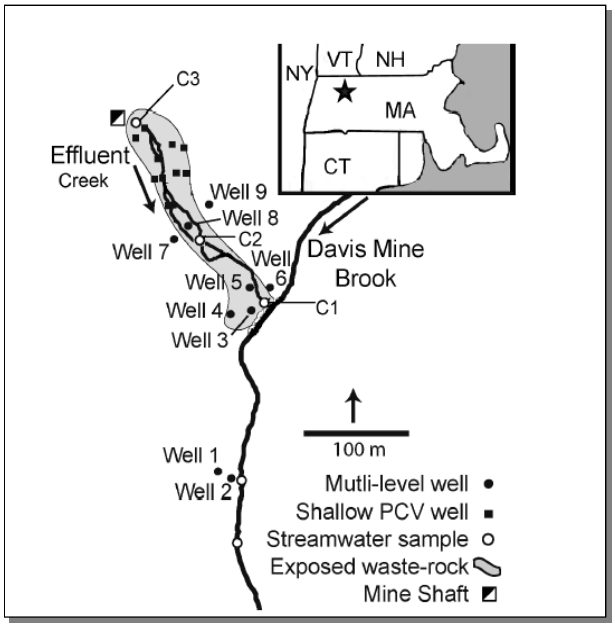

Figure 2: Davis Mine Locus Map and Monitoring Well Locations

In the intervening 100 years, the 3000 m^2 (0.3 ha) area of tailings has been reclaimed partially by acid-tolerant plants and forest, with the effluent stream lined by species typical of bogs (sphagnum moss, blueberry, sundew), and the valley walls forested with conifers (pine and hemlock). Some sections of tailings are barren and covered by an ochreous crust. A conclusion drawn from the last 25 years of study is that the site has become an example of natural attenuation, in dynamic equilibrium between acid generating and attenuating processes (Gál, 2000, Bloom, 2005).

Part of a hydrothermal massive sulfide deposit, the Davis Mine deposit was formed during Ordovician time and subsequently metamorphosed in Taconic and Acadian orogenic events. The sulfide ore itself is ~60 volume % pyrite (FeS_2), with some chalcopyrite ($FeCuS_2$) and sphalerite (ZnS). The ore-body is hosted in the lower part of the Hawley Formation, a unit formed of schist, gneiss, and amphibolite and containing quartz, hornblende (actinolite), plagioclase feldspar (albite) and chlorite (Field, 1985, Hatch and Hartshorn, 1968).

In general, the prevalence of low pH (2-3) water, the absence of carbonate minerals in the host rock, and the duration of acid drainage production (~100 yrs) are consistent with geochemical neutralization by mainly aluminosilicate mineral dissolution (Gál, 2000 Bloom, 2005). Further evidence of neutralization via aluminosilicate weathering is the presence of secondary clay minerals produced through incongruent weathering and the relatively high concentrations of aluminum, silicon and major cations in the effluent water.

As the subject of a 5 year multidisciplinary study (2003-2008), the Davis Mine has been used to characterize the contributions of dilution, co-precipitation / sorption, geochemical neutralization, and bacterial remediation to the improved quality of the effluent, with later focus given to means of stimulating the bacterial processes of attenuation.

A principal focus of current research at Davis Mine is documenting natural methods of attenuation by the *in situ* microbial population and stimulating the activity of sulfate- and iron-reducing bacteria.

Members of the Davis Mine research team have performed characterization and stimulation of the indigenous bacterial community at Davis Mine and at Mam Tor, an analogous ARD site in Derbyshire (UK). Selected findings from these studies are summarized in Table 3. At Davis Mine, bacterial communities were hypothesized to be most active at the periphery of the acidic effluent's reach, and so the focus area likely to host these bacteria was designated the acidity "Attenuation Zone" (AZ). Well numbers shown in Table 3 correspond to the those shown

in Figure 2; where the Well 1 and 2 area was often sampled as to represent the AZ and the Well 3 area likewise sampled to represent the acidity "Generation Zone" (GZ).

Table 3: Previous Bioremediation Experiments at Davis Mine and Mam Tor

Author	Type	Materials	Amendment	Selected Findings
Monserrate (2004)	column	sediment and water DM AZ (Well 2)	(none)	Effluent S^{2-} > Influent S^{2-} Effluent pH > Influent pH black precipitate
Harrison (2005) and Adams *et al.* (2007b)	microcosm	sediment and water Mam Tor, surficial	Postgate's B medium	pH 5.5→7, ORP -100→-400mV Fe^{tot} =Fe^{2+}, SO_4^{2-} 20→15mM
	microcosm	sediment and water Mam Tor, surficial	municipal waste digestate	pH 5.5→6.5, ORP-100→-300mV increasing Fe^{tot}, SO_4^{2-} increase
Becerra *et al.* (2009)	microcosm	sediment and water DM AZ (Well 14)	(none)	pH 3→6, ORP 150→-50 mV Fe^{2+} 50→175 mg/L, SO_4^{2-} steady
	microcosm	sediment and water DM AZ (Well 14)	glycerol+ N+ P	pH 3.5→6, ORP 200→ -100 mV Fe^{2+} 50→200mg/L, SO_4^{2-} varied
López-Luna (2008)	microcosm	sediment and water DM AZ (Well ~1)	glycerol+ N+ P	pH 2.7→5.0, E_H540→200mV increasing Fe^{tot}, black precipitate
	in situ microcosm	(sediment and water) DM AZ (Well ~1)	glycerol+ N+ P	pH 3-4; E_H 400-600mV; no trends increasing Fe^{tot}, SO_4^{2-} decreasing

Bacterial sulfate reduction was suggested when a column filled with field-collected sediment from Davis Mine's attenuation zone (AZ) consistently produced effluent with higher pH and sulfide (S^{2-}) concentrations than the field-collected AMD influent (Monserrate, 2004). In this study, bacterial sulfate reduction appeared likely under natural conditions, without any organic carbon amendment. A similar column was constructed with sediments and waters collected from the acidity generation zone, and found no (S^{2-}) generation but rather suspected sulfide oxidation.

Methods of augmenting bacterial iron and sulfate reduction through the addition of carbon sources and nutrients have also been explored successfully in the laboratory. Working at Mam Tor, a ~3000 yr old ARD site where biogeochemical iron cycling processes are well established, Harrison (2005) gathered sediments from the acidic and oxidizing ochreous surface formations. By cultivating these sediments in Postgate's B medium, she selected for sulfate reducing bacteria, finding cells even from a surficial oxidizing environment that were capable of affecting changes in microcosm consistent with iron and sulfate reducing metabolisms;

specifically raising pH, decreasing ORP, decreasing SO_4^{2-} concentration, and finding all dissolved Fe^{tot} present as Fe^{2+}. After adding a complex carbon source (municipal waste digestate), similar transformation to a less acidic, more reducing environment were observed in microcosm, suggesting some components of this organic carbon amendment were bio-available for reducing bacteria. Slight increases in sulfate concentration were also observed, possibly released from metastable secondary minerals (i.e. jarosite $KFe_3OH_6(SO_4)_2$) as pH increased.

Returning to sediments taken from Davis Mine's Attenuation Zone, Becerra *et al.* (2009) measured changes in an unamended microcosm that where suggestive of reducing activity, namely; increasing pH, decreasing ORP, and increasing dissolved Fe^{2+}. After amending similar microcosms with a simple carbon source (glycerol $C_3H_5(OH)_3$), nitrogen and phosphorous, similar improvements in water quality were observed, suggesting simple carbon sources were bio-available to these bacteria. Culture independent genomic sequencing of sediment taken from the AZ for this study confirmed a small presence of δ-proteobacteria, the phylogenetic group to which sulfate reducers belong.

In paired lab and field experiments, López-Luna (2008) began extrapolating the results of laboratory studies to the field. Laboratory microcosms prepared with AZ field gathered sediment and water (from near Well 1) and amended with glycerol, nitrogen, and phosphorous showed increases in pH, decreases in oxidation-reduction potential (ORP) and increasing dissolved Fe^{2+}, again suggestive of reducing activity. In the next step, the same nutrient amendments were added to an in-situ microcosm was installed underground in AZ. Here the trends were less clear-cut; pH did not rise and ORP did not fall on comparable scales. Rain events and influxes of different composition water complicated interpretation of changes in pH, ORP, and Fe^{tot} because these parameters varied in response in part due to "new" water and not the remediation amendments. Natural systems will of course have seasonal geochemical fluctuations and influx of different waters; however this hydrogeochemical complexity presents a challenge to providing controls and contexts for field studies.

Although the SO_4^{2-} and Fe^{3+} reducing bacteria found at Davis Mine respond to nutrient stimulation in laboratory settings, it is challenging to describe the degree to which they are metabolically active in the field. This previous work lays a foundation for attempting to stimulate bioremediation in the diversity of conditions found in the natural setting.

1.4 Treatment of Acid Mine Drainage: Remediation Options

A number of technologies for the remediation of acid mine drainage exist, including those using chemical treatment systems, biological treatment systems, or some combination of the two (Doshi, US EPA 2006). These include active treatment options such as bioreactors which require relatively more upkeep and continual operating costs than passive treatment options such as constructed wetlands, anoxic limestone drains, or permeable reactive barriers. These passive treatment options are intended as low operating cost, low maintenance alternatives and are preferable for use at remote sites. A flow diagram of AMD treatment strategies is reproduced from Johnson and Hallberg (2005) below, with notes added describing each method's treatment strategy, specifically the addition of alkalinity, the redox state of iron, and how metals are sequestered.

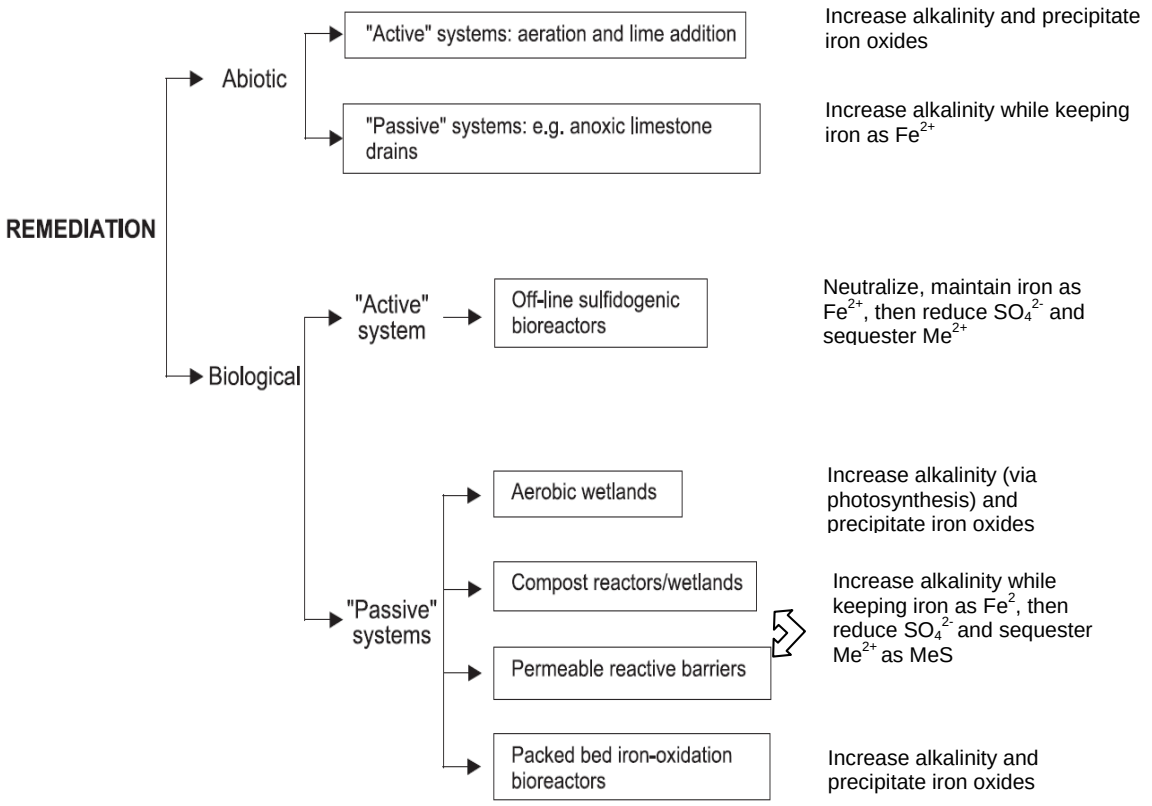

Figure 3: Overview of AMD treatment options (after Johnson and Hallberg 2005).

The several treatment systems may differ in engineering design, but they make use of only a few treatment chemistries. In all systems alkalinity is increased, either by limestone ($CaCO_3$) dissolution, bacterial transformation of organic carbon to bicarbonate, or photosynthetic release of OH^-. Dissolved iron is removed from the water through one of two strategies; either by maintaining oxidizing conditions and removing dissolved iron as an Fe^{3+} oxide, or by maintaining reducing conditions and removing dissolved iron as an Fe^{2+} sulfide. Fe^{2+} sulfides are preferred based on their stability as a sink, provided they are kept from re-oxidation. In some cases the treatment systems may be combined or staged to sequentially treat AMD; for example, acidic drainage may be partially neutralized before entering a sulfidogenic bioreactor to avoid stressing or inactivating the sulfate-reducing bacterial community. Likewise, reducing conditions should be created for water entering an anoxic limestone drain, so that dissolved iron enters as Fe^{2+}. In cases where water carrying Fe^{3+} is introduced to limestone gravel, precipitation of Fe^{3+} oxides

directly onto the limestone surface can lead to coating or "passivating" the mineral grains (Benner *et al.*, 1999, Caraballo *et al.*, 2009), impeding dissolution.

Permeable reactive barriers (PRBs) are trenches of reactive material installed below ground in the path of migrating contaminated groundwater. In the case of AMD-impacted groundwater, the intended treatment mechanism is alkalinity addition via bacterial sulfate reduction and metals sequestration via combination with bacterially produced sulfide (Benner *et al.*, 1997, Benner *et al.*, 1999, Blowes *et al.*, 2005). The reactive material will contain a bio-available organic carbon substrate and alkalinity source, with coarser materials sometimes added to increase porosity. Alkalinity sources may include calcite ($CaCO_3$), dolomite ($CaMg(CO_3)_2$), quicklime (CaO), crushed concrete, pulp waste, oyster shells or any other soluble acidity-consuming compounds (Catalan *et al.*, 2003). A wide variety of organic carbon substrates may be used; generally those containing mixes of composted or digested natural material perform well (Waybrant *et al.*, 1998, Gibert *et al.*, 2003.) Because the sulfate-reducing bacteria are dependent on other heterotrophic bacteria to break-down more complex substrates, it may be that mixed sources support these bacterial consortia or release simpler carbon leachate as a result of previous decomposition. As the effluent passes through the barrier, it is treated via carbonate neutralization, sulfate reduction, and metal sulfide precipitation.

An adaptation of a permeable reactive barrier was used for this thesis experiment, since this passive treatment option was manageable on a small scale and likely to be non-disruptive to the natural mechanisms of attenuation occurring at the site.

1.5 Davis Mine: Well 8 Waste-rock pile site specifics

Extensive data was collected from 2003 through 2005 during the characterization of Davis Mine's aqueous geochemistry performed by Bloom (2005), whose thesis work centered on data collected from May 2003 to May 2004. A monitoring well (Well 8) was installed within a waste-rock pile of weathered pyritic material (boring log reproduced in Appendix A). The average yearly pH, ORP, and Fe^{tot} concentrations measured from 2003-04 by depth are

summarized in Figure 4. The shallowest groundwater was collected from an additional PVC drive-point well (port 2, 1.5m depth) located in the vadose zone, which intermittently held adequate water for collection, as shown by the minimum and maximum water table elevations measured that year. Remaining groundwater was collected from ports 3, 5 and 7 of Well 8, which respectively correspond to the shallow groundwater (2.1 m depth), the groundwater-bedrock interface (3.7 m depth), and the bedrock groundwater (4.6 m depth).

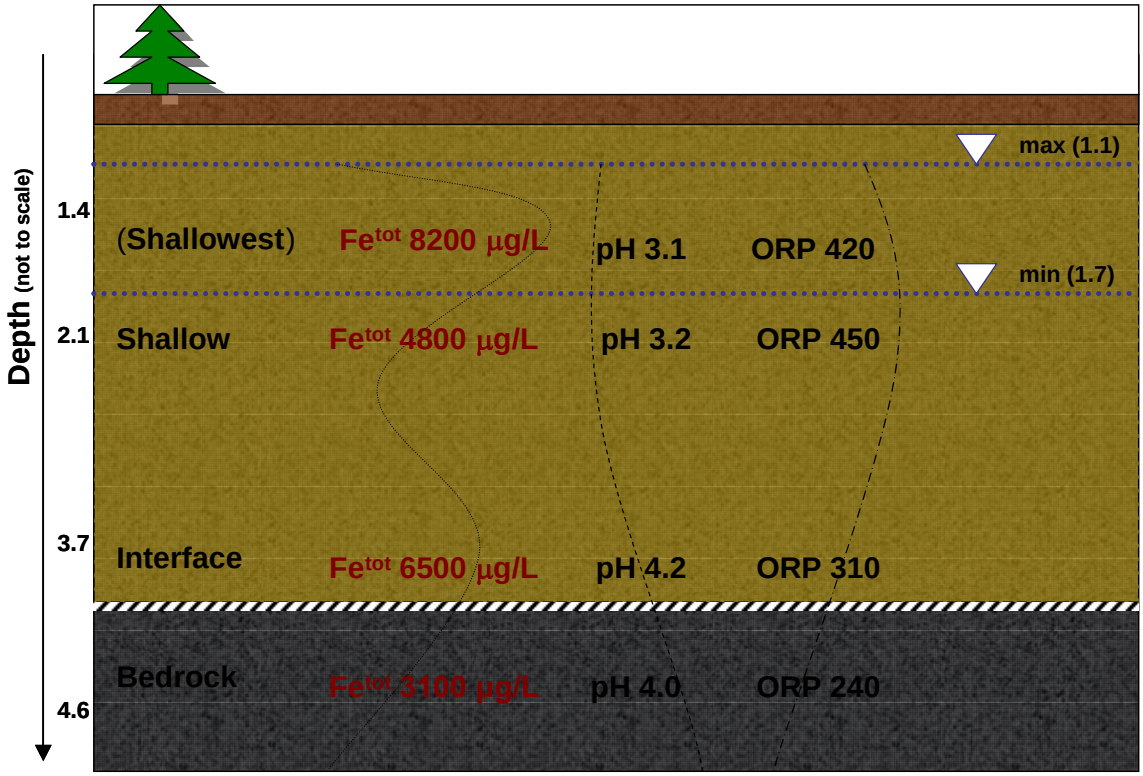

Figure 4: Well 8 Waste Rock-pile Schematic showing Fe^{tot}, pH and ORP by Depth (Bloom 2005)

Data collected during that time period showed a transition from more to less acidic and oxidizing with depth, as pH increased from ~3 to ~4 and ORP decreased from ~420 to 240 mV. Fe^{tot} concentrations fluctuated, with the largest amount of Fe^{tot} measured in the most acidic shallowest water, decreasing substantially in the next most shallow water, then rebounding in the water from the groundwater bedrock interface, and fairly low in the bedrock. Previous measurements (2003-04) of oxidation-reduction potentials (ORP) were strongly positive

(oxidizing) down to the groundwater-bedrock interface depth, with the lowest values observed within the isolated bedrock water.

Partial iron speciation data collected in 2003-04 found Fe^{tot} transitioning from mainly Fe^{3+} in the shallow groundwater to mainly Fe^{2+} with depth, shown here as Figure 5 (Bloom 2005).

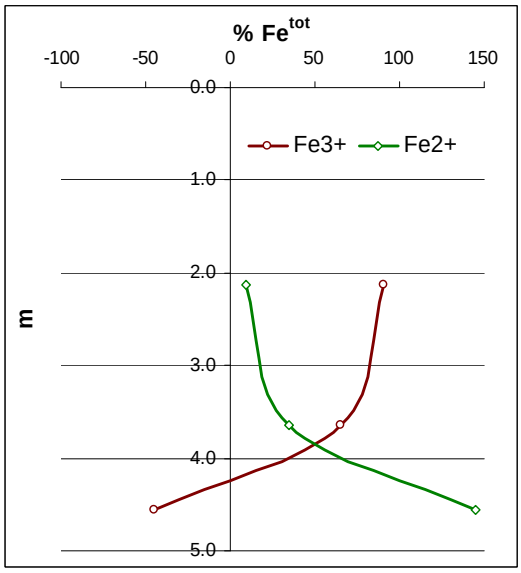

Figure 5: Well 8 Fe^{2+} and Fe^{3+} vs. Depth (Bloom 2005)

From the combined pH, redox and iron speciation data, it is reasonable to propose that Fe^{2+} oxidation appears to be active and ongoing within the shallow tailings, given the high Fe^{3+} concentrations measured in the shallow groundwater. Fe^{2+} oxidation can proceed either biotically (pH<4) or abiotically (pH>4) and is most active in surficial environments. The variability in measured Fe^{tot} concentrations within the waste rock and tailings-pile may be in part due to changing pH and redox conditions.

Previous studies have also found the hydraulic conductivity (K) in the vicinity to be fairly high, on the order of sand or sand-silt aquifers, with bail tests giving K estimates of 10^{-4} to 10^{-6} m/s (Gál, 2000) and grain-size measurements giving K estimates of 10^{-4} to 10^{-5} m/s (Cerato, 2003).

The small valley immediately south / southeast of the collapsed mine-shaft was partially filled partially during mining activities with crushed waste rock; this valley contains the effluent creek and waste rock and tailings-pile studied. The depth of spoil overlying the bedrock varies, in the vicinity of this tailings-pile the spoil depth increases down valley from 2 to 4m as described during seismic studies undertaken by Gál (2000).

1.6 Objectives

This pilot-scale field study of organic carbon and limestone addition continues the work of bridging flask and field studies at Davis Mine by further characterizing the possibility of stimulating bacterial sulfate reduction. While previous work by the Davis Mine research teams has shown the indigenous bacteria are responsive to stimulation in mainly laboratory studies, this experiment will be a remediation study undertaken in the field. This pilot scale project is intended to provide "proof of concept" for studies using organic carbon and limestone amendments at AMD sites. This study will also contribute to understanding of the multiple biogeochemical mechanisms operating within these treatment systems.

The purpose of this thesis will be to characterize the changes in aqueous geochemistry following the introduction of geochemically and microbially reactive media in the path of moving groundwater. This material will include a mixed-source, partially digested organic carbon substrate and adequate limestone to increase the system pH towards one favorable for bacterial sulfate reduction.

1.6.1 Hypotheses and Comparisons

Following the installation of a modified organic carbon and limestone permeable reactive barrier, the acidic, metals-laden groundwater will show evidence of remediation. This will be indicated by;

Hypothesis 1.) pH increasing

Hypothesis 2.) ORP decreasing

Hypothesis 3.) SO_4^{2-} decreasing

Hypothesis 4.) Ca^{2+} increasing

Hypothesis 5.) Fe^{tot}, Cu^{2+}, and Zn^{2+} decreasing

Potential change in these parameters will be evaluated relative to;

Comparison 1.) Previous measurements of the same parameters taken during 2003-2005

Comparison 2.) Simultaneous measurements of the same parameters from adjacent untreated surface water

Comparison 3.) Analogous acid mine treatment studies

CHAPTER 2

METHODS

2.1 Installation

An adaptation of a permeable reactive barrier was installed at Davis Mine within the waste-rock and tailings-pile. The specific site chosen is 2m in a presumed up-gradient direction from Well 8 (Figure 6). The site of the waste rock and tailings-pile was chosen for its relatively level ground surface, where groundwater had the best chance of prolonged contact with the reactive fill. This area has the smallest slope along any reach of the effluent stream before it joins Davis Mine Brook. Because groundwater from this area is moderately acidic, ranging from pH 3 to 5, it was necessary to use a relatively high proportion of limestone within the reactive mix in order to approach values amenable to bacterial sulfate reduction. Well 8 is drilled through 3.9m of weathered tailings to the bedrock contact and 0.6 m into bedrock. It is located approximately in the middle of the effluent stream's reach, in the acidic drainage generating zone. It is bounded by two branches of the shallow, ochreous deposit-lined effluent stream; each branch at 5-6 m distance from Well 8. Photos of the sampling locations are provided in Appendix B .

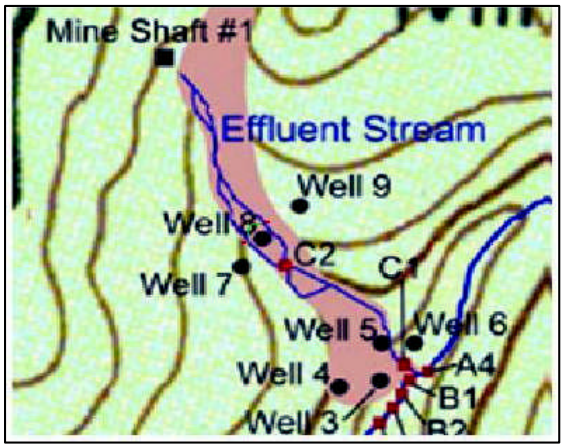

Figure 6: Tailings Pile Area (shown in red)

The reactive fill material chosen consists of 50% granular dolomitic limestone ($CaMg(CO_3)_2$ at: 85mol% Ca, 15mol% Mg), 25% composted cow manure (possibly an additional source of sulfate reducing bacteria), and 25% seaweed compost (organic carbon, nitrogen and phosphorus addition) by volume. Approximately 318kg of limestone, 110 kg of manure, and 110 kg compost was added over 5 days in August

2007. A total of 11 closely spaced columnar holes were excavated with an 8hp mechanical auger (Little Beaver®) and finished by hand. The saturated zone was encountered at about 1.7 m below ground, and a bucket auger was used to continue removing ~30-45cm of the groundwater/sediment slurry. Reactive fill was added to these 11 "columns" closely placed in a half circle up-gradient from the sampling well (Well 8); this curtain structure is ~0.15m thick by 4 m diameter by 2m depth (Figure 7; scale given by well-to-fill distances). Since the water table is fairly shallow at this site (~1m) at least some of the fill would be saturated at all times. Precipitation events, vadose zone movement, and interactions with soil moisture are expected to introduce reactive fill components from the unsaturated portion to the water table.

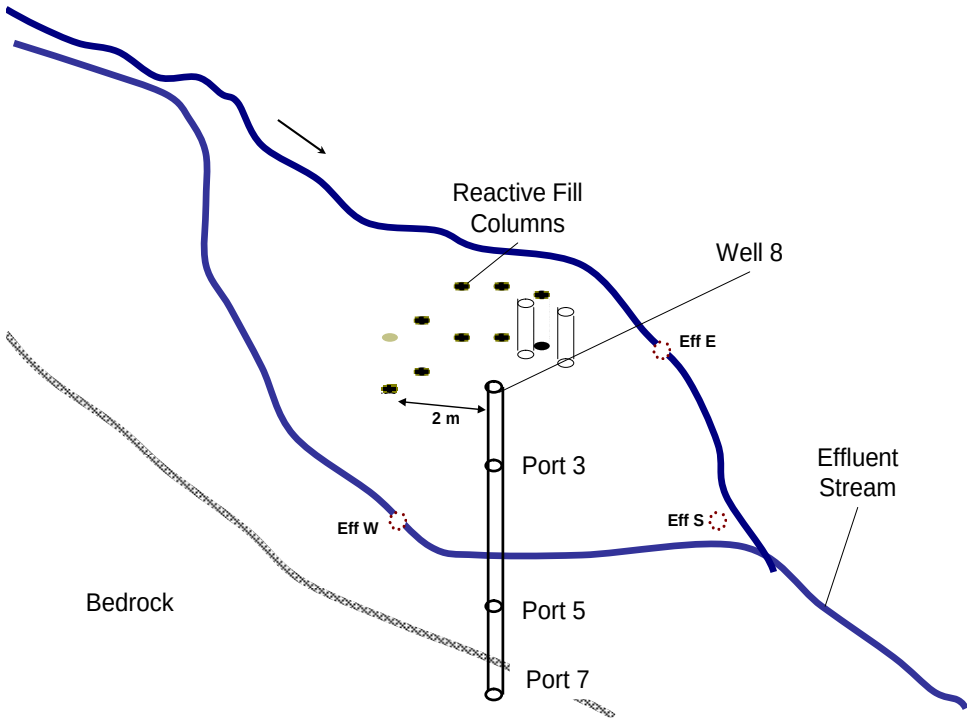

Figure 7: Permeable Reactive Barrier Schematic: Oblique View

Table 4: Reactive Fill Components

Fill Material	% (volume)	mass (kg)
Allyndale® Limestone (granular)	50%	318
Foster's® Composted Cow Manure	25%	110
Conrad Fafard® Shrimp and Seaweed Compost	25%	110

Figure 8 represents the adapted permeable reactive barrier in cross-section, the location of the sampling ports, and summarizes the previous hydraulic conductivity measurements (K) by Gál and Cerato.

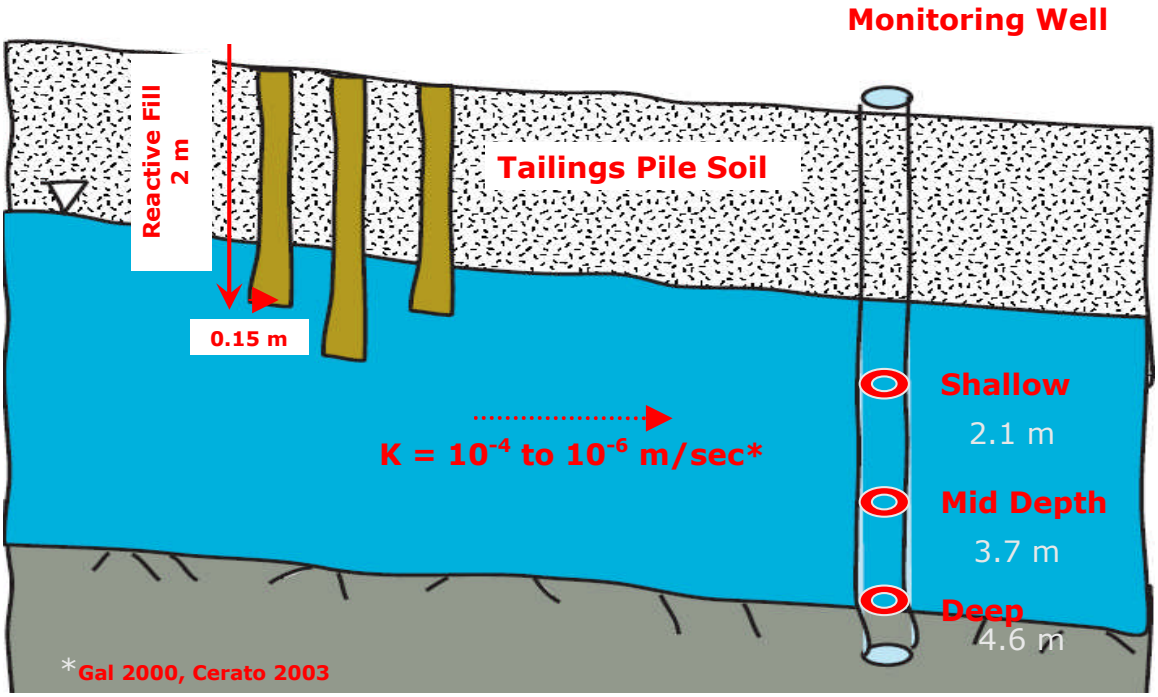

Figure 8: Permeable Reactive Barrier Schematic: Cross Section

2.2 Field Monitoring

Water samples were collected from the study site at Davis Mine once or twice monthly for a 16 month period starting June 2007 and ending October 2008.

Three groundwater samples were taken from Well 8; from its ports 3, 5, and 7, corresponding to shallow groundwater at 2.1m (7') depth, bedrock interface groundwater at 3.7m (12') depth, and groundwater from within the bedrock at 4.6m (15') depth. The monitoring well used was constructed with Solinst® tubing, a radially sectioned plastic well tubing which was opened at different intervals to allow separate depths of groundwater to be accessed from a single well casing. The depth to groundwater was measured with a Soiltest® conductance water level meter prior to sampling. The well was purged for ~3 min before sampling to remove any water stored in the well-bore. Approximately 500 mL of sample was pumped into a 1 L Nalgene® beaker, which had been pre-rinsed with the sample 3 times; this portion was used for field measurements of pH, ORP, Temperature, and Conductivity. An acid-washed 500 mL Nalgene® bottle was also rinsed 3 times with the sample and filled to the top (to minimize oxidation from air); this portion was used for laboratory analyses.

Two surface water samples were taken from the east and west braids of the shallow, ochre lined effluent stream. These two sampling sites representing the nearest surface water are located 5-6 horizontal meters away from Well 8 and in depressions 0.5-1 vertical meter below the ground surface in the middle of the tailings-pile. The west branch (Eff W) of the effluent stream is bounded by an uphill slope, is shaded by overhanging branches, with water flowing through pools which may be up to 50 cm deep. The west branch is underlain by iron oxide stream bed, in which the ochreous lining is well formed and cemented. The east branch (Eff E) of the effluent stream is also bounded by a gentler uphill slope, is generally not shaded, and is relatively shallower; with water depths of ~10-15 cm. The east branch is underlain by a less developed iron oxide stream bed, in which some sediments are not cemented by the ochreous coating and are visibly loose. A third surface water sample was taken from the water actively seeping from the

base of the tailings-pile (Eff Seep); this water represents emerging groundwater. This water was accessed by digging a small hole (~15 cm diameter) at the seep and letting it fill with water. For both the water from the east branch of the effluent stream and the tailings-pile seep, it was sometimes necessary to "bail" water with a beaker to fill the sampling bottle. Samples from these three surface water sites were taken in the manner described in the groundwater section above (Photos: Appendix B).

The pH was measured in the field using an ORION® 250 portable meter and an ORION® low maintenance pH triode (Cat #9107BN) calibrated previously the same day with 3 pH buffers (Fisher Scientific®, pH 4, 7, and 10). Temperature was recorded with this automatic temperature correcting pH probe. ORP was measured with the same meter and an Accumet® Pt Ag/AgCl probe (Cat # 13-620-81) which was satisfactorily checked against a Zobell's solution prior to sampling. Conductivity was measured using a YSI® 30 portable conductivity probe.

All samples were placed in a cooler with an ice-pack, and were brought same day to the Environmental Geochemistry Laboratory. The samples were filtered through a 0.45 μm inline filter (Millipore®, Billerica, MA) and split into two 125mL portions. One portion was kept at 4°C for anion analysis; the other was acidified below pH 2 with 3-4 drops of concentrated HNO_3 for cation and DOC measurements. Anions analysis was performed usually within a week. Cations and DOC were analyzed within 2-3 months.

2.3 Laboratory Analyses

2.3.1 Cations

Cations were analyzed using Inductively Coupled Plasma Optical Emission (ICP-OES) Spectroscopy with a Spectro® Flame M120 sequential instrument (Kleve, Germany). Calibration was performed with a 6 point calibration curve using secondary standards prepared daily by diluting NIST traceable single element standards (SPEX CertiPrep) with double deionized water (resistivity > 18 MΩ/cm). Waters were analyzed for major cations (Na^+, Ca^{2+}, Si, K^+, Mg^{2+}) and trace cations (Fe^{total}, Al^{3+}, Cu^{2+}, Zn^{2+}, Mn^{tot}, Pb^{2+}) in separate runs. Table 5 lists the standard

ranges and an example of the associated detection ranges. It was necessary to run samples diluted 1:10 for the major cations and some samples were run at multiple dilutions and the results confirmed as comparable.

Table 5: ICP Calibration and Detection Ranges

Analyte	Calibration Std. Range (µg/L)	Example Detection Range (µg/L)
Na^{+}	0 – 5000	1.3 – 6000.0
Ca^{2+}	0 – 5000	6.3- 6000.0
Mg^{2+}	0 – 1000	3.6 – 1200.0
K^{+}	0 – 5000	3.4 – 6000.0
Si	0 – 5000	11 – 6000.0
Cu^{2+}	0 – 1000	7 – 1200.0
Pb^{2+}	0 – 1000	15 – 1200.0
Mn^{total}	0 – 1000	0.7 – 1200.0
Fe^{total}	0 – 5000	0.8 – 6000.0
Al^{3+}	0 – 5000	0.6 – 6000.0
Zn^{2+}	0 – 5000	5.8 – 6000.0

Check standards were run as unknowns at least every 10 samples, with variation from known concentration generally within 10%, and variation did not increase in any direction during the analytical runs.

2.3.2 Anions

Anions (F^{-}, Cl^{-}, NO_2^{-}, Br^{-}, NO_3^{-}, PO_4^{3-}, SO_4^{2-}) were analyzed via ion exchange chromatography (IC) using a Lachat® 5000 Ion Chromatograph (Milwaukee, WI) equipped with a ~15 cm long ~0.15 I.D. column packed with an ammonium resin ($R\text{-}NH_4^{+}$) stationary phase. A 2.0/2.6 mM HCO_3^{-}/CO_3^{2-} eluent was used as the mobile phase which was chemically suppressed before conductivity detection. Calibration was done with a 5 point calibration curve; standards were prepared from reagent grade salts as outlined in the EPA 300.0 method using the high range option. It was necessary to dilute samples 1:2 or 1:5 with double deionized (>18MΩ/cm) water for sulfate analysis; samples were frequently run at serial dilution with comparable results.

Table 6: IC Calibration Ranges

Analyte	Calibration Std. Range
F-, NO_2-, Br-, $^-$	0 – 5.0 mg/L
Cl-, NO_3-, PO_4^{3-}	0 – 10.0 mg/L
SO_4^{2-}	0 – 200.0 mg/L

Variance of check standards from known concentrations was generally within 15% and remained similar during the run.

2.3.3 Dissolved Organic Carbon

Dissolved Organic Carbon was measured on filtered samples using a Shimadzu 5000® TOC analyzer with the help of Ken Mercer and Boning Liu from the Reckhow Lab in Engineering Lab 2.

2.4 Geochemical and Statistical Calculations

2.4.1 Saturation Indices and Iron Speciation

The USGS equilibrium and speciation model PHREEQC Interactive version 2.14 (2008) was used for the calculation of saturation indices and iron speciation. All calculations were made using the "*phreeqc.dat"* database, which incorporates thermodynamic data from Nordstrom *et al*. (1990) and WATEQ4F (Ball and Nordstrom, 1991) into the previous PHREEQE program (Parkhurst *et al,* 1980).

Saturation indices and speciation were calculated by inputting the field measured temperature, pH, redox environment (as pe) and laboratory measured elemental concentration data for each sample at each sampling date using the solution description function. (Redox unit conversions reported in Appendix C.)

A saturation index is the ratio of the ion activity product to the solubility product and is used to describe a specific minerals tendency to either dissolve or precipitate in a solution.

$$SI = \frac{IAP}{K_{sp}}$$

Where the ratio is equal to 1, the activity of the ions measured in solution is equal to the amount present at saturation, and the water is at equilibrium with respect to a mineral. Strongly positive values indicate a solution is oversaturated with respect to the mineral and it is thermodynamically predicted to precipitate, negative values indicate a solution is undersaturated with respect to that mineral and it is thermodynamically predicted to dissolve.

2.4.2 Sorption

During the course of the field experiment, reactions between the added limestone and dissolved iron likely resulted in precipitation of iron (hydr)oxides. The formation of the oxides would have resulted in changes in the concentrations of dissolved metals. Observational evidence of change in dissolved metals concentrations was compared with modeled change in dissolved metals concentrations resulting from precipitation of ferric oxides. A semi-quantitative prediction of sorption onto a hydrous ferric oxide surface was also using PHREEQCi. Default values for the sorptive capacities of hydrous ferric oxide were used, since any iron precipitates formed would be of approximately hydrous ferric oxide composition. Average composition solutions representative of Davis Mine groundwaters were set to equilibrate with the oxide surface in a batch reaction step. Solution compositions were: summer average 2008 (May to Oct; n=8) summer average 2007 (June to Oct; n=8), and whole year 2004 (May to May; n=7). These three solutions were inputted into the solution spreadsheet, along with field measured pH and pe. The composition of these solutions is given in Appendix D. Surface reactions were calculated using a Dzombec and Morel simplified two layer model. Sorbates are organized into those held strongly to the oxide surface by bonds of an ionic or covalent character (i.e. inner-sphere complexes between transition metals and ferric oxides's hydroxyl functional groups) and those held weakly to the inner sorped layer by electrostatic interactions (i.e. anions in outer-sphere complexes). In this study, the predicted occupancy of the strong sites only is reported.

2.4.3 Statistical Calculations

Yearly average concentrations for this study were calculated using data from June 2007 through June 2008 (n = 19 for most ions). One full year was assumed to include a complete period of seasonal variation.

Summer averages were calculated using data from April through October of 2008, April through October of 2007, April through July for 2004 (best available), April through October for 2003 for comparisons. When data is plotted by month and 2 data-points exist, the average is used, with some years also not having data for a given month.

The *Analysis Toolpak* for Microsoft Excel 2003 was installed and used for calculations of the Student's T Test and the Pearson correlation coefficient (r).

CHAPTER 3

RESULTS

3.1 Hydrogeologic Background

For the purposes of this study, it was necessary to confirm that the reactive fill was placed in the up-gradient direction from the monitoring well. The hydraulic gradient within the waste rock and tailings pile valley was measured during a single day (7/15/09). A 1.5 m slotted drive-point 4" diameter PVC temporary well ("temp well") was installed 2 m horizontal meters North of a similar PVC well immediately next to Well 8 (previously identified as Well 8 "Port 2"). The wider diameter PVC wells were used to accommodate an available water-level meter and both wells were assumed to be at equal elevation, based on the locally flattened slope of the Well 8 vicinity. The depth to water was measured three times in each well (Table 7).

Table 7: Waste-Rock Pile Hydraulic Gradient

	depth to water (m)	-casing above ground (m)	corrected (m)	average
temp well	1.15	0.05	1.10	*1.097*
	1.15	0.05	1.10	
	1.14	0.05	1.09	
Port 2	1.33	0.15	1.18	*1.18*
	1.33	0.15	1.18	
	1.33	0.15	1.18	

$$\frac{\Delta h}{\Delta l} = \frac{1.097 - 1.18 \text{ m}}{2.0 \text{ m}} = -0.0415$$

A hydraulic gradient of approximately 4% was calculated between the two wells from these measurements. The higher hydraulic head was found in the temp well North of Well 8 Port 2, in agreement with the water table contour map drawn by Bloom (2005; Figure 18). These measurements confirm that the reactive fill was installed in the up-gradient direction (N/NW) from Well 8 and that groundwater taken from Well 8 would have come in contact with this reactive material with the potential to flow through it.

Depth to groundwater in the shallow groundwater sampling port averages 1.24m below ground surface, and ranges from 0.9 to 1.7m (Fig. 9). Depth to groundwater is similar in the

groundwater-bedrock interface sampling depth. Hydraulic heads found in the bedrock port are slightly greater than either the shallow or interface levels; averaging 1.09m, and ranging from 0.8 to 1.4m. The higher heads measured in the bedrock groundwater indicate a limited potential for downward migration of shallow groundwater. Regardless of depth interval, the location of the saturated zone fluctuates seasonally, with lows during the drier summer months of 2007 and highs during the winter and spring. Monthly average precipitation data from the weather station approximately 10 miles south of the study site (Ashfield MA, COOP ID 190213) is also included in Figure 9.

The reactive fill was introduced in August 2007, a time during which the water table was at its lowest (1.7m). Since the fill depth of this material was 2m, it was minimally saturated at the time of installation. Water table elevation rose during the fall and winter, reaching its highest (0.9m) in March of 2008. The proportion of saturated reactive fill would have been highest at this time. Water table elevations were slightly lower in the summer months of 2007 vs. those of 2008, with June-October averages of each year respectively 1.37 m and 1.35m below ground in the shallow groundwater.

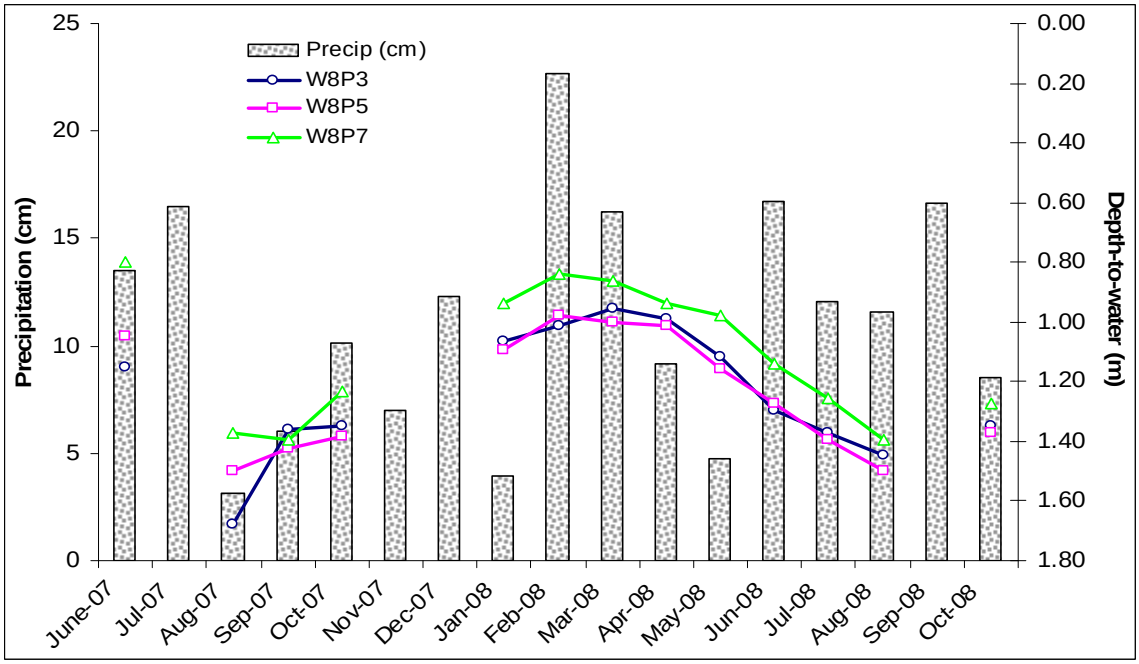

Figure 9: Depth to Groundwater in Well 8, 2007-2008. Well 8 Ports 3, 5, and 7 represent the shallow, groundwater-bedrock interface and bedrock groundwater, at respectively 2.1, 3.7 and 4.6m below ground surface. Monthly average precipitation from a local weather station is also provided. (Missing data points due to water level meter malfunction)

3.2 Groundwater Chemistry

3.2.1 pH and Oxidation-Reduction Potential

Groundwater within the tailings-pile is acidic and oxidizing, with the most severe conditions found in the shallow groundwater (Figure 10). At this level 2.1m below ground, pH averages 3.8 and Oxidation Reduction Potential (ORP) averages 485±63 mV over a 1 year period (June 2007-June 2008, n=19). Within the shallow groundwater, no immediate decrease in redox potential is observed following August PRB installation. After approximately six months the ORP actually becomes more oxidizing, rising from 480 to 624 mV (from 0.7 to 0.85V as E_H) in February 2008. From this maximum, the redox potential declines to a minimum of 323 mV (0.54V as E_H) in October of 2008. Similarly, following the introduction of PRB materials, pH does not increase for several months, ranging from 3.4 to 4.4 from August 2007 through April 2008. In May of 2008, pH rises to 4.8, a value greater than was observed at any time during the

2003 to 2005 monitoring period. This condition continued through the end of periodic monitoring in October 2008.

Ground water taken from an intermediate depth (3.7 m below ground surface) at the groundwater-bedrock interface is also acidic and oxidizing, but less so, with a pH averaging 4.3 and an Oxidation Reduction Potential averaging 334±37 mV (0.55V as E_H) during the 1 year period (Figure 11). The Oxidation-Reduction Potential measured at the interface varied over a smaller range than the shallower ground water, from 235 to 431 mV. Interface groundwater is slightly less acidic than the shallow ground water.

At 4.6m depth, the sampling port located within bedrock, the water is slightly less acidic and oxidizing, consistent with furthest removal from the air, averaging a pH of 4.2 and an ORP of 358±54 mV (0.55 as E_H), (Figure 12). ORP at this interval is similar to that of overlying groundwater bedrock interface water, and both are less oxidizing than the shallow groundwater through most of the observation period. The ORP is less variable. At depth, pH varies between 3.4 and 5.2, exceeding pH 5.0 twice during the fall of 2007.

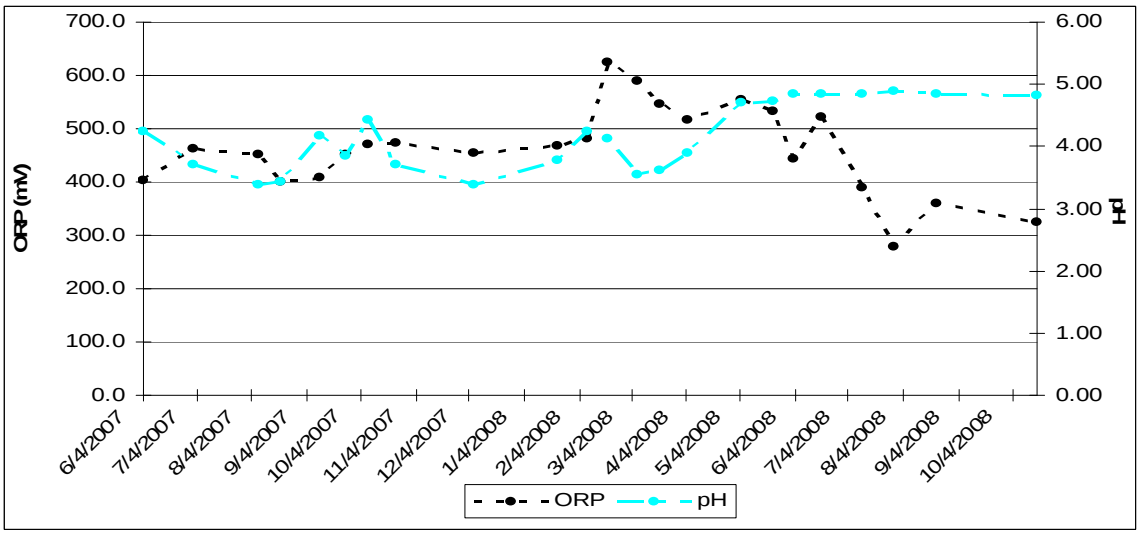

Figure 10: Shallow Groundwater pH and ORP

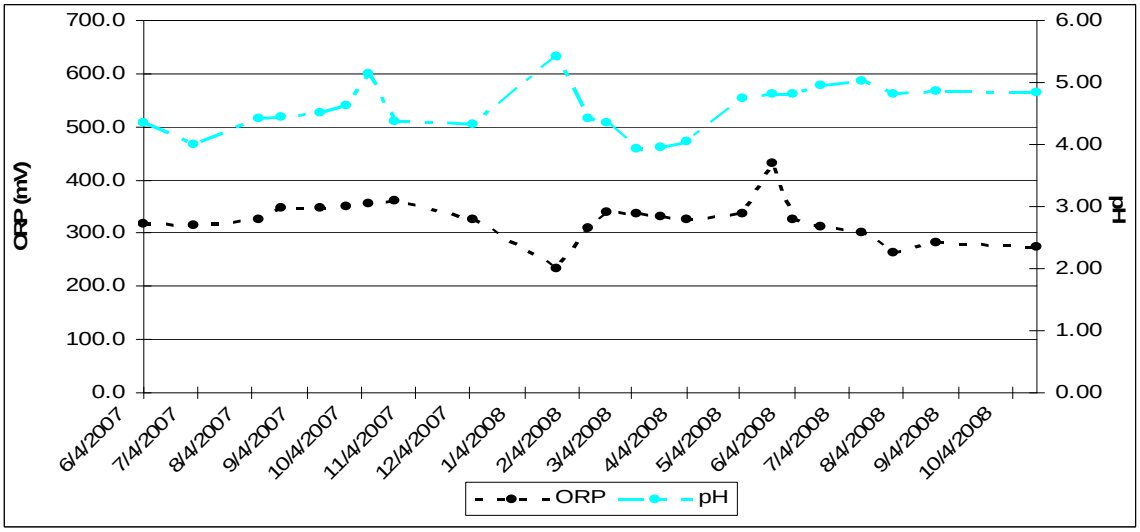

Figure 11: Interface Groundwater pH and ORP

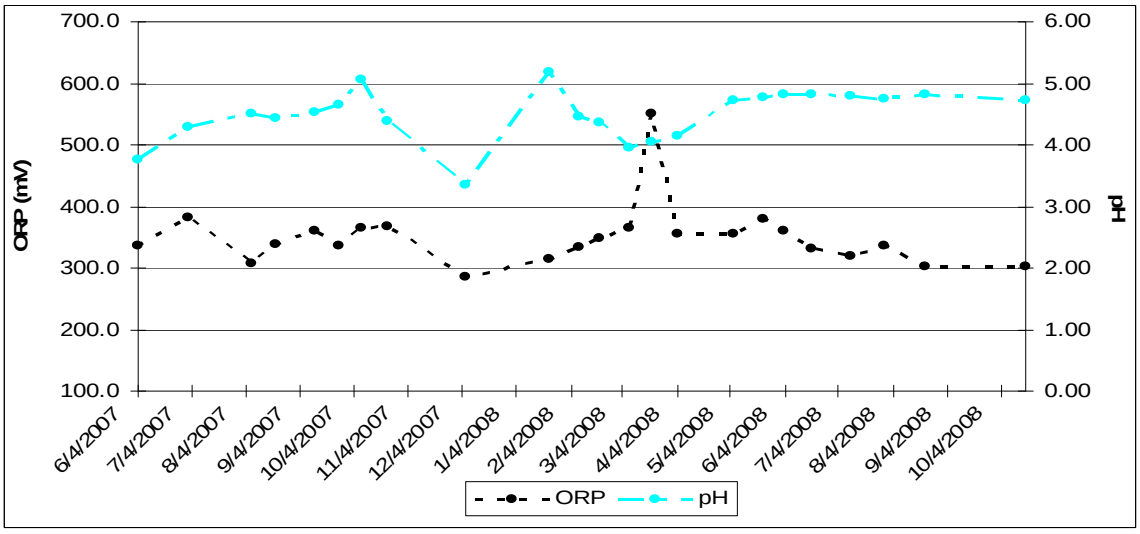

Figure 12: Bedrock Groundwater pH and ORP

3.2.2 Major Cations

As the acidic drainage comes in contact with the aluminosilicate host rock, major cations and silicon are released to solution.

The average yearly concentrations of the major cations at all three sampling depths are reported in Table 8. Generally speaking, concentrations of the major cations increase from the shallow to bedrock-interface groundwater. The shallow groundwater contains the least amount of dissolved components, the groundwater bedrock interface contains the most, and the bedrock groundwater contains almost as much as the interface. At all three intervals, Ca^{2+}, Si, and Mg^{2+} are the largest contributors to the solution chemistry from the major cations, with minor K^{+} and Na^{+} are also present.

Table 8: Groundwater Average Major Cation Concentrations

(μg/L)	**Ca^{2+}**	**Si**	**Mg^{2+}**	**Na^{+}**	**K^{+}**
Shallow	43953	13415	10173	1804	4663
±	*8220*	*2019*	*1104*	*273*	*881*
Interface	69935	15432	13241	1789	5806
±	*6352*	*1542*	*997*	*106*	*657*
Bedrock	65372	12544	12519	1569	5541
±	*5868*	*817*	*1015*	*114*	*660*

The shallow groundwater sampling interval is the freshest with regards to the major cations Ca^{2+}, Mg^{2+}, Si and K^{+} (Figure 13). At this level, concentrations of Ca^{2+} and Mg^{2+} show a slight upward trend during the year, and correlate closely (Pearson's r= 0.89).

The interface groundwater has relatively the highest concentrations of Ca^{2+}, Mg^{2+} and Si, and K^{+}, with Ca^{2+} levels ~1.5x higher than the shallow groundwater (Figure 14). Ca^{2+} and Mg^{2+} again show good correlation (Pearson's r= 0.88).

Lastly, Ca^{2+}, Mg^{2+}, and Si are again the largest major cation contributors to solution in the bedrock groundwater, and the dissolved load is comparable to, though slightly smaller than water from the overlying groundwater bedrock interface (Figure 15). Again, trends in Ca^{2+} and Mg^{2+} track each other closely (Pearson's r =0.95). The groundwater sampled from the bedrock shows the least variation in major cations seasonally.

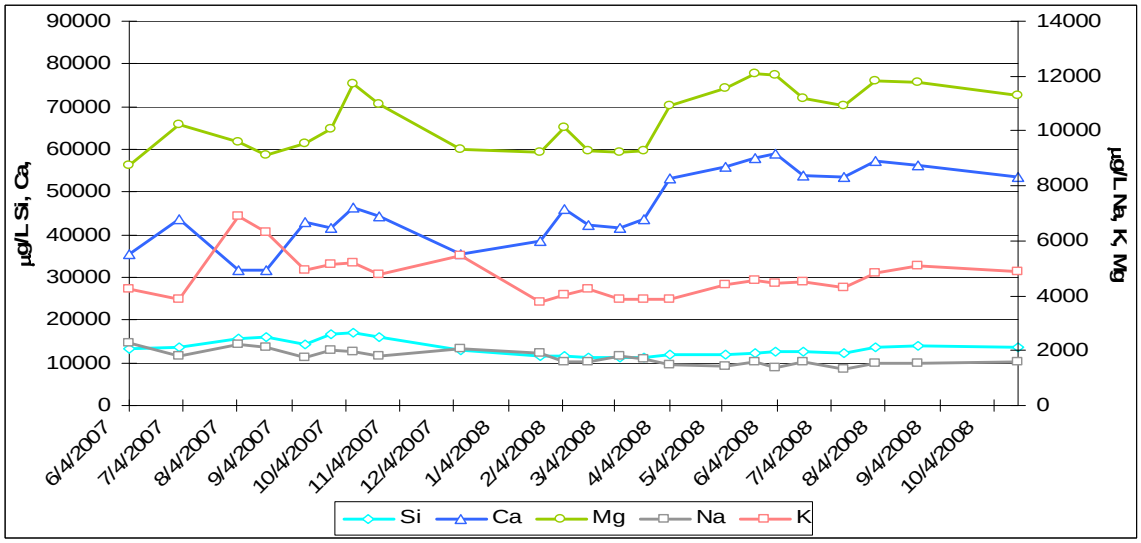

Figure 13: Shallow Groundwater Major Cations (note two vertical axes)

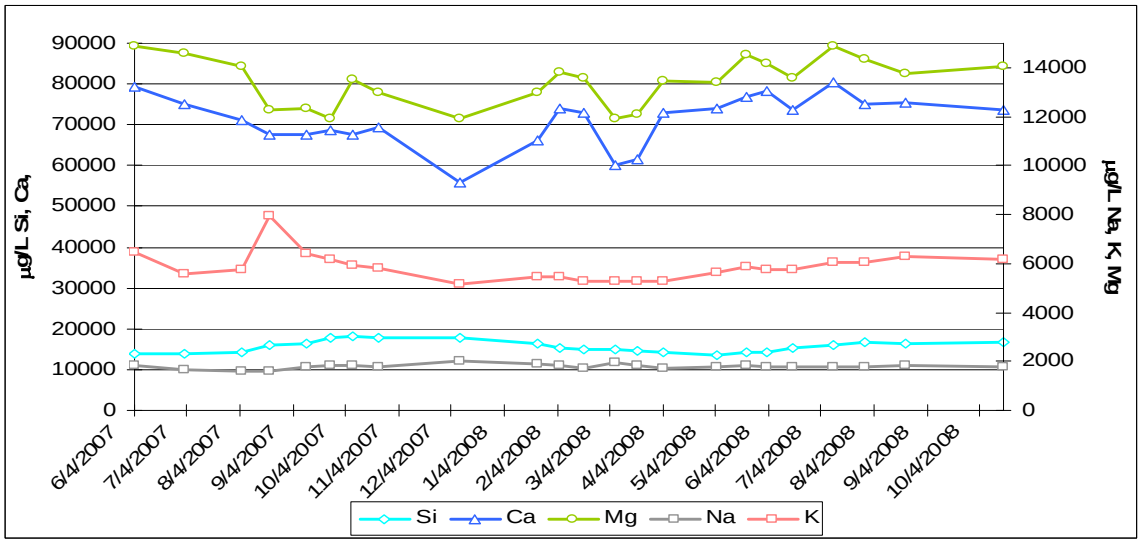

Figure 14: Interface Groundwater Major Cations

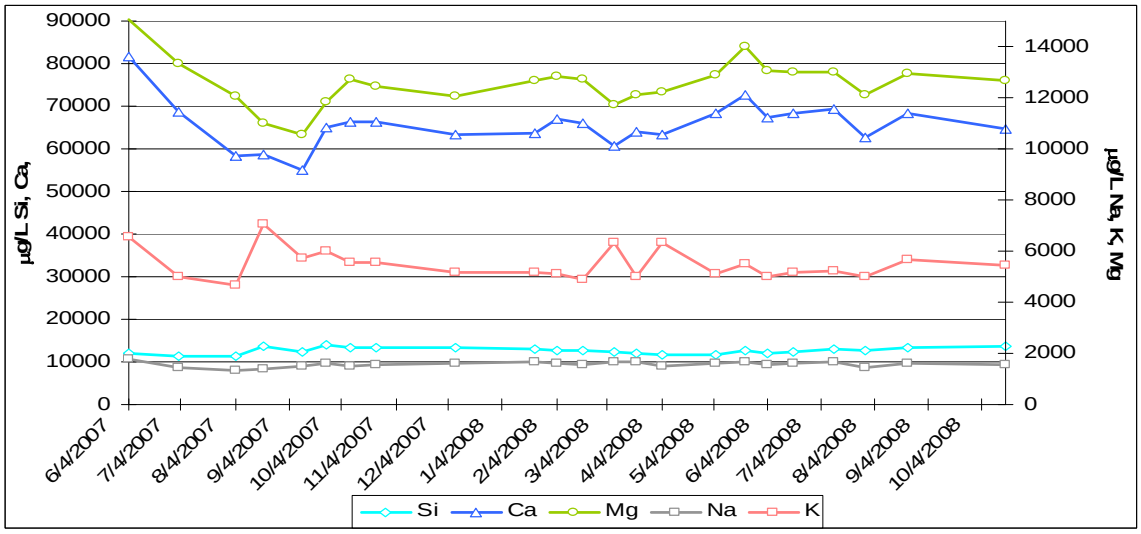

Figure 15: Bedrock Groundwater Major Cations

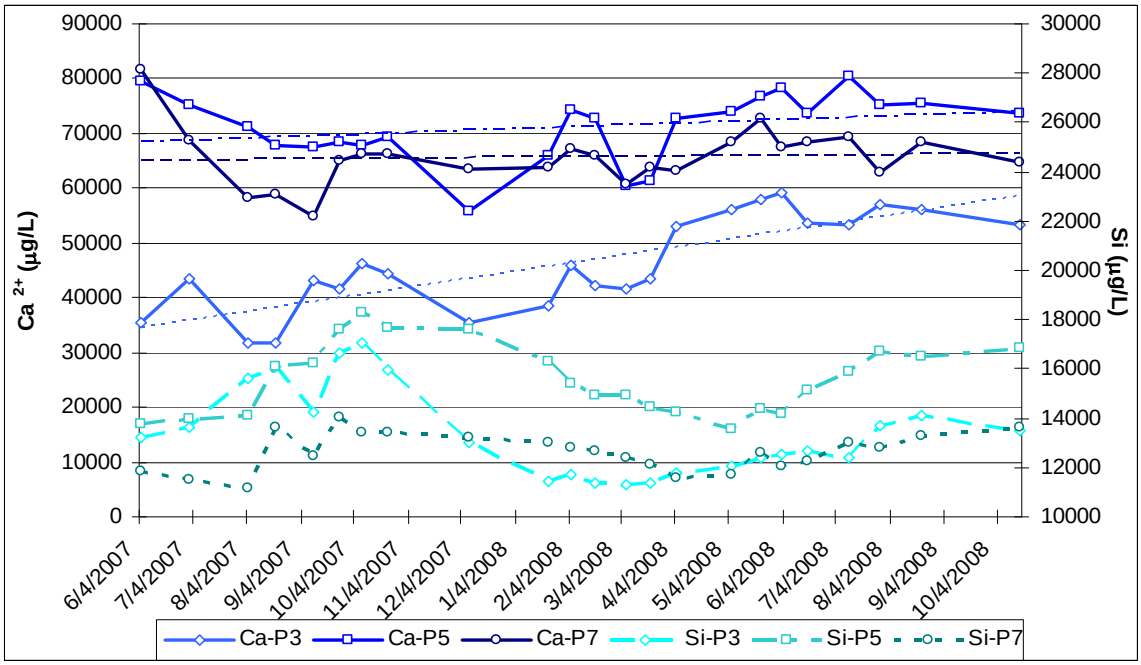

Figure 16: Groundwater Ca^{2+} and Si Concentrations; All Depth Intervals

The groundwater concentrations of Ca^{2+} and Si from all well intervals (Ports 3, 5, and 7) show differing trends (Fig 16). At this scale, it is possible to see seasonal fluctuations in conservative Si concentrations, with higher concentrations observed in summer months. Though commonly sourced, Ca^{2+} and Si trends are somewhat de-coupled, with groundwater Ca^{2+} concentrations showing less periodic variation but instead more constant values. The upward trend in Ca^{2+} is not mirrored by one in Si, suggesting that the increasing contribution of this ion is not coming from the host rock but rather from the added calcite.

Table 9: Ca^{2+} Trend-line Equations

Ca-P3	y = 48.16x - 2E+06
	R^2 = 0.6556
Ca-P5	y = 11.293x - 374690
	R^2 = 0.069
Ca-P7	y = 2.4429x - 30791
	R^2 = 0.0044

A gradual, clear upward trend in Ca^{2+} is observed only in the shallow groundwater. The equations of the Microsoft Excel generated trend-lines are shown in Table 9. From shallow to bedrock groundwater, the slope of the trend-lines decrease from 48 to 11 to 2, as does the goodness of correlation (R^2), quantifying an upward trend in dissolved Ca^{2+} measurable only in the shallow groundwater.

3.2.3 Trace Cations

Remnants of sulfide ore are disseminated throughout the tailings-pile, providing a source of Fe^{tot}, Cu^{2+} and Zn^{2+}. Whereas the shallow groundwater was the most dilute with respect to major cations, it contains the highest amounts of trace cations Al^{3+}, Zn^{2+}, and Cu^{2+}. Water taken from the groundwater-bedrock interface contains the highest concentrations of Fe^{tot} and Mn^{tot}. Average yearly concentrations of Fe^{tot}, Al^{3+}, Zn^{2+}, Cu^{2+}, and Mn^{2+} are summarized in Table 10 (n=19). Dissolved Pb^{2+} concentrations are frequently low; the average reported for this element is for all data above detection limit (n=8-10).

Table 10: Average Groundwater Yearly Trace Metal Concentrations

(μg/L)	**Fe^{tot}**	**Al^{3+}**	**Zn^{2+}**	**Cu^{2+}**	**Mn^{2+}**	**Pb^{2+}**
Shallow	622	2056	2791	407	888	72
±	*417*	*709*	*463*	*97*	*145*	*58*
Interface	5296	1356	2337	237	1568	72
±	*1847*	*241*	*222*	*51*	*123*	*78*
Bedrock	1599	1331	2215	261	1308	80
±	*952*	*88*	*78*	*22*	*99*	*76*

The shallow groundwater contains relatively the highest levels of Al^{3+}, Zn^{2+}, and Cu^{2+}, but relatively the lowest levels of Fe^{tot} and Mn^{tot}. In molar amounts, the shallow groundwater's trace metal composition is mainly an Al^{3+} solution, followed by Zn^{2+}, then Fe^{tot}, Mn^{2+} and Cu^{2+}.

Table 11: Average Summer (May-Oct) Trace Metal Concentrations

(μg/L)	**Fe^{tot}**	**Al^{3+}**	**Zn^{2+}**	**Cu^{2+}**	**Mn^{2+}**
W8P3	90	1222	2321	275	1007
±	*42*	*95*	*101*	*21*	*46*
%	-85.6	-40.5	-16.8	-32.3	13.4

The regular periodic variation seen in the major cations is not mirrored in the trace cations, but instead the concentrations of these ions are more variable throughout the year (Figure 17). Beginning in May of 2008 Fe^{tot}, Al^{3+}, Zn^{2+}, Cu^{2+} are consistently low during a 6

month period lasting until the end of sampling in October 2008. This time period of stable, decreased trace metal concentrations seems to be the clearest effect resulting from the limestone and organic carbons addition. These summer averages are reported in Table 11, along with the % decrease relative to the June-June average. Fe^{tot} concentration is most decreased at this time, with the summer average concentration of 90µg/L low enough to be compliant with the US-EPA's 300µg/L Fe^{tot} secondary drinking water standard (US-EPA 2010)

At the bedrock-groundwater interface, water composition reflects a more isolated, less oxic environment. Fe^{tot} now predominates as the most common trace metal, at concentrations 1-2 orders of magnitude greater than the shallow groundwater (Figure 18; note larger scale). Mn^{2+} is also two times more concentrated. In molar amounts, Fe^{tot} is followed by Al^{3+}, Zn^{2+}, Mn^{2+}, Cu^{2+} then Pb^{2+}. Iron concentration is largely stable, but shows two major decreases; one August 7th, 2007 and one December 6th, 2007. On the December sampling date, Zn^{2+}, Al^{3+}, and Cu^{2+} increase whereas Fe^{tot} and Mn^{2+} decrease, showing a composition more similar to the shallow groundwater, possibly resulting from a hard freeze forcing dissolved components from groundwater downward. Zn^{2+}, Al^{3+}, and Cu^{2+} concentrations are otherwise consistent.

The trends of decreasing concentrations over time as measured in the shallow groundwater are not observed at the groundwater-bedrock interface interval.

Within the bedrock groundwater, trends in trace metal concentrations are not easily recognized (Figure 19). Concentrations of iron fluctuate broadly between ~2500 µg/L and ~500µg/L. Bedrock Fe^{tot} concentrations average ~30% of the interface values, whereas Al^{3+}, Zn^{2+}, Mn^{2+} and Cu^{2+} concentrations are very similar. Generally, Mn^{tot} trends often match Fe^{tot}, in the direction but not in the magnitude, and Al^{3+}, Zn^{2+}, and Cu^{2+} trends are similar. With the exception of Fe^{tot}, bedrock groundwater trace metal concentrations show little variability. The pH and redox conditions, and related iron chemistry, of this bedrock well's recharge area for this groundwater are unknown. The lower summer concentrations observed in the shallow groundwater are again not observed at this sampling interval.

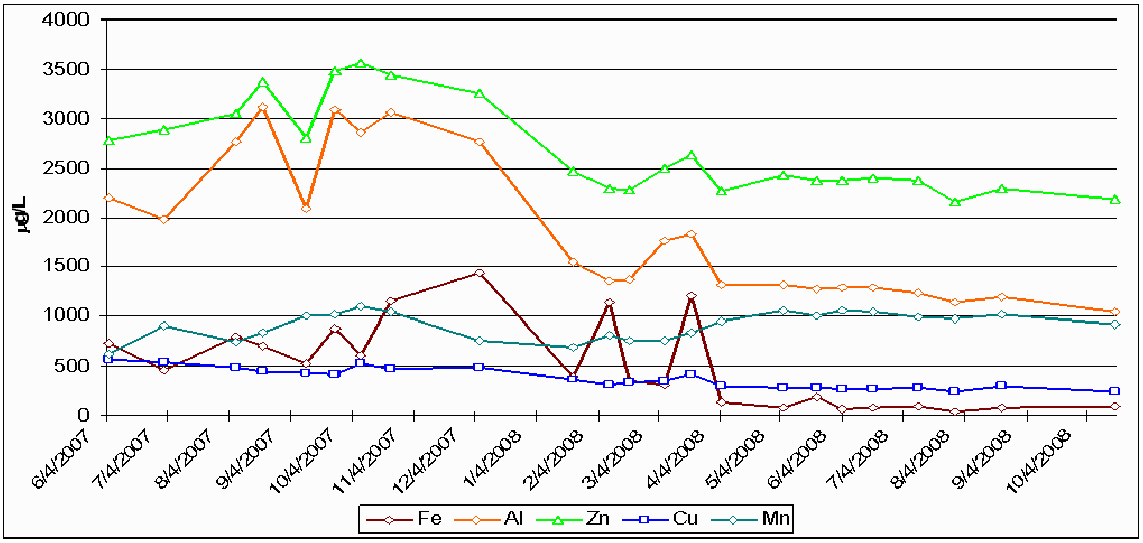

Figure 17: Shallow Groundwater Trace Metal Concentrations

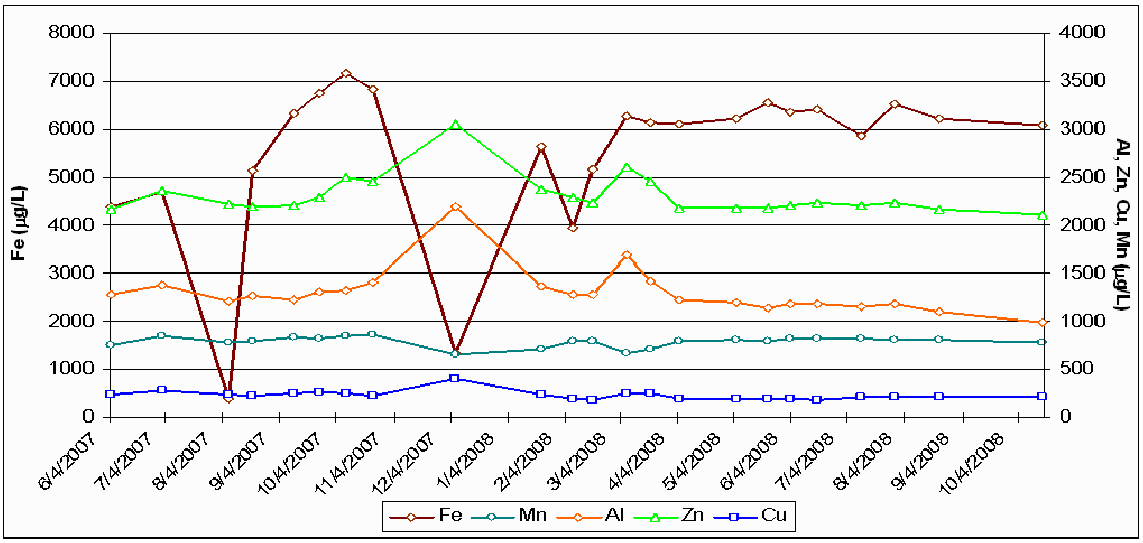

Figure 18: Interface Groundwater Trace Metal Concentrations (note Fe^{tot} scale)

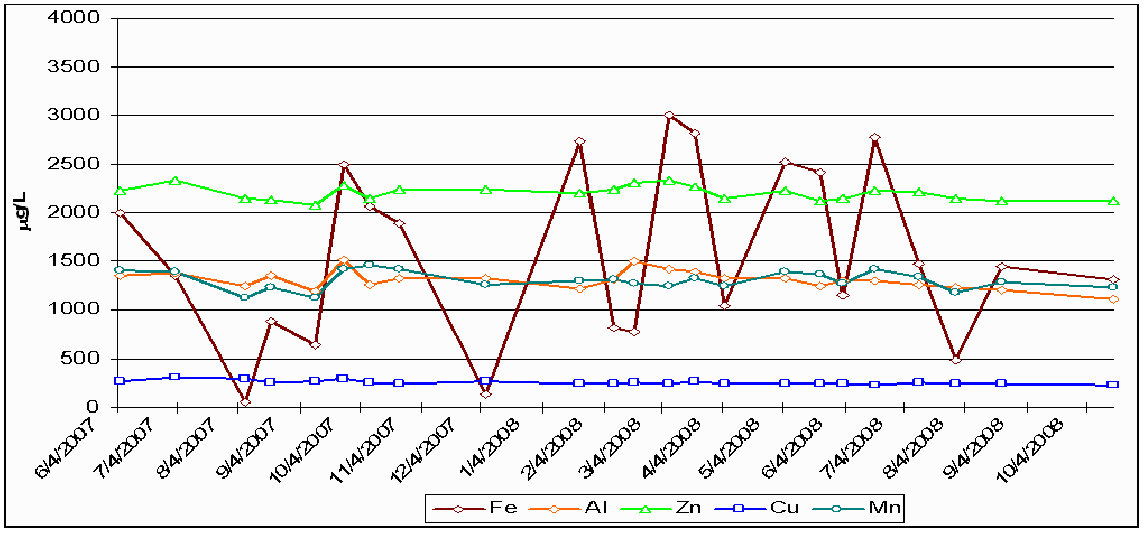

Figure 19: Bedrock Groundwater Trace Metal Concentrations

3.2.4 SO_4^{2-}

Concentrations of sulfate within the tailings-pile are lowest in the shallow groundwater, intermediate in the bedrock groundwater and highest in the interface groundwater (Figure 20). At all intervals, elevated concentrations of sulfate characteristic of sulfuric acid mine drainage are found, with sulfate generally the most prevalent anion or cation in solution. From shallow to deep, groundwater SO_4^{2-} averages respectively 202±35, 277±28 and 245±25 mg/L (2.11, 2.88, and 2.55 mmol/L) over a 1 yr period.

In the shallow groundwater sulfate concentrations are highest in the fall of 2007, lowest in the winter, and rebound slightly in the summer of 2008, showing generally conservative behavior. Concentrations measured at the interface and bedrock depth are less variable, with no seasonal trends. The small decrease in sulfate concentrations observed in the shallow groundwater occurs during the winter month. Shallow groundwater sulfate concentrations fall generally in two groups; data points before December 2007 average higher amounts (229 mg/L) and those from January onward average less (182 mg/L).

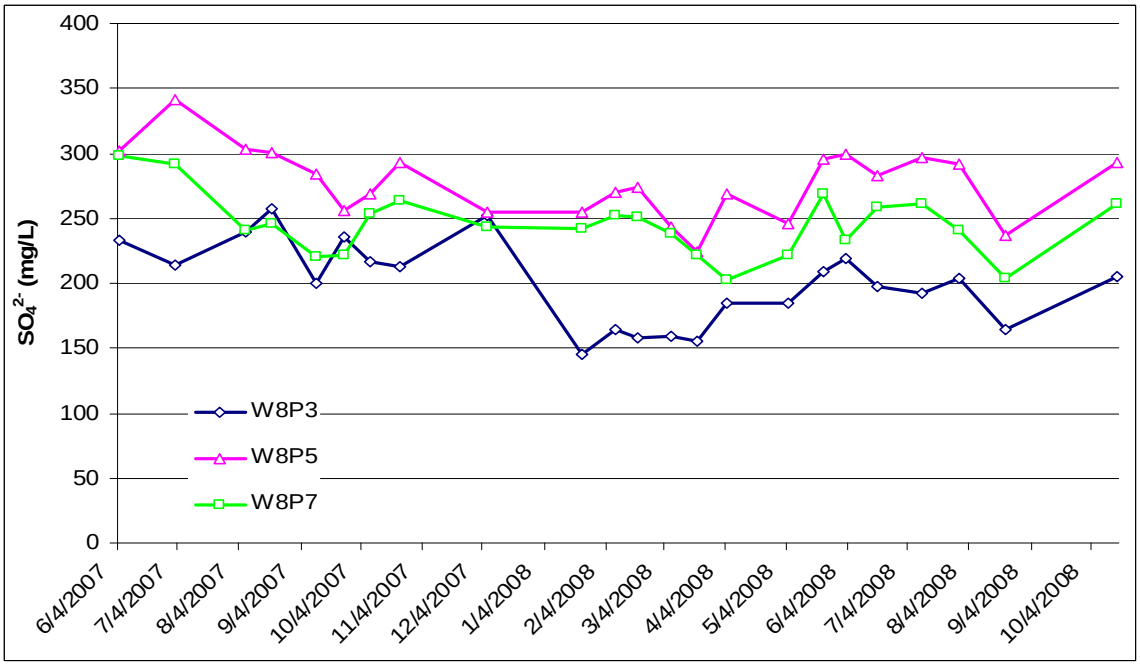

Figure 20: Groundwater Sulfate Concentrations; all intervals.

3.2.5 DOC and Cl^-

Groundwater concentrations of Dissolved Organic Carbon (DOC) are low; consistent with the tailings pile area being composed of mineral soil with scant organic layer formation. Organic carbon was added as part of the reactive fill in order to stimulate the activity of carbon-limited heterotrophic iron and sulfate reducing bacteria. Guided by studies which cited mixed-carbon sources as the most effective, a mix of commercially available partially decomposed organic carbon was chosen to add; this mix contained 50% composted cow manure (an additional SRB source) and 50% seaweed compost (high N and P, possible Cl^- source).

Groundwater Cl^- concentrations are also somewhat low; with a limited amount introduced under natural conditions through amphibole weathering and as a result of road salting. Cl^- is subject to limited removal processes and is often understood to move through groundwater conservatively.

In the shallow groundwater, DOC exceeds a trace amount a few times after the installation of the reactive fill (Figure 21). Immediately following PRB installation in August of 2007, DOC peaks at 12.46 mg/L. Another large peak in DOC occurs in a freeze event in December 2007. Addition of DOC from the reactive fill's carbon mix otherwise seems limited.

Cl^- also follows a declining pattern in the shallow groundwater. It reaches a maximum concentration of 12.8mg/L after the reactive fill was added and again at 9.3 mg/L during December 2007. Other smaller peaks are observed in the shallow groundwater. Cl^- concentrations at depth show more or less constant concentrations over time.

It is likely that increased concentrations of DOC and possibly Cl^- measured immediately following the installation of the PRB were released from the material. The organic carbon source was expected to have at least a small water soluble fraction which would be measured as DOC. The Cl^- content of the organic carbon mix is unknown, however may have contained Cl^- from the marine-derived compost.

In this case, these components act as inadvertent tracers for the most mobile soluble components added from the reactive fill. The largest amounts of DOC and Cl^- are present in August and in December of 2007, decreasing afterwards and suggesting the more mobile soluble components are absent by the summer of 2008.

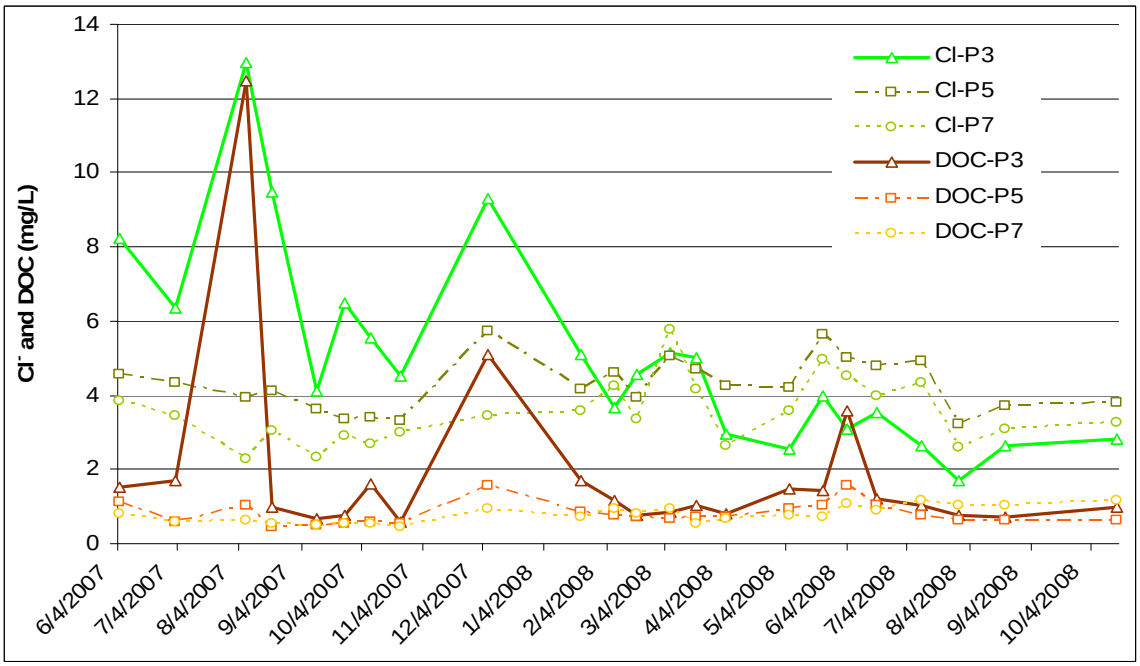

Figure 21: Groundwater Dissolved Organic Carbon and Cl^-, all intervals

3.3 Surface water Chemistry

3.3.1 pH and Oxidation Reduction Potential

The pH and Oxidation-Reduction Potential (ORP) of the surface water samples are uniformly more acidic and oxidizing than groundwater sites. The East and West Branches of the effluent stream also show little variation in pH and ORP.

At the East branch (Effluent East), pH fluctuates between 3 and 4, with an average value of 3.36 (Figure 22). Oxidation-Reduction Potential ranges between 450 and 530 mV, with an average of 484 mV (0.69V as E_H), approaching the stability limit of water with respect to O_2. Although stream discharge varies, no appreciable dilution effects are observed; in fact pH and ORP conditions are fairly stable over the whole period of observation. No data is recorded when the stream is frozen.

Conditions in the West Branch (Effluent West) are comparable (Figure 23). Here the pH ranges from 2.9 to 4.1, averaging 3.26 and Oxidation-Reduction Potential ranges from 450 to 610 mV, averaging 478 mV (0.69V as E_H). Again, pH and ORP values fluctuate within a narrow range, even as the volume increases during the spring melt.

At the Effluent Seep sampling location, water seeping from the base of the tailings-pile is visibly flowing, stirring clay particles while seeping, indicating that it is being sampled soon after exiting the groundwater system. As such, it is not in contact with the amorphous red iron (hydr)oxide riverbed which the other effluent samples are, but rather is in contact with yellow tailings-pile materials.

The Effluent Seep reflects the most severe conditions observed in this study (Figure 24). The oxidation reduction potential is approximately as oxidizing as the other effluent samples, ranging from 450 to 570 mV, averaging 514 mV (0.73V as E_H). pH ranges from 1.83 to 3.62, averaging 2.45. In this case, lowest pH is observed in the winter and spring months with highest water table, dipping below 2.0 in March and April.

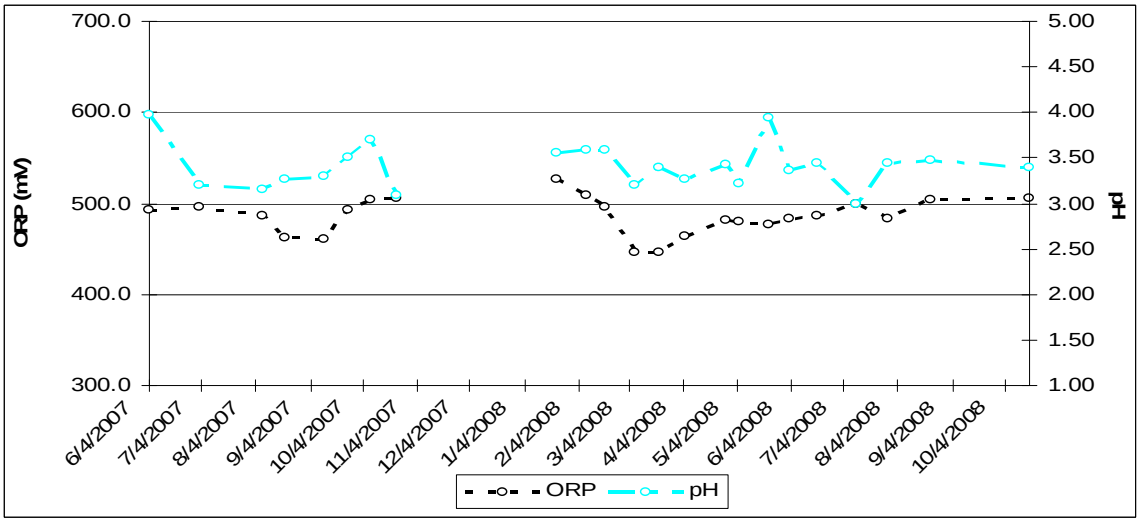

Figure 22: Effluent East pH and ORP

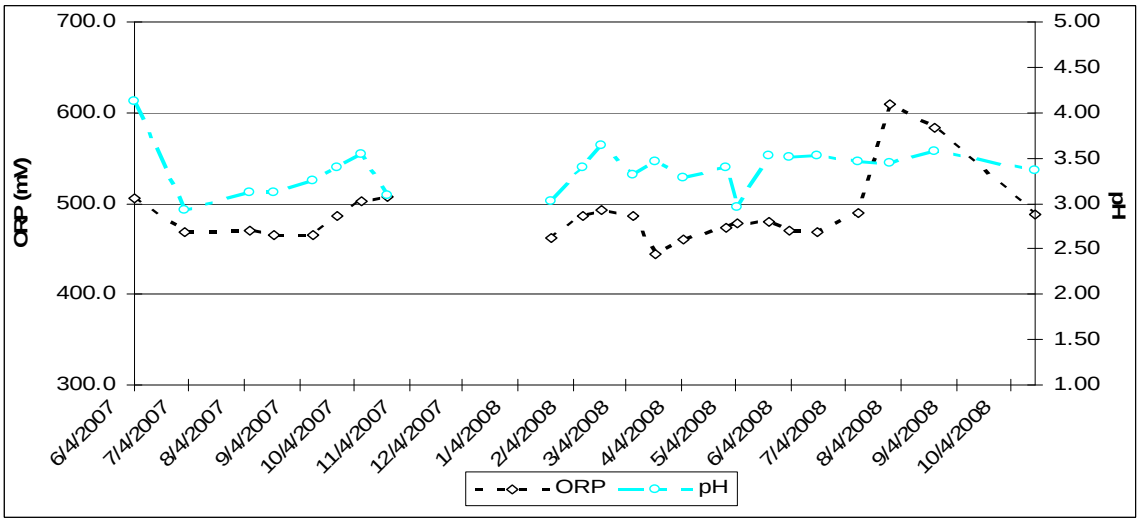

Figure 23: Effluent West pH and ORP

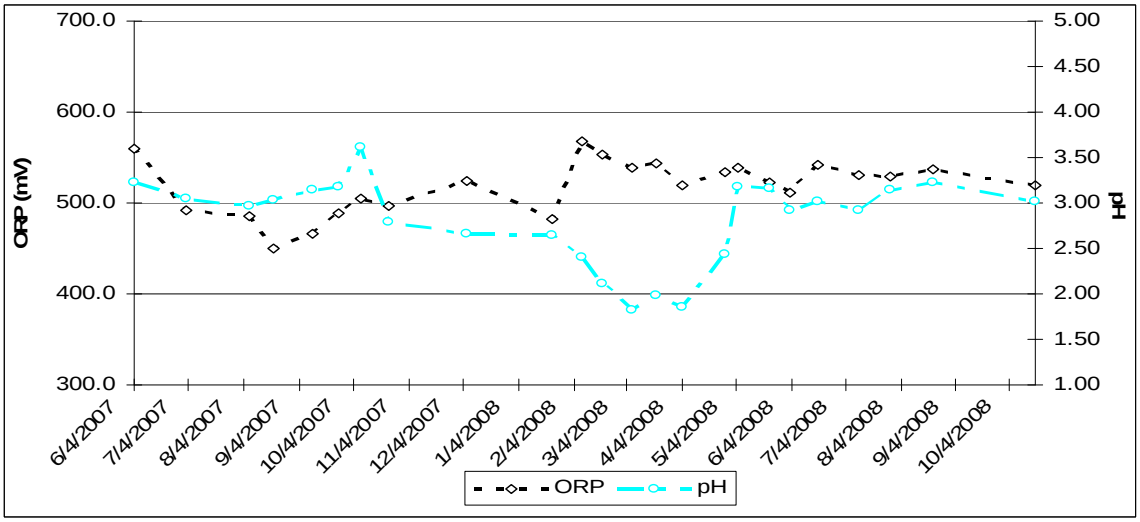

Figure 24: Effluent Seep pH and ORP

3.3.2 Major Cations

Similarities in major cation trends are apparent between three surface water sampling sites, with all sites showing seasonal variation related to conservative transport.

Table 12: Average Surface Water Major Cation Concentrations

(μg/L)	Ca^{2+}	Si	Mg^{2+}	Na^{+}	K^{+}
Eff E	21199	13497	7301	1776	3765
±	*4573*	*3877*	*1651*	*200*	*1120*
Eff W	17647	10677	6213	2331	3320
±	*5653*	*2876*	*1863*	*308*	*1471*
Eff S	17554	14550	6647	2348	3275
±	*5333*	*4457*	*2137*	*303*	*1396*

In the east branch (Eff E) of the effluent stream is predominantly a Ca^{2+}, Si and Mg^{2+} solution (Figure 25). Seasonal trends in Ca^{2+}, Si, Mg^{2+}, and K^{+} concentration are well highlighted in this sample; with higher concentrations measured in the summer and fall of both years, and lows from February through April. A rain event in September is visible.

The west branch of the effluent stream (Eff W) is also mainly a Ca^{2+}, Si, and Mg^{2+} solution (Figure 26). There are slightly smaller concentrations of Ca^{2+}, Si, Mg^{2+} and K^{+}, and slightly more Na^{+}, than in the neighboring east branch, but overall values are comparable. Also comparable is the periodicity of concentration fluctuations, again showing highs in the summer and fall and lows from February through April.

The effluent south seep water is again mainly a Ca^{2+}, Si, and Mg^{2+} solution (Figure 27). The values of Ca^{2+}, Mg^{2+}, Na^{+} and K^{+} are very similar to the west branch, although Si concentrations are higher in the tailings-pile seep water. This sampling location shows the smoothest periodic variation in concentrations of Ca^{2+}, Si, and Mg^{2+}.

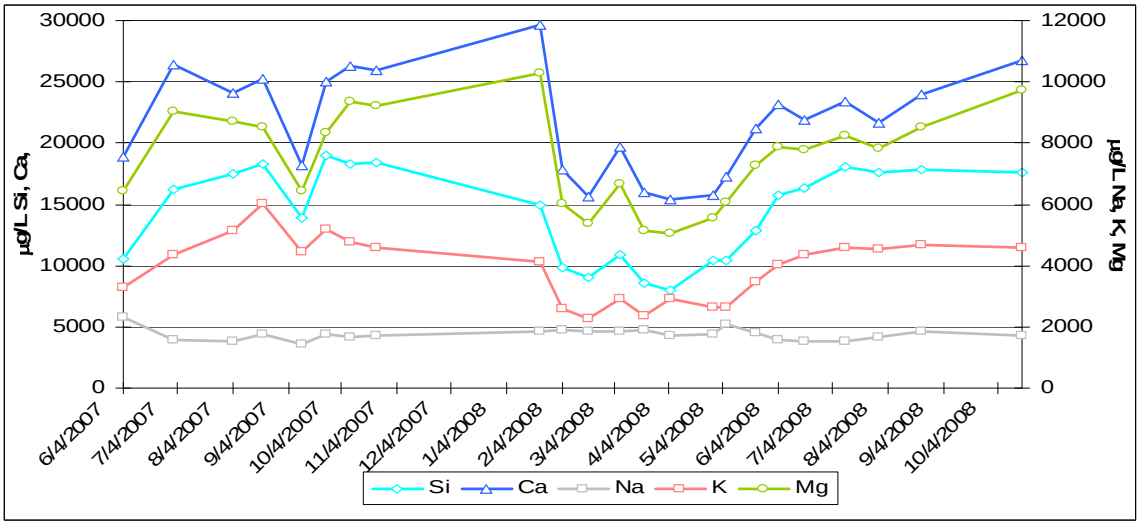

Figure 25: Effluent East Major Cation Concentrations

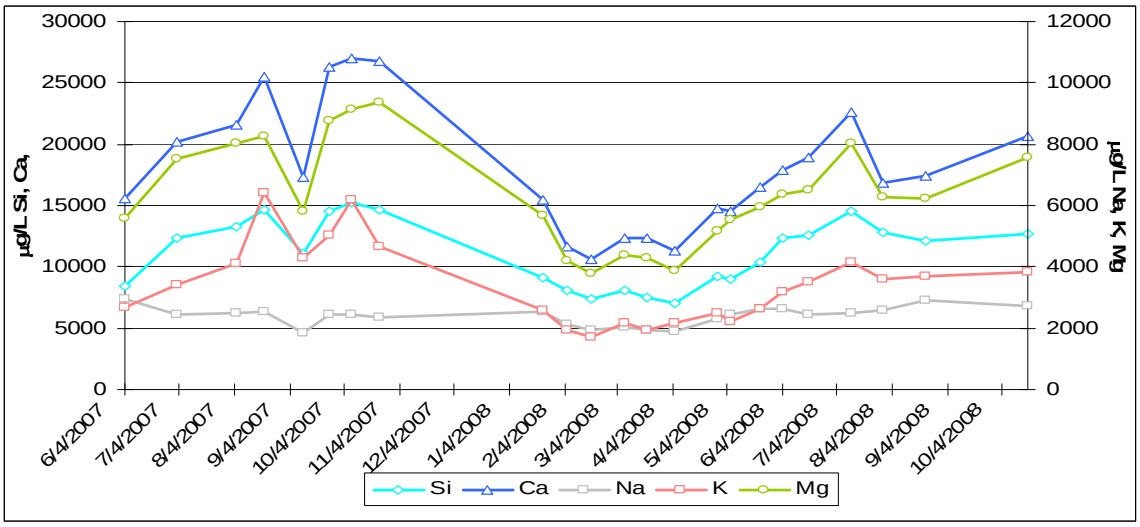

Figure 26: Effluent West Major Cation Concentrations

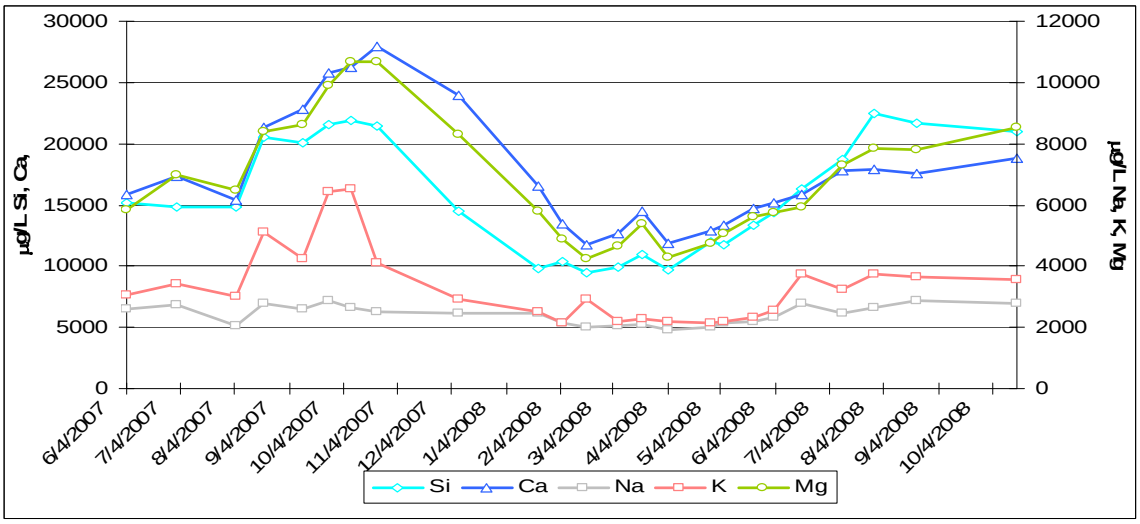

Figure 27: Effluent Seep Major Cation Concentrations

3.3.3 Trace Cations

Average yearly concentrations of trace metals Fe^{tot}, Al^{3+}, Zn^{2+}, Cu^{2+}, Mn^{2+}, and Pb^{2+} measured in the surface waters are shown in Table 13.

Table 13: Average Surface water Trace Metal Concentrations

(μg/L)	**Fe^{tot}**	**Al^{3+}**	**Zn^{2+}**	**Cu^{2+}**	**Mn^{2+}**	**Pb^{2+}**
Eff E	4999	2385	3255	376	743	60
±	*2364*	*513*	*445*	*86*	*246*	*54*
Eff W	8915	2334	3440	282	529	46
±	*4113*	*515*	*901*	*129*	*256*	*57*
Eff S	2692	3436	3380	446	541	58
±	*2336*	*1182*	*767*	*151*	*255*	*104*

Generally speaking, the composition of the two braids of the effluent stream is similar, whereas the tailings-pile seep is unique.

Trace metal concentrations in the East Branch (Eff E) of the effluent stream show predominantly an Fe^{tot} and Al^{3+} solution, followed by half as much Zn^{2+}, and smaller amounts of Mn^{tot} and Cu^{2+} (Figure 28).

During the course of the year, concentrations of Al^{3+}, Zn^{2+}, Cu^{2+} fluctuate slightly, being at their highest in January, dipping slightly in the spring melt months, but the scale of this variability is small, and these elemental profiles differ strongly from those of the major cations. Manganese however is very similar to the major cations Ca^{2+} or Si. Mn^{tot} and Fe^{tot} do not follow the same pattern, but rather anti-correlate (Pearson's r=-0.60) Iron follows a profile similar to Al^{3+}, Zn^{2+} and Cu^{2+}, with one major exception. During the period of spring melt, iron increases 2-3 fold, from ~3000 to 10,000 μg/L.

In the effluent stream's West Branch (Eff W), concentrations of Fe^{tot} are 78% higher than in the east branch, averaging 8915 and 4999 μg/L respectively (Table 13 and Figure 29). Concentrations of Al^{3+} and Zn^{2+} are comparable to those measured in the east branch. Cu^{2+} concentrations are also slightly less in the west branch, but show more clearly peaking with iron in the spring melt event. Mn^{tot} concentrations are slightly lower in the west branch, and display better correlation with Fe^{tot} (Pearson's r=0.57).

At this surface water site, dissolved Fe^{tot} rises in the fall of 2007 and again in the summer of 2008, both in addition to the peak observed during spring melt. The spring melt peak event is marked by Fe^{tot} concentrations increasing ~7.5 fold, from ~2000 to 15,000μg/L.

The tailings-pile seep water (Eff S) shows elemental profiles which are distinct relative to the two effluent samples (Figure 30). Mn^{tot} and Zn^{2+} are most comparable in concentration to the other effluent samples, and display seasonal lows in January and February. Al^{3+} and Cu^{2+} concentrations are higher in the seep than they are in the surface water samples. Al^{3+} and Mn^{tot} show good correlation (Pearson's r =0.91), and show a conservative profile similar to that of Mntot in the effluent west. Fe^{tot} and Cu^{2+} show good correlation (Pearson's r=0.77) The tailings-pile seep water is most acidic water measured, yet Fe^{tot} is low; routinely below 5000 μg/L, although it peaks at 10,500 μg/L in December of 2007. Iron concentrations in the effluent seep are more similar to shallow or bedrock-groundwater interface groundwater $Fe^{tot.}$

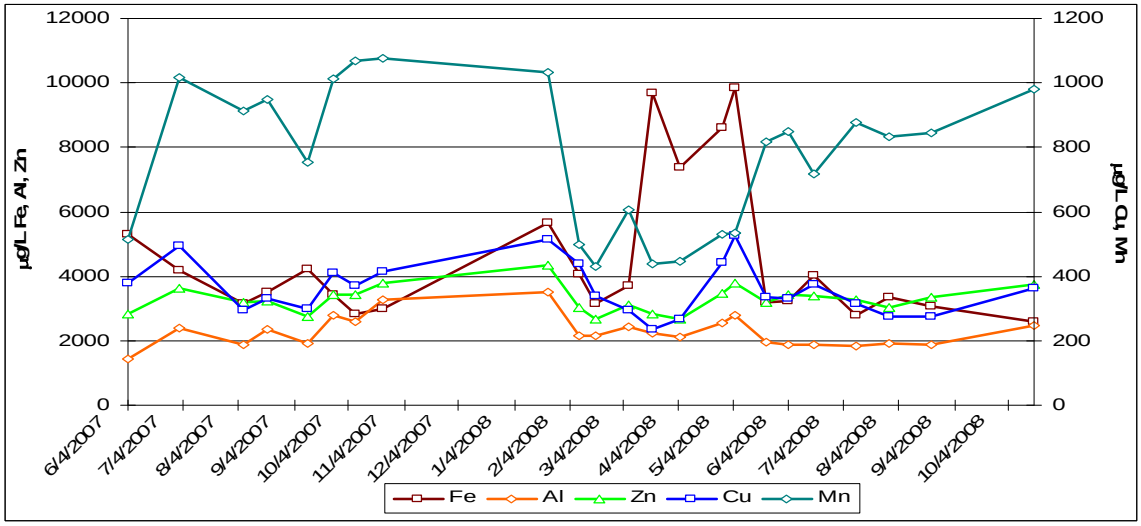

Figure 28: Effluent East Trace Metals (note 2 vertical scales)

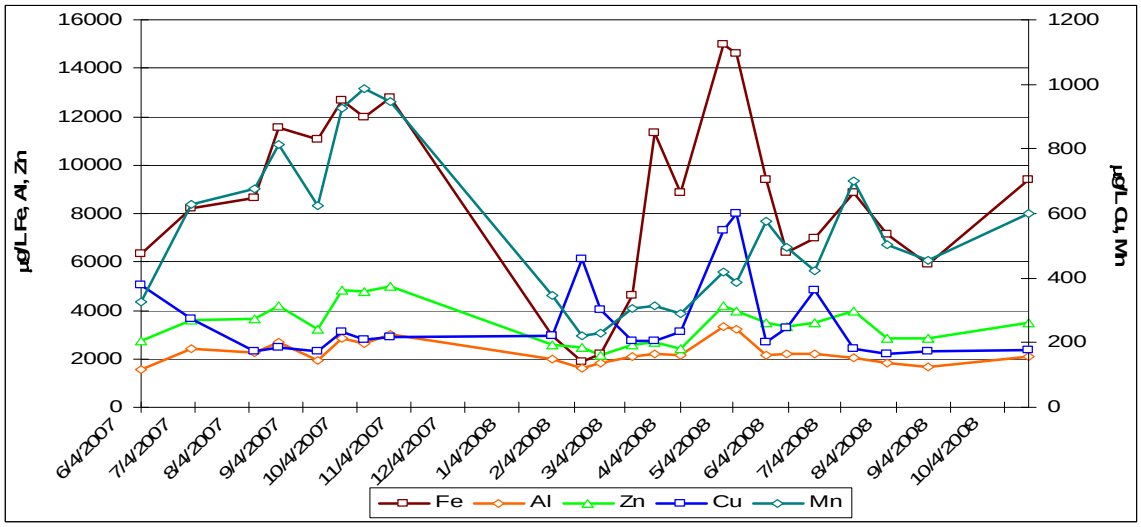

Figure 29: Effluent West Trace Metals (note larger Fe^{tot} scale)

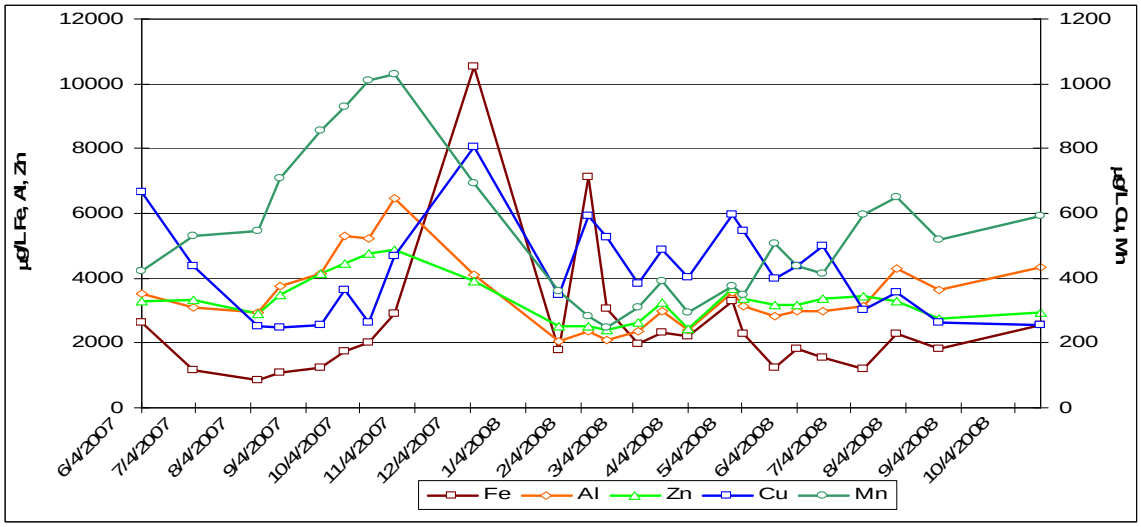

Figure 30: Effluent Seep Trace Metals (note 2 vertical scales)

3.3.4 SO_4^{2-}

Surface water sulfate (SO_4^{2-}) concentrations are all fairly similar to each other in concentration, with the east, west, and seep averaging 201±75, 210±105, and 264±110 mg/L, respectively.

The slightly higher sulfate concentrations in the seep water are more comparable to groundwater (i.e. 202-277mg/L). The seep water continued to flow during the winter months, providing a continuous record of sulfate behavior when the other effluent waters are frozen.

Seasonal trends are well displayed by surface water sulfate, with highest concentrations in the summer and fall and lowest in winter and spring. This suggests sulfate is behaving fairly conservatively in these moving waters. Summer highs in 2008 are lower than those of 2007.

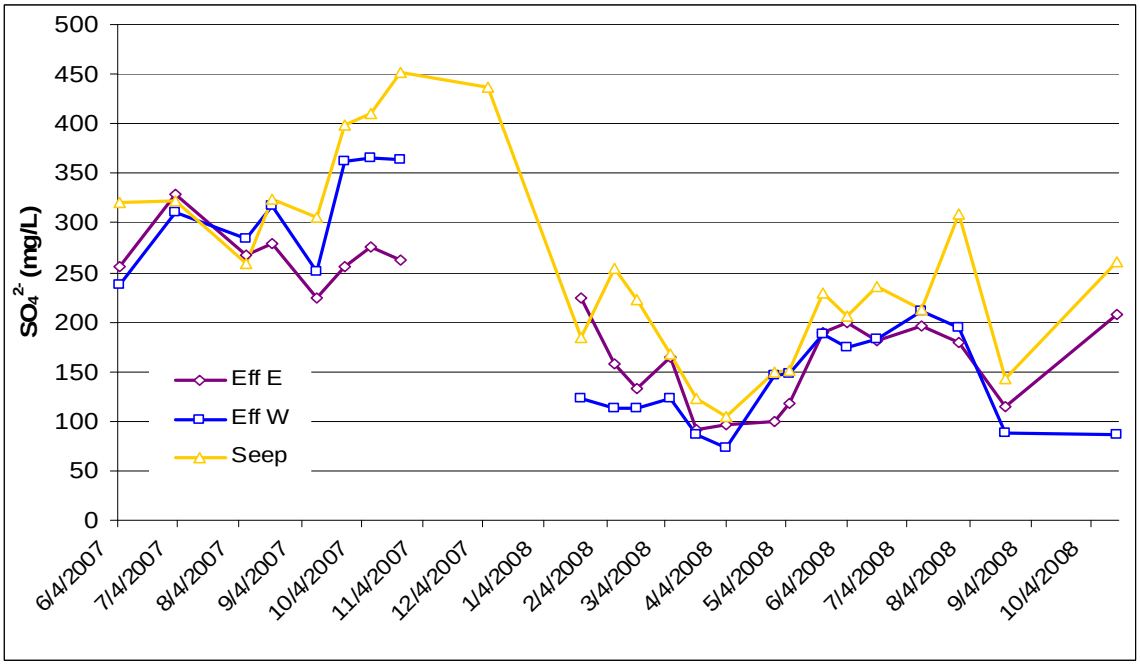

Figure 31: Surface water Sulfate Concentrations

3.4 May 2009 Check Measurement

During a check measurement in May of 2009, the shallow groundwater had a pH of 4.6 and an E_H of 0.42 V, similar conditions to those measured last in October of 2008. The redox measurement is the most reducing recorded for the shallow groundwater during the time period of this study. At this time, the concentrations of trace metals in the shallow groundwater were also found to be low, similar to levels measured last in October of 2008 (Table 14) . As of about 6 months after the end for formal monitoring, the groundwater seems to remain less acidic, less oxidizing, and with decreased concentrations of trace metals.

Table 14: May 2009 Trace Metal Concentrations

(μg/L)	**Fe^{tot}**	**Al^{3+}**	**Zn^{2+}**	**Cu^{2+}**	**Mn^{2+}**	**Pb^{2+}**
W8P3	58.6	1174	2210	252.9	929	59.8
± 1 ICP STD	20.3	27.29	43.79	9.34	25.81	10.16

CHAPTER 4

DISCUSSION AND INTEPRETATION

4.1 Water Table Elevation

At 2.1m below ground surface and ~2m down-gradient from the reactive fill, the shallow groundwater (Well 8 Port 3) was best poised to record any changes resulting from this addition and realistically the only changes observed were measured at this depth.

The reactive fill was added during the first week of August 2007, which was particularly dry, resulting in a groundwater elevation in the shallow groundwater which was the lowest measured (Figure 32). A low water table at the start of the project would have saturated only a small portion of the reactive fill. By February of 2008 more than half of the material was saturated, and the late winter timing of the first changes in shallow groundwater pH/ORP corresponds to maximum saturation (Figure 9).

The groundwater elevation data for all years (2003-04, 2004-05, 2007-08 and 2008-09) generally shows a falling water table leading in to August or September and a rising water table towards February or March. No discharge data was collected for the stream branches sampled in this study, however previous synthesis of precipitation and stream discharge data cite comparable seasonal hydrologic variations, with August noted as the driest month and April as the wettest month (Adams 2007a).

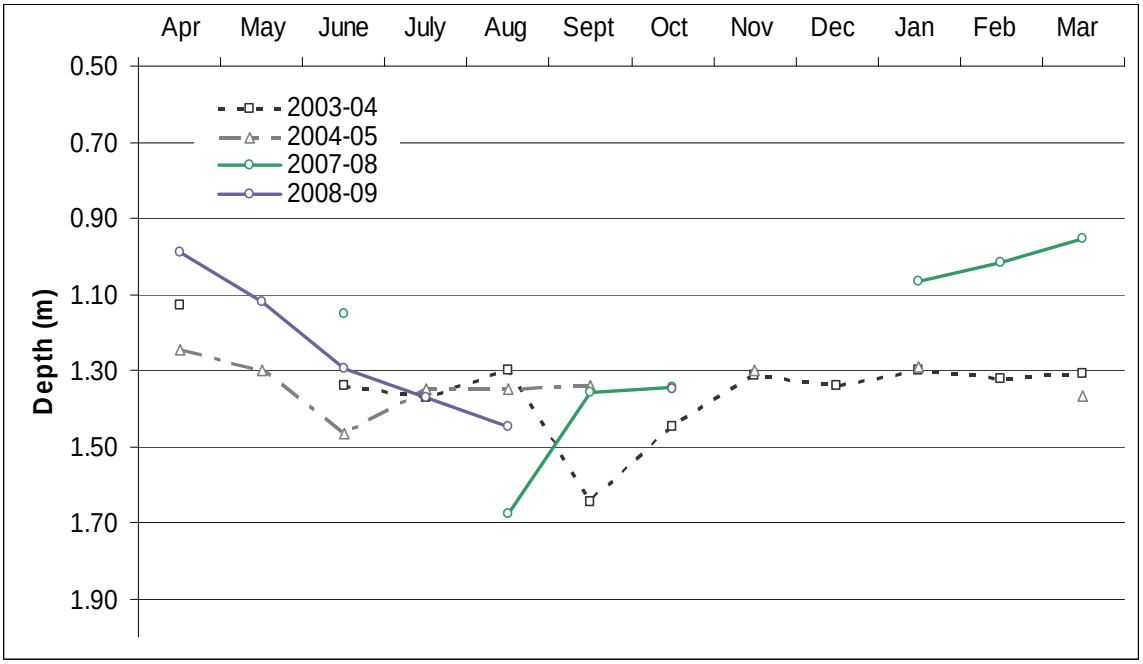

Figure 32: Shallow Groundwater Water Table Elevation over time

4.2 Indices of Change

4.2.1 pH and Redox

The availability of sulfate (SO_4^{2-}) as an electron acceptor in acid waste streams has lead to the use of organic carbon based treatment systems, intended to stimulate sulfidogenesis and divalent metal sequestration as MeS_2. In order to successfully stimulate the activity of sulfate-reducing bacteria, adequate pH and redox conditions must be already existing or attained. Bacterial sulfate reduction (BSR) can occur in acidic environments which have plentiful SO_4^{2-} and bio-available organic carbon.

In reviews of acid mine drainage treatment systems using bacterial sulfate reduction, Gibert *et al.* (2002) recommends as a minimum a pH of 5 and an E_H of -0.200 V to stimulate this bioremediation, whereas Neculita *et al.* (2007) recommends a pH of 5 and an E_H of 0 V, with some low pH exceptions noted. In reviewing data from the Davis mine site, Ergas *et al.* (2006) found some evidence that bacterial sulfate reduction can occur at pH as low as 3 under experimental conditions.

In this study, the pH range observed in the shallow groundwater varies from 3.2 before treatment to 4.8 by the end of measurement. The pH approaches the literature recommendations and exceeds the low pH observances made by the Davis Mine group; pH may be adequate to allow bacterial sulfate reduction to occur, especially where acid-tolerant sulfate reducing bacteria are present.

The Oxidation-Reduction Potential rises to a very oxidizing value of 624 mV (0.85V as E_H) during the middle of this experiment, after which it falls to a minimum of 323 mV (0.54 as E_H.) On the scale of groundwater sampling, the treatment effect on redox environment is not sufficient; this environment is still too oxidizing for bacterial sulfate reduction to be favorable.

The extent of pH and redox shifts measured in this field study is a 1.6 pH unit increase from pH 3.2 (2003-04 average, Bloom 2005) to the summer 2008 average of 4.8, and a 122mV ORP decrease from 445 mV to 323 (2003-04 average, Bloom 2005), affected only in the shallow groundwater. Though small, these changes are the first ones unequivocally affected in a field study at Davis Mine. From the shifts in environmental measurements like pH and ORP, it is not possible to conclusively support or rule out bacterial sulfate reduction as an ongoing process, and other indicators and mechanisms are therefore considered.

4.2.2 Ca^{2+} and Mg^{2+}

The reactive fill consisted of 317.5 kg (3.175 kmol) of slightly dolomitic limestone (85: 15 mol% Ca^{2+}:Mg^{2+}), some of which was immediately saturated by acidic groundwater, but most of which was not saturated until the winter of 2007-2008.

Calcite addition was not clearly signaled by an immediate increase in groundwater Ca^{2+} concentrations, possibly because the proportion of saturated fill was low at the start of the study and the receiving solution had high background Ca^{2+} concentrations. This was surprising considering calcite's relatively quick dissolution rate relative to groundwater velocity, which at undersaturation and pH 4, would have a dissolution rate constant on the order of 10^{-4} mmol/cm^2/sec (Morse and Arvidson, 2002). However, other factors can slow $CaCO_3$ dissolution,

such as Mg^{2+} for Ca^{2+} substitution (Berner and Morse, 1974) or as discussed relative to acid mine waters, Fe^{3+} precipitation onto the $CaCO_3$ surface. Indeed, Ca^{2+} levels through much of 2007 are comparable to the variable background levels measured in whole years 2003-05 (Figure 33). At two times, Ca^{2+} concentrations are actually higher before calcite addition; in June 2003 and April 2004 (Bloom 2005). The whole-year average Ca^{2+} concentration measured in the shallow groundwater in 2007-2008 is slightly higher than the average measured for 2003-04, though slightly lower than that of 2004-05. Finally, by the summer of 2008, Ca^{2+} levels are consistently within the upper range of concentrations measured, and are uniformly higher than the values measured during the same months in 2007.

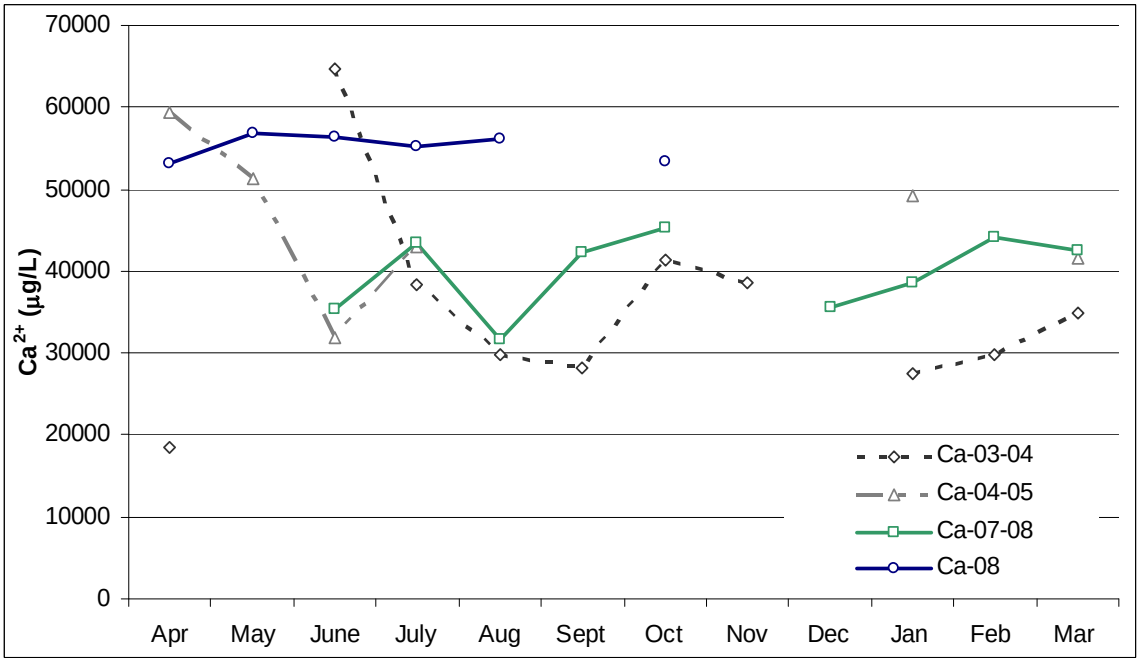

Figure 33: Shallow Groundwater Calcium Concentrations over time

Table 15: Average Shallow Groundwater Ca^{2+} by year

Ca^{2+}	2003-04	2004-05	2007-08	2008
(µg/L)	35149	46028	39894	55216

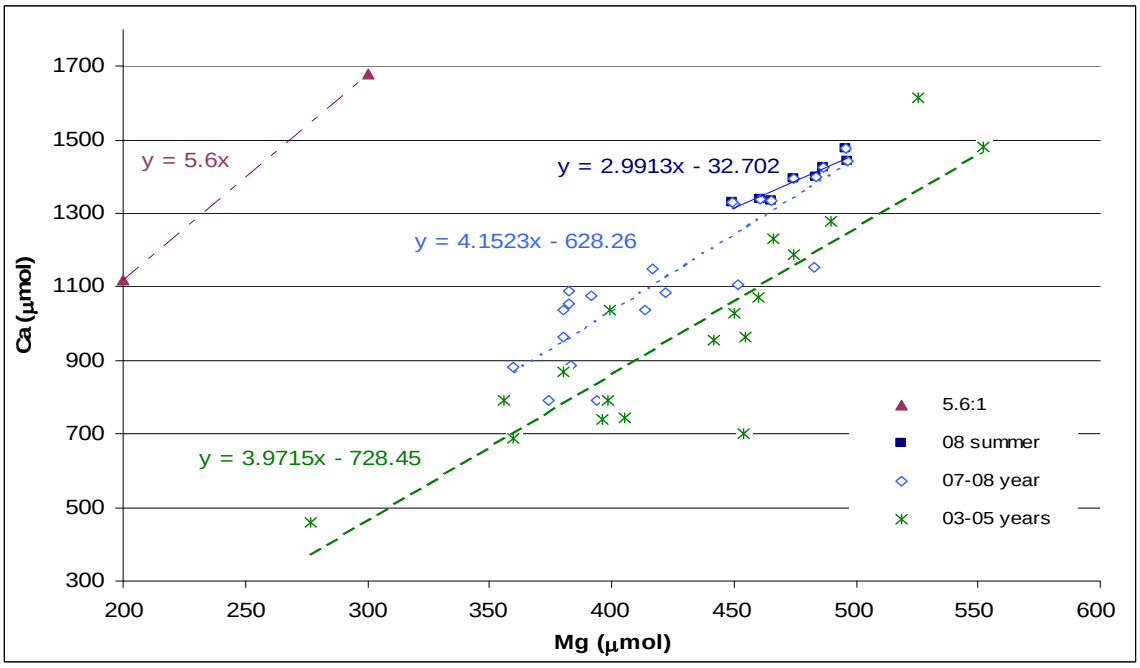

Figure 34: Shallow Groundwater Ca^{2+} vs. Mg^{2+} (µmol), combined data-sets from 2003-2005 and 2007 -2008 and molar ratio of added calcite.

4.2.2.1 Ca^{2+}/Mg^{2+} Ratio

Ca^{2+}/Mg^{2+} ratios were also examined to look for evidence of Ca^{2+} or Mg^{2+} from calcite addition. These same Ca^{2+} concentrations and Mg^{2+} concentrations from the 2003-2005 (Bloom 2005) and 2007-2008 data-sets were combined to examine if the added calcite influenced Ca^{2+}/Mg^{2+} ratios in the groundwater (Figure 34).

The micromolar Ca^{2+}/Mg^{2+} ratios from the 2003-2005 groundwater data reflect Ca^{2+} and Mg^{2+} concentrations which were quite variable with amounts of Ca^{2+} and Mg^{2+} which were both higher and lower than those observed in 2007-08. Though the 2007-2008 shallow groundwater data is quite similar in slope to the previous data, it is consistently offset, in the direction of more Ca^{2+} per unit Mg^{2+}. As more Ca^{2+} per unit Mg^{2+} was introduced during the limestone addition, this offset may be interpreted to be addition signal.

4.2.2.2 Ca^{2+}/Mg^{2+} Mixing Equation

The treatment limestone was acid digested and dissolved Ca^{2+} and Mg^{2+} determined. The ratio of Ca^{2+}/Mg^{2+} in the added calcite was 85:15 mol % or $5.6Ca^{2+}:1Mg^{2+}$. The field gathered groundwater Ca^{2+}/Mg^{2+} ratios were used in a simple mixing equation, since new Ca^{2+} and Mg^{2+} were added without new water volume. An average Ca^{2+}/Mg^{2+} molar ratio of 2.69 is calculated for 2007-08, and a Ca^{2+}/Mg^{2+} molar ratio of 2.28 is calculated for 2003-05. A small proportion of the 5.6 Ca^{2+}/Mg^{2+} treatment limestone would shift the groundwater Ca^{2+}/Mg^{2+} average ratio from 2.28 to 2.69.

$$2.69\ (1) = 5.6\ (x) + 2.28(1-x) \qquad \text{(EQ. 12)}$$

In the mixing equation 12, an x-value of 0.12 would satisfy this equality, meaning the added limestone would therefore contribute a small but measurable 12% of the moles of Ca^{2+} and Mg^{2+} measured in the groundwater.

4.2.3 Sulfate Concentration

Shallow groundwater sulfate concentration decreases slightly in January of 2007 (Figure 20). Although decreasing sulfate concentration would be expected as an indicator of bacterial sulfate reduction, it is not a unique indicator. Dissolved sulfate concentrations could decline through either an increase in a removal process or a decrease in a supply process. Removal processes include dilution, bacterial sulfate reduction, or increased secondary mineral formation and supply processes include FeS_2 weathering (abiotic or biotic) or secondary mineral weathering.

The small decrease in sulfate concentration during the winter months co-occurs with a high oxidation-reduction potential (0.70 to 0.85V as E_H) and the low temperature (~3°C), meaning this trend is unlikely to have been caused by a bacterial process. Although reducing microenvironments may certainly exist within the organic carbon fill, the shallow groundwater on the whole does not reflect an environment where activity via this mechanism would be favorable.

Of the other mechanisms described which could account for the small sulfate decrease, some support is found for dilution, which would be expected to act upon SO_4^{2-} as the water saturated zone increased. Additionally, inclusion within or sorption to Fe^{3+}/Al^{3+} secondary minerals would decrease dissolved sulfate concentration.

4.2.4 Proton Activity vs. Sulfate

Proton activities within the shallow groundwater decrease in May of 2008, 9 months after the limestone containing reactive fill is placed. As changes in sulfate concentration removal were small, sulfate concentrations were compared to pH, to in order to rule out the alternative that a decrease in FeS_2 weathering could account for the increased pH observed in the summer months of 2008. Stoichiometric amounts of sulfate and proton are initially generated during the oxidative dissolution of FeS_2, either a.) $1SO_4^{2-}$: $1\ H^+$ in the abiotic mechanism (EQ 1) or b.) $1\ SO_4^{2-}$: $8\ H^+$ in the biotic mechanism (EQ 4). Equations 1 and 4 are repeated from the introduction.

$$FeS_2 + 7/2\ O_2 + H_2O \rightarrow Fe^{2+} + 2\ SO_4^{2-} + 2\ H^+ \qquad \text{(EQ 1)}$$

$$FeS_2 + 14\ Fe^{3+} + 8H_2O \rightarrow 15\ Fe^{2+} + 2SO_4^{2-} + 16H^+ \qquad \text{(EQ 4)}$$

The proton activity (log aH^+, where $aH^+ = 10^{-pH}$) and the sulfate concentration (log mol) in the shallow groundwater are shown Figure 35. With dissolution of FeS_2 as their common source, sulfate and proton concentrations should co-vary, although proton is clearly more reactive than sulfate. Some proportionality between the two FeS_2 weathering products remains; here measured proton activities are 1-2 orders of magnitude lower than that of sulfate. Also shown is the proton measured as a percent of the predicted proportional amount (for simplicity, assuming a 1:1 relation under abiotic conditions). From July 2007 through April 2008, the amount of proton generated by pyrite oxidation which is accounted for in the pH measurement ranges between ~2 and 16% (average 8.9%) of the predicted amount, and is quite variable. The remaining ~98 to 84% appear lost to weathering and subsequent reactions.

During the May-October 2008 period, proton concentration decreases more than sulfate concentration does, and the percent of SO_4^{2-} proportional proton drops 10-fold, to below 1%

(average 0.67%). The sulfate concentration changes much less than the proton activity does; making it possible to infer that supply of these ions from FeS_2 weathering has been fairly constant.

The large change in proton concentration with small change in SO_4^{2-} concentration then suggests proton removal by an added component or new process, at least during the last 6 months of observation. New processes would include carbonate dissolution, as supported by an increased concentration in Ca^{2+}. Presumably, some carbonate species are present at this time period; but at pH 4.8, would be present largely in the form of H_2CO_3. The decline in proton concentration may be caused by a consumption of proton to convert limestone CO_3^{2-} to H_2CO_3.

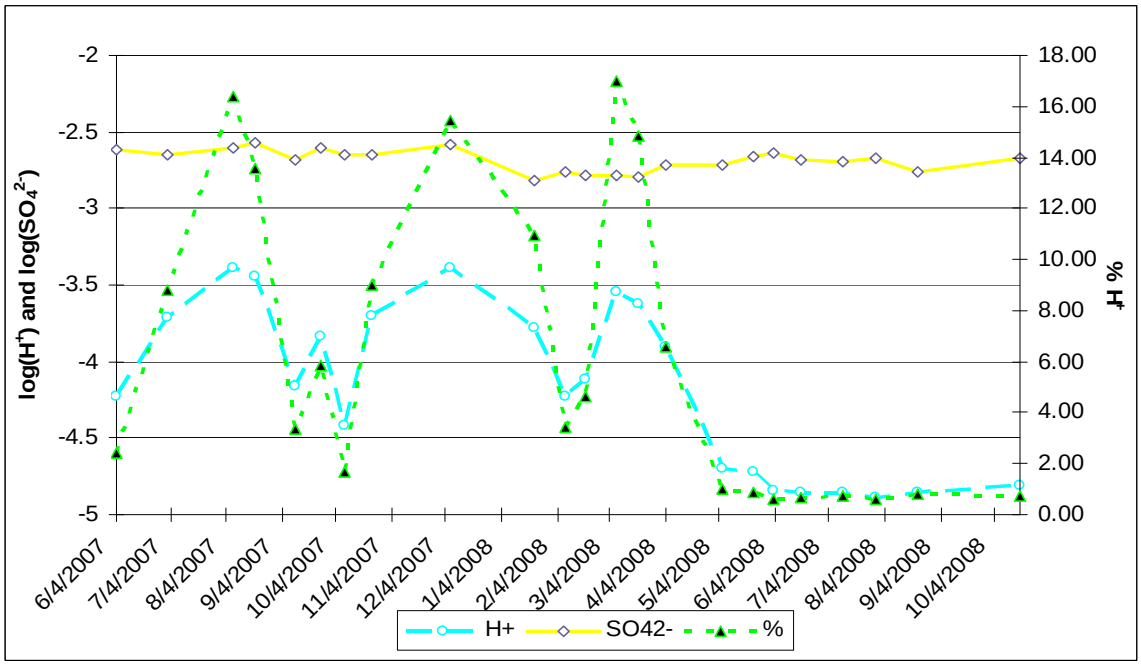

Figure 35: Log H^+ and SO_4^{2-} concentrations and % of H^+ proportional to SO_4^{2-}.

4.2.5 Trace Metal Concentrations

The geochemical parameter which was most responsive to the addition of the reactive fill was the concentration of dissolved trace metals (Figure 17).

These trace metals are plotted as a percent of their June-June yearly average concentrations shown in Figure 36. This approach highlights which metals are most changed,

since this ranking may be helpful to identify which mechanisms (e.g., bacterial sulfate reduction, Fe^{3+} hydrolysis, etc.) are most responsible. The shallow groundwater pH is also shown since it is related to the change.

In the early months of the experiment, trace metal concentrations are variably high and seem unaffected by the treatment addition. From May to October of 2008, the behavior of the trace metals clearly shifts and concentrations are decreased and stabilized. During this 6 month time period, the "acid" cations Fe^{tot} and Al^{3+} are decreased the most; at -85.6 and -40.5% of their average June-June concentrations, respectively. The next most affected are the divalent metals Cu^{2+} and Zn^{2+}, at -32.3 and -16.8% decreased. Mn^{tot} concentrations are not affected.

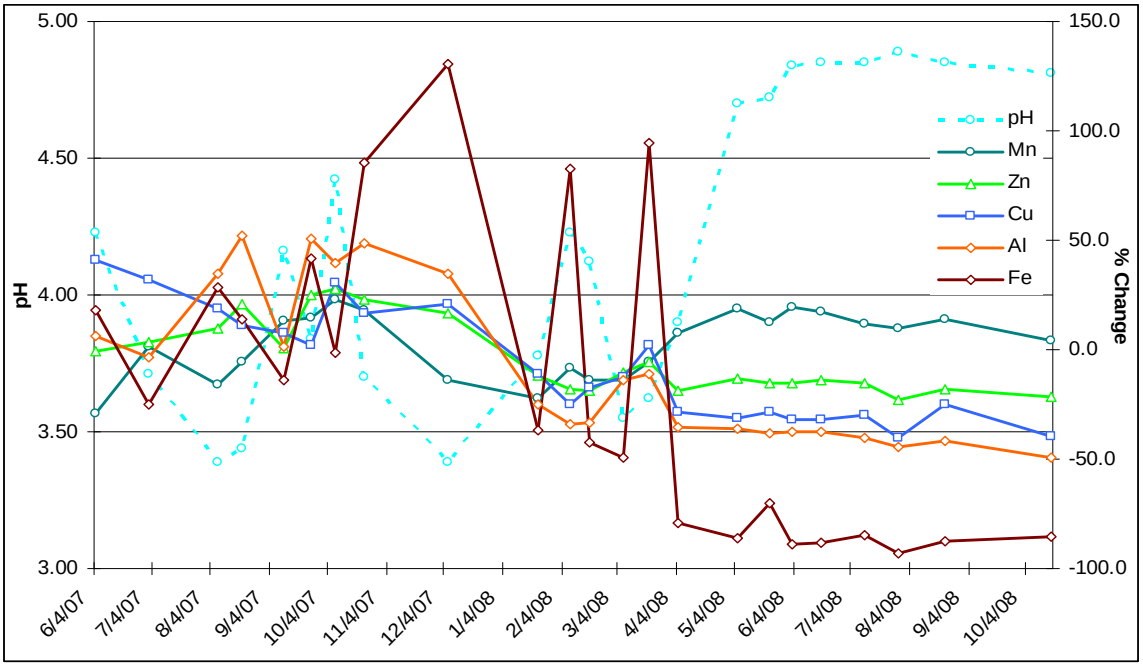

Figure 36: Shallow Groundwater: % Change in Trace Metals and pH

From this data, the ranking of elements most affected is:

$$Fe^{tot} > Al^{3+} > Cu^{2+} > Zn^{2+}$$

Because the intended treatment mechanism of sulfidogenesis ($Me^{2+} + S^{2-} \rightarrow MeS_2$) acts upon divalent metals, the decrease in Al^{3+} suggests influence of an additional or alternate mechanism.

Table 16: MeS_2 Complexation Constants

Me^{2+}	pK
Cu^{2+}	37.5
Pb^{2+}	29.4
Zn^{2+}	26
Fe^{2+}	17
Mn^{2+}	15

Sillén and Martell (1964) compiled the aqueous complexation constants for S^{2-} and Me^{2+}, reporting the values for experiments at 25°C as projected to zero ionic strength, as shown in Table 16. The less soluble sulfides have higher pK values (lower K values for dissociation). The thermodynamically favored removal of trace metals by combination with biogenic S^{2-} would rank:

$$Cu^{2+} > Pb^{2+} > Zn^{2+} > Fe^{2+} > Mn^{2+}$$

The profile of metals which would be most removed under a reducing, sulfide-generating scenario does not align with the changes observed in the shallow groundwater. For example, if dissolved metals were combining with biogenic S^{2-}, a larger removal of Cu^{2+} than Fe^{2+} would be expected.

However, even when sulfidogenesis has been successfully stimulated and identified in AMD characterization and treatment studies, only partial agreement with the thermodynamic prediction is observed. Rowe *et al*. noted preferential removal of CuS over FeS in a sulfidogenic biofilm, even when Fe^{tot} concentrations were greater than those of Cu^{2+} (2007). Johnson *et al.* were able to selectively recover Zn^{2+} as ZnS from an acidic waste while leaving Fe^{tot} in solution (2006). Benner *et al* (1999 and 2002) confirmed active bacterial sulfate reduction by measuring evolving S^{2-} concentrations and recovering amorphous FeS precipitates, although they also observed major Al^{3+} removal, a change not anticipated under influence of bacterial sulfate reduction alone. In other studies, removal of several or all trace metals is near-complete and no preference can be determined for the metal counter-ion to biogenic S^{2-} by comparing percent removal (Waybrant *et al* 2002, Ludwig *et al* 2002). Adherence to the thermodynamically

predicted profile for metals removal under bacterial sulfate reduction is only sometimes observed, limiting mechanistic explanations.

The relatively larger decreases in the acid sensitive cations Fe^{tot} and Al^{3+} suggest removal by a pH dependant secondary mechanism at work in this study. In this case, Fe^{3+} and Al^{3+} hydrolysis is the next most likely mechanism, in response to rising pH; above ~pH 3.5 for Fe^{3+} and above ~pH 5 for Al^{3+} (EQs 3 and 7). This has been described as a secondary mechanism in other experiments which sought to treat AMD affected groundwater with organic and inorganic carbon mixes where the proportion of limestone was high (Carrera *et al.*, 2001, Bolzicco *et al.*, 2004). Though iron precipitation in response to limestone addition is generally viewed as unfavorable in reducing AMD treatment systems, some designs make use of this reaction (Rötting *et al.*, 2008, Caraballo *et al.*, 2009).

Smaller amounts of Cu^{2+} and Zn^{2+} were absent from solution. The hydrolysis of these metals is not expected until higher pH (>6), suggesting a different removal mechanism for these metals. The minor removal of Cu^{2+} and Zn^{2+} may be caused by co-precipitation or sorption onto newly formed Fe^{3+}/Al^{3+} oxides.

4.3 Mechanisms of Change

4.3.1 Hydrolysis and Secondary Mineral Formation

Iron and aluminum secondary minerals (oxides and sulfates) are ubiquitous at acid mine drainage sites, where they provide a local sink for mobile metals and sulfate and provide mineral buffering with their dissolution and precipitation.

As a first approximation of whether conditions were favorable for the formation of iron and aluminum secondary minerals within the shallow groundwater, their saturation indices (SI) over time were calculated using the USGS equilibrium software PHREEQCi.

A saturation index is the ratio of the ion activity product to the solubility product,

$$SI = \frac{IAP}{K_{sp}}$$

where the ratio equals 1, the activity of the ions measured in solution is equal to the amount present at saturation, and the water is at equilibrium with respect to that mineral. Strongly positive values indicate a solution is oversaturated with respect to the mineral and it is thermodynamically predicted to precipitate, negative values indicate a solution is undersaturated with respect to that mineral and it is thermodynamically predicted to dissolve. Since PHREEQCi bases these predictions on thermodynamic data, the more stable crystalline phase is favored, although first occurrences in the field may be amorphous.

Models which predict saturation states under equilibrium conditions are used with an understanding that these conditions may never be reached, and that kinetics and transport are not accounted for. However, for reactions which are less limited kinetically (rate constants on timescales of minutes, days, etc.), these predictions are useful.

4.3.1.1 Iron Saturation Indices and Speciation

Some of the well characterized secondary Fe^{3+} (hydr)oxides and hydroxysulfates are listed below in Table 16, along with general outlines of the environments in which they form, as discussed by Bigham *et al.* (1996) and Hammarstrom *et al.* (2005). These minerals may form together as mixtures where the environmental conditions overlap. The Fe^{3+} oxides include the metastable ferrihydrite or amorphous $FeOH_3$ which may occur with, and will transition to, goethite (α-FeOOH) and eventually hematite (Fe_2O_3) with time. In waters rich in both Fe^{3+} and SO_4^{2-}, Fe^{3+} sulfates may be formed. These include the metastable schwertmannite (which may transition to jarosite and goethite), and more commonly in low pH (<3) environments, the Fe^{3+} sulfate Jarosite ($(K)Fe_3(OH)_6(SO_4)_2$).

Table 17: Iron Secondary Mineral Formation Overview

Mineral	Bigham (1996)	Hammarstrom (2005)
Jarosite $(K)Fe_3(OH)_6(SO_4)_2$	---	$1.5 > pH > 3$ $[SO_4^{2-}] > 3000mg/L$
Schwertmannite $(Fe_8O_8(OH)_6SO_4)$	$2.8 > pH > 4.5$	$3 > pH > 4$ $[SO_4^{2-}]$ ~1000mg/L
Ferrihydrite $(Fe_5HO•4H_20)$	$pH > 6.5$	$pH > 5$, $[SO_4^{2-}] < 1000mg/L$
Goethite α-FeOOH	---	pH variable $[SO_4^{2-}] < 1000mg/L$

The shallow groundwater saturation indices for representative Fe^{3+} secondary minerals, including amorphous iron oxide ($Fe(OH)_3$), goethite (α-FeOOH), and K-Jarosite ($KFe_3OH_6(SO_4)_2$) are shown in Figure 37. During all times in this study, the shallow groundwater is supersaturated with respect to the Fe^{3+} mineral goethite, representing that an Fe^{3+} mineral is generally supersaturated in the shallow groundwater. The water is also approaching equilibrium with amorphous $Fe(OH)_3$ and K-Jarosite. Since an Fe^{3+} mineral like goethite is strongly supersaturated in this groundwater interval, it seems that the measured changes in Fe^{tot} concentration, pH, and redox are not large enough to be reflected in any change on this mineral's saturation index.

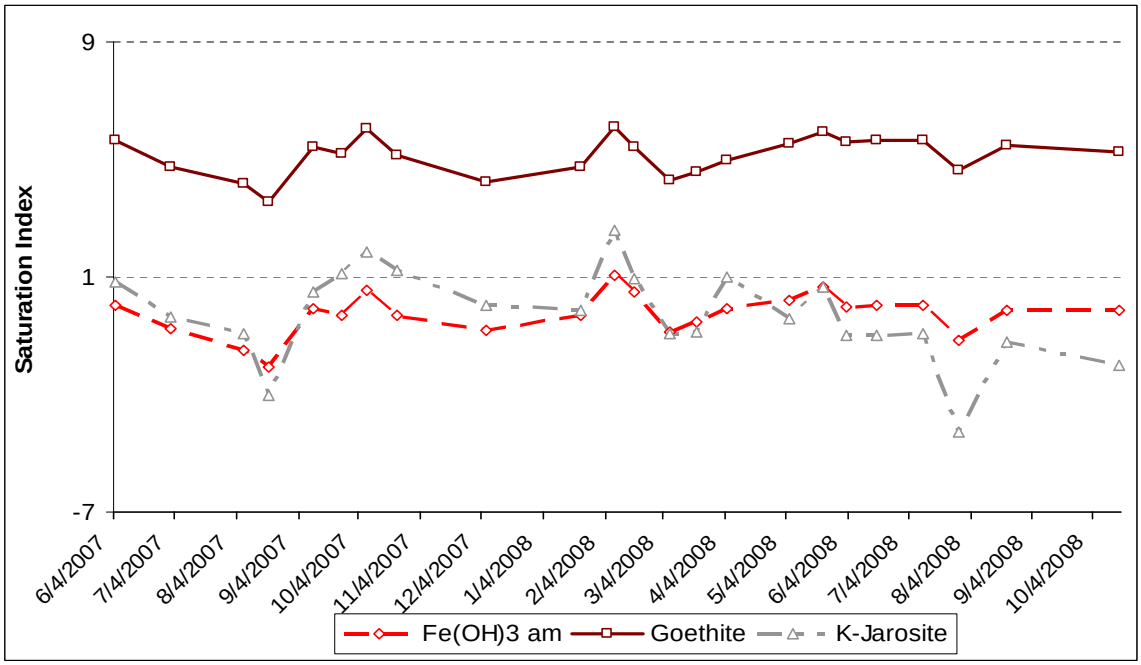

Figure 37: Shallow Groundwater Saturation Indices for Fe^{3+} Secondary Minerals

To form these minerals, some of the Fe^{total} must be present as Fe^{3+}; however that proportion was unmeasured during this study. The amount of Fe^{3+} measured in previous studies was variable; though in the data compiled by Bloom for the same monitoring well port, the Ferrozine-determined Fe^{3+} concentration ranged from 61 to 113% of ICP-determined Fe^{tot} (2005).

In place of measured of Fe^{3+} and Fe^{2+} concentrations, modeled concentrations are given by dividing dissolved Fe^{total} concentration via the solution speciation in PHREEQCi. The measured Fe^{tot}, °C, pH and redox potentials along with the other elemental data were used as input. Since iron oxidation occurs on the order of minutes-hours-days; (Johnson 1986, Schwertmann 1991) the use of the thermodynamic model PHREEQCi to predict a kinetically "fast" reaction is reasonable.

Predicted Fe species concentrations range over several orders of magnitude; hence they are reported in log (mol) units (Figure 38). Roughly equivalent amounts of Fe^{3+} and Fe^{2+} are predicted from June 2007 through February 2008, similar to what had previously been measured. As redox potential climbs in early winter 2008, Fe^{3+} iron is predicted to be up to 10^4 times more common than ferrous iron. This condition continues from February through June, with Fe^{3+} and

Fe^{2+} predicted to return to equivalent amounts during the later summer, accompanied by a decline in redox and Fe^{tot} values.

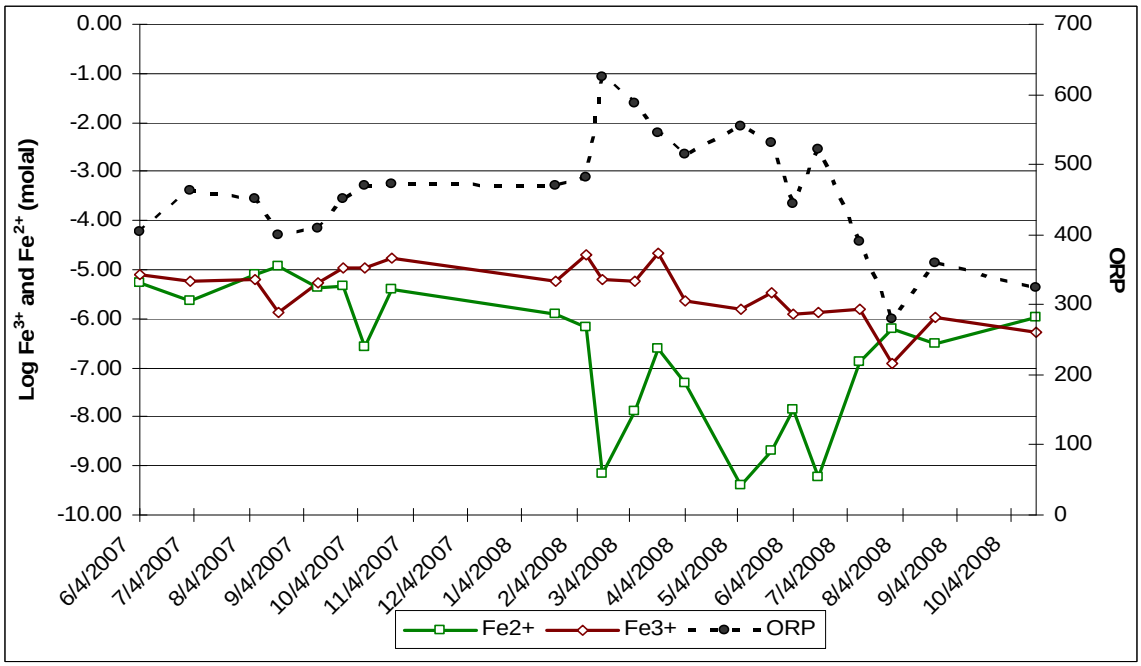

Figure 38: Modeled Fe^{3+} and Fe^{2+}concentrations shown with measured ORP.

According to this model, it is likely that under initial conditions at least some Fe^{tot} is present as Fe^{3+}, and during the months preceding and co-occurring with the decreased trace metal concentrations, most iron is predicted to be present as Fe^{3+}. The ratio of Fe^{3+} to Fe^{2+} is highest from February through June, leading and overlapping with the period of the decreased metals concentrations. As pH rose above 4 during the late spring and summer months, Fe^{3+} would have been unstable with respect to $FeOH_3$ and therefore prone to hydrolysis. Hydrolysis in turn would have decreased pH, possibly detracting from the anticipated pH rise from carbonate dissolution.

The sequential rise and then fall of redox potential, oversaturation of Fe^{3+} minerals, modeled predominance of dissolved Fe^{3+} in the winter and spring, and the near absence of dissolved Fe^{tot} in the summer months all support presence of Fe^{3+} and subsequent removal to a solid phase.

4.3.1.2 Aluminum Saturation Indices

The common Al^{3+} minerals include amorphous $Al(OH)_3$, gibbsite ($Al(OH)_3$) and the Al^{3+} sulfate alunite ($KAl_3(OH)_6(SO_4)_2$). Unlike Fe^{tot}, Al^{3+} is neither redox sensitive nor likely to be removed via sulfidogenesis. However, aluminum solubility is pH sensitive, with the more toxic inorganic monomeric Al^{3+} species losing solubility over a pH window of 4.5 to 5.0 pH (Klöppel *et al.*, 1997).

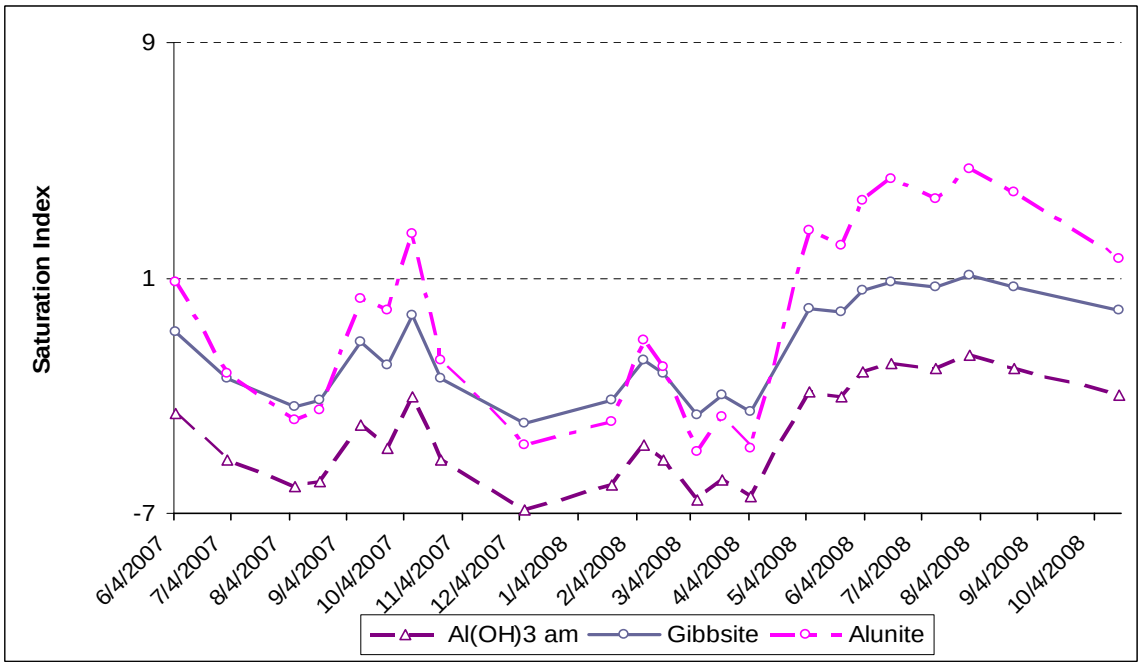

Figure 39: Shallow Groundwater Saturation Indices for Al^{3+} Secondary Minerals

The saturation indices of representative aluminum secondary minerals are shown in Figure 39, including the oxides amorphous $Al(OH)_3$ and crystalline gibbsite ($Al(OH)_3$) and the aluminum sulfate alunite ($KAl_3(OH)_6(SO_4)_2$). As with the iron minerals, field occurrences are often amorphous. For the aluminum minerals, the solution approaches equilibrium with respect to gibbsite for the first time during the summer months of 2008.

Although the decrease in Al^{3+} is relatively smaller than the decrease in Fe^{tot} (40% vs. 85% in Figure 36), Al^{3+} was present at greater initial concentration than iron, meaning more

moles of Al^{3+} are absent from solution. It is possible Al^{3+} was removed as an Al-hydroxide, Al-hydroxysulfate or a mixed Fe^{3+}/Al^{3+} hydroxide precipitate.

Decreases in Al^{3+} concentration with increasing pH and dilution were also previously noticed at the stream confluence site B2 by Bloom (2005, p. 68) where an increase from pH ~3.5 to ~5.8 corresponded with an Al^{3+} decrease from 700 to 100 µg/L. Additionally, other Davis Mine researchers have detected or suggested the presence of Al^{3+} secondary phases, such as the hydrated Al^{3+} sulfate hydrobasalunite [$Al_4(SO_4)(OH)_{10}\cdot 12\text{-}36H_2O$)] (Cerato 2003).

Lastly, in consideration of the potential dissolution and precipitation of iron and aluminum secondary minerals, though the solubility of iron and aluminum oxides have been discussed separately, mixed Al^{3+} and Fe^{3+} oxides and sulfates may occur. Up to 30 mol% Al^{3+} for Fe^{3+} substitution is observed in natural goethites (Schwertmann, 1991) and mixed Fe^{3+}/ Al^{3+} oxide precipitates have been formed in AMD hydrolysis experiments (Rötting *et al.*, 2008, Gibert *et al.*, 2005).

In this field experiment where both dissolved Fe^{3+} and Al^{3+} concentrations were decreased, if solid phases were formed, it then seems reasonable to expect some mixing in the precipitates. Additionally, the steady pH recorded during the summer of 2009 ranged from 4.7 to 4.8, a pH value that is greater than the Fe^{3+} hydrolysis pH range of 2.5 to 3.5 and but less than the Al^{3+} hydrolysis pH of 5.0.

4.3.2 Cu^{2+}, Zn^{2+} and Pb^{2+} sorption to Hydrous Ferric Oxide

With relatively large decreases in dissolved Fe^{3+} and Al^{3+} concentrations most likely related to precipitation of hydroxides, the relatively smaller decreases in dissolved Cu^{2+} and Zn^{2+} are then most likely related to sorption onto the newly formed oxides. The hydrolysis of Cu^{2+} and Zn^{2+} themselves is not predicted to occur until a pH > 6, making removal via that mechanism unlikely.

Cu^{2+} and Zn^{2+} have a good affinity for pH dependent sorption to the surface of various Fe^{3+} hydroxides. Studies of the oxide-rich streambed sediments taken from Davis Mine have found the majority of the easily and moderately-easily displaced sorped metals on these iron sediments to be Pb^{2+}, Cu^{2+} and Zn^{2+} (Russell 2003, Keddie 2007).

During this experiment at Davis Mine, both Fe^{3+} and Al^{3+} were removed from solution. For Fe^{3+} or Al^{3+} rich AMD waters undergoing hydrolysis, Lee *et al.,* (2002) found similar sorption edges of Cu^{2+} and Zn^{2+} onto either solid phase, suggesting Al^{3+} substitution into an Fe^{3+} does not significantly alter the characteristics of Fe^{3+} solids as sorbents.

The USGS model PHREEQCi was again used, this time to semi-quantitatively describe sorption to a hypothetical Fe^{3+} hydroxide surface. In this case, the default hydrous ferric oxide surface was used, since it is compositionally appropriate. Solution compositions were: summer average 2007 (June to Oct), summer average 2008 (May to Oct) and whole year 2004 (May to May; n=7) were inputted into the solution spreadsheet, along with field measured pH and redox potential as pe. Though fresh hydroxides are thought to be formed in 2008, 2007 and 2004 are shown to describe sorption to any pre-existing weathering product hydroxide. Surface reactions were calculated using the Dzombec and Morel simplified two layer model. The Davis Mine input solutions and hydrous ferric oxide surface were allowed to equilibrate in a batch reaction step; the predicted occupancy of the strong site is reported.

The distribution of species modeled as sorbed to the “strong” adsorption sites on hydrous ferric oxide are reported as fraction of the total available sites for 2004, 2007 and 2008 (in Figures 40, 41, and 42). In this prediction Fe^{tot} and Al^{3+} are not represented among the sorbed cations because they are assumed to be in a new solid phase.

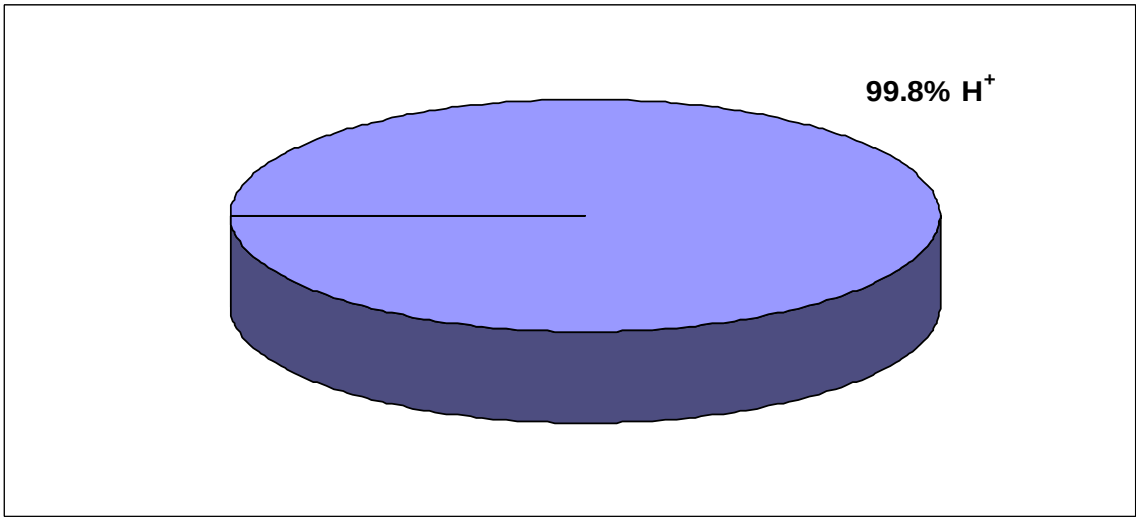

Figure 40: Site Occupancy on Hydrous Ferric Oxide: 2004 (pH 3.09, without Pb^{2+})

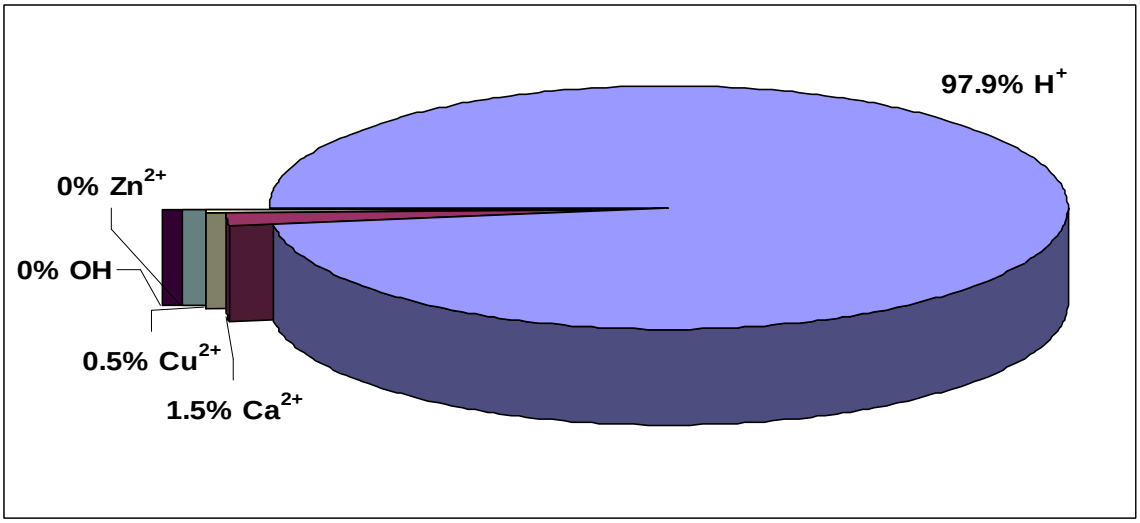

Figure 41: Site Occupancy on Hydrous Ferric Oxide: 2007 (pH 3.73, without Pb^{2+})

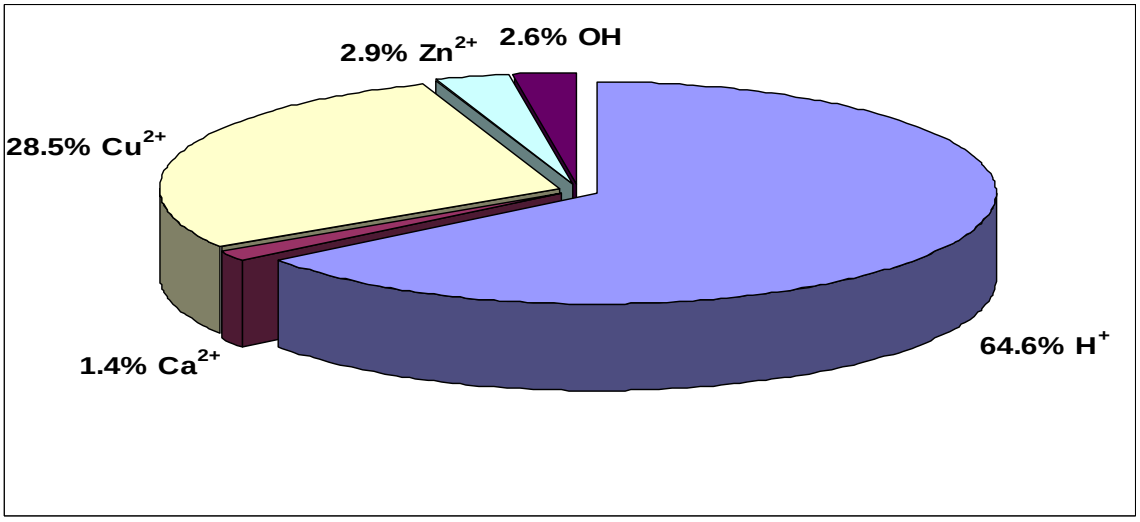

Figure 42: Site Occupancy on Hydrous Ferric Oxide: 2008 (pH 4.81, without Pb^{2+})

At the lower pH conditions representative of 2004 and summer 2007 (3.1 and 3.7) , the majority of surface sites on any pre-existing hydrous ferric oxide would be filled with proton (H^+); 99.8 and 97.9% respectively. For data year 2004-05, it is an entirely protonated surface. In summer 2007, where pH values were slightly higher, the surface remains almost entirely saturated with proton, and a small fraction of sites available to sorb trace Ca^{2+} and Cu^{2+}.

During the strongly oxidizing conditions measured in late winter and spring months of 2008, we hypothesize that new Fe^{3+} hydroxide was formed. At the pH measured during the summer months of 2008 (~4.8), the model predicts an iron oxide surface which is only partially filled by proton, at 64.6%. On this newly formed oxide, the majority of available sites are filled by Cu^{2+} (28.5%), followed by Zn^{2+} (2.9%) and then Ca^{2+} (1.4%). Preferential removal of Cu^{2+} over Zn^{2+} is modeled in this sorption scenario.

Preferential removal of Cu^{2+} over Zn^{2+} was observed in field study, with Cu^{2+} decreased 32% relative to the yearly average and Zn^{2+} 16%. The observed changes in Cu^{2+} and Zn^{2+} align with those expected in the sorption scenario descriptively and semi-quantitatively.

The modeling of sorbed metals on a hydrous ferric oxide surface is repeated incorporating average concentrations of dissolved Pb^{2+} from the partial data (Figures 43, 44, 45). During this study period, dissolved Pb^{2+} was frequently below detection limit, so the average of data points above detection limit were used to calculate the average for the input solutions.

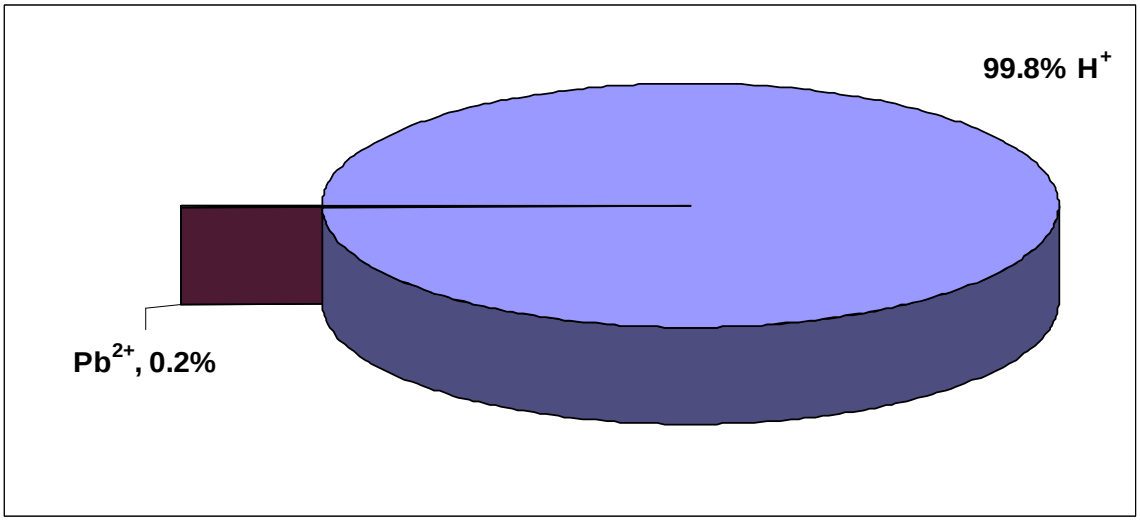

Figure 43: Site Occupancy on Hydrous Ferric Oxide: 2004 (pH 3.09, with Pb^{2+})

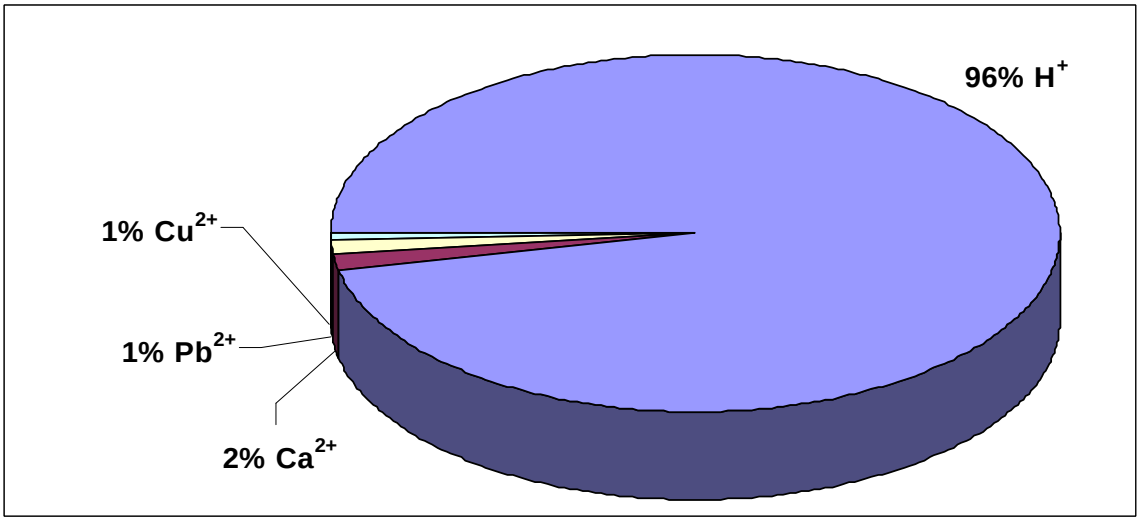

Figure 44: Site Occupancy on Hydrous Ferric Oxide: 2007 (pH 3.71, with Pb^{2+})

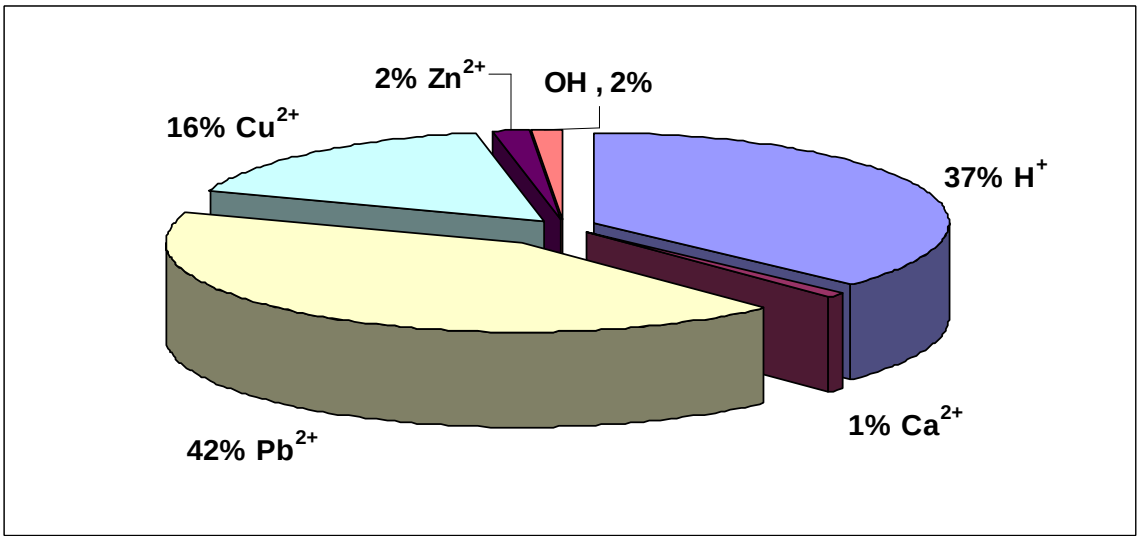

Figure 45: Site Occupancy on Hydrous Ferric Oxide: 2008 (pH 4.81, with Pb^{2+})

In the low pH conditions of 2004 and summer 2007, the surface of any pretreatment hydrous ferric oxide would be again almost entirely lined with proton, at 99.8% and 96% proton filled, similar to the models without Pb^{2+}. The remainder of sites in 2007 would have been taken up by trace Pb^{2+}, Cu^{2+} and Ca^{2+}.

In 2008, at pH 4.8, the surface of any iron oxide formed would be largely taken up by Pb^{2+} (42%), followed by proton (37%), Cu^{2+} (16%) and Zn^{2+} (2%). When Pb^{2+} is accounted for in the solution, it takes up the largest portion of the surface, and the relative amount of sorped Cu^{2+} is smaller (28.5% vs. 16%). With Pb^{2+} included, the affinity of trace metals for an oxide surface is $Pb^{2+}>Cu^{2+}>Zn^{2+}$. The shallow groundwater's frequently below-detection limit levels of dissolved Pb^{2+} found may in fact be due to the affinity of Pb^{2+} to sorb to solid phases.

The formation of iron or aluminum oxides would remove major Fe^{3+} and Al^{3+} from solution, and these oxides would carry along with them minor sorped Pb^{2+}, Cu^{2+} and Zn^{2+}. Regardless of whether dissolved Pb^{2+} is included in the calculation, the modeled trace metals removal via sorption onto hydrous ferric oxide is compatible with the measured changes in Cu^{2+} and Zn^{2+}.

4.4 Comparisons and Contexts

4.4.1 Graphical and Statistical Comparisons with Previous Years

The groundwater data collected in 2007-08 is compared to the data collected in 2003-04 and 2004-05; these data-sets overlap in such a way that data for four summer periods (April through October of 2003, 2004, 2007 and 2008) is available. The shallow groundwater (Well 8 Port 3) was the only sampling interval to show evidence of change, so data from this location is the focus of interpretations. The behavior over time of sensitive parameters pH, ORP, trace metals, Ca^{2+}, and SO_4^{2-} are shown in Figures 46-54. Accompanying these plots are the results of a 2-tailed Student's T Test for difference of means (Tables 17-20). Significant differences which have less than a 0.10 chance of being randomly caused are shown in italics, those which have less than a 0.05 chance are shown in bold.

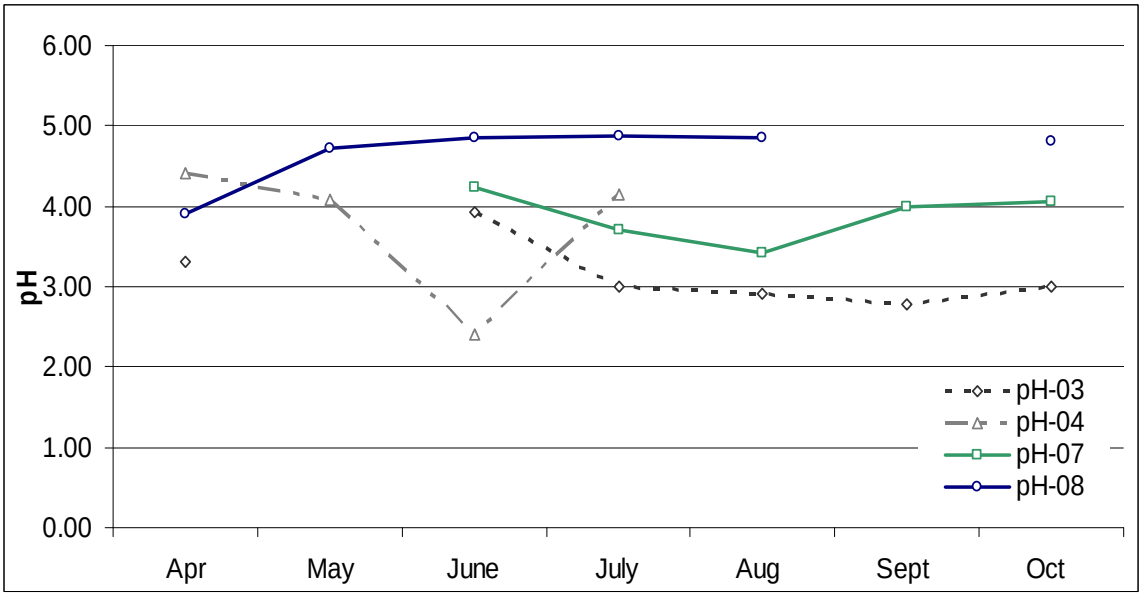

Figure 46: Summer pH; 2003, 2004, 2007 and 2008

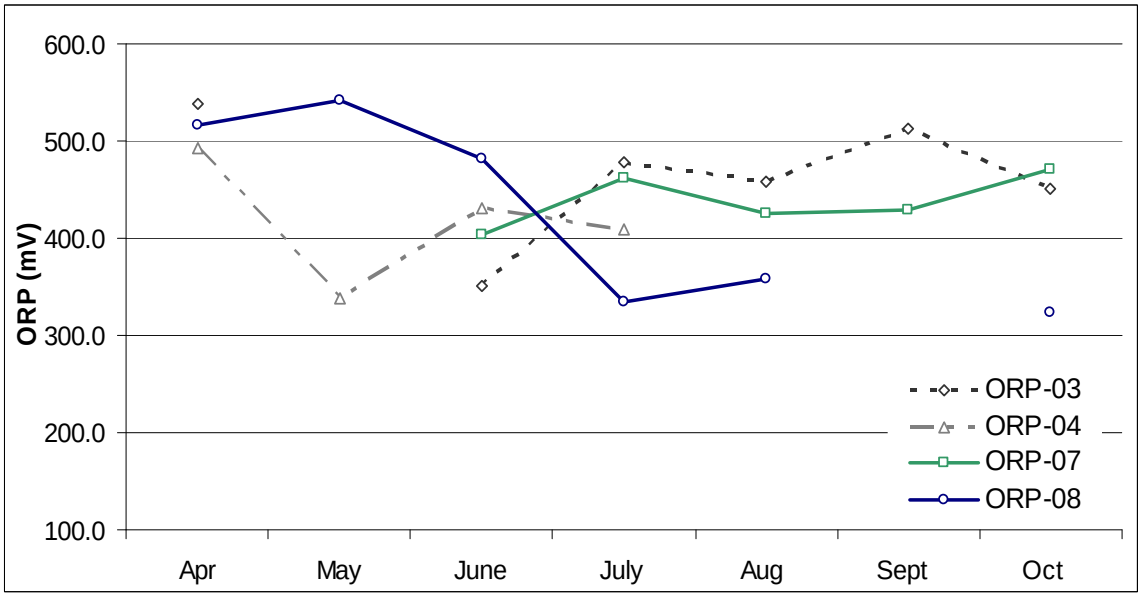

Figure 47: Summer ORP; 2003, 2004, 2007 and 2008

Table 18: p values: ORP and pH

	ORP	pH
2004 vs.		
2003	0.84	0.64
2007 vs.		
2003	0.66	**0.03**
2004	0.80	0.52
2008 vs.		
2003	0.36	**0.02**
2004	0.44	0.39
2007	0.29	0.11

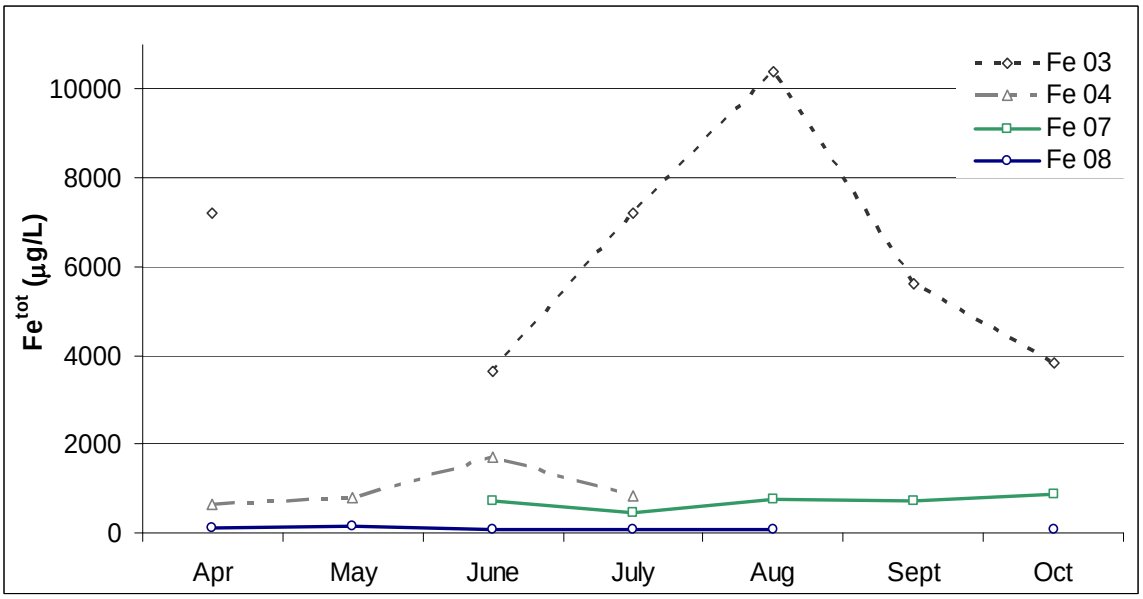

Figure 48: Summer Iron Concentrations; 2003, 2004, 2007 and 2008

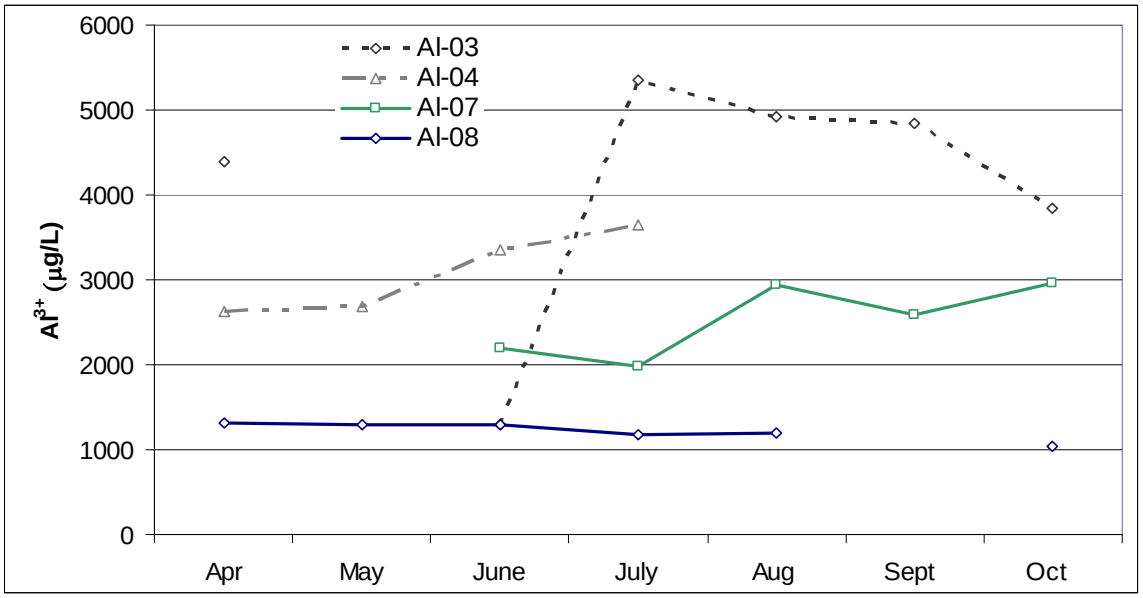

Figure 49: Summer Aluminum Concentrations; 2003, 2004, 2007 and 2008

Table 19: p values: Fe^{tot} and Al^{3+}

	Fe^{tot}	**Al^{3+}**
2004 vs.		
2003	*0.08*	0.75
2007 vs.		
2003	**0.01**	0.10
2004	0.26	0.11
2008 vs.		
2003	**0.01**	**0.01**
2004	**0.00**	**0.00**
2007	**0.00**	**0.02**

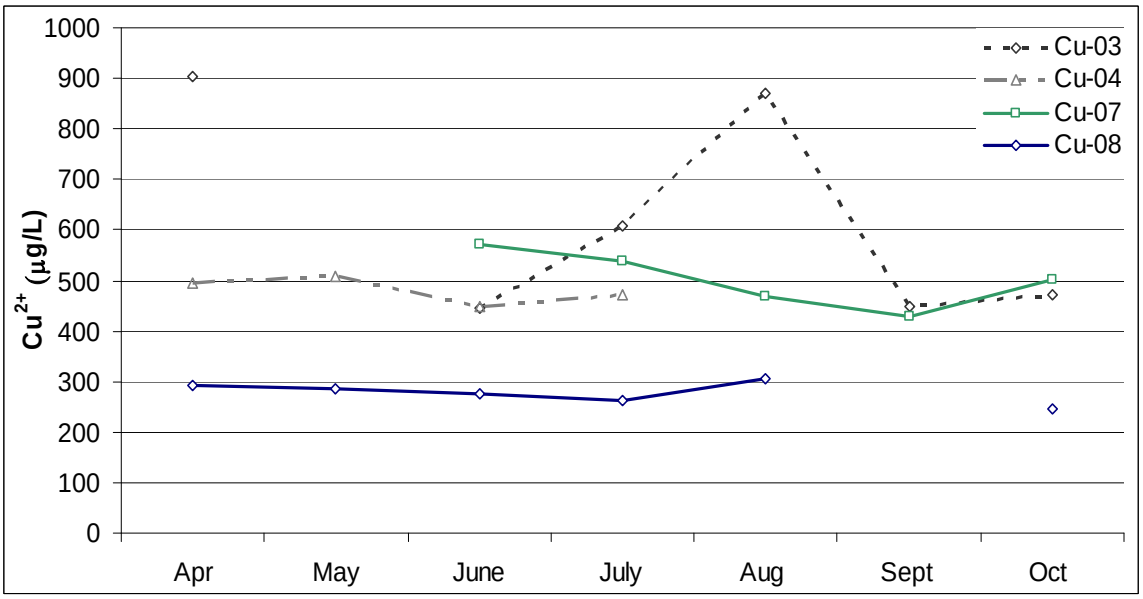

Figure 50: Summer Copper Concentrations; 2003, 2004, 2007 and 2008

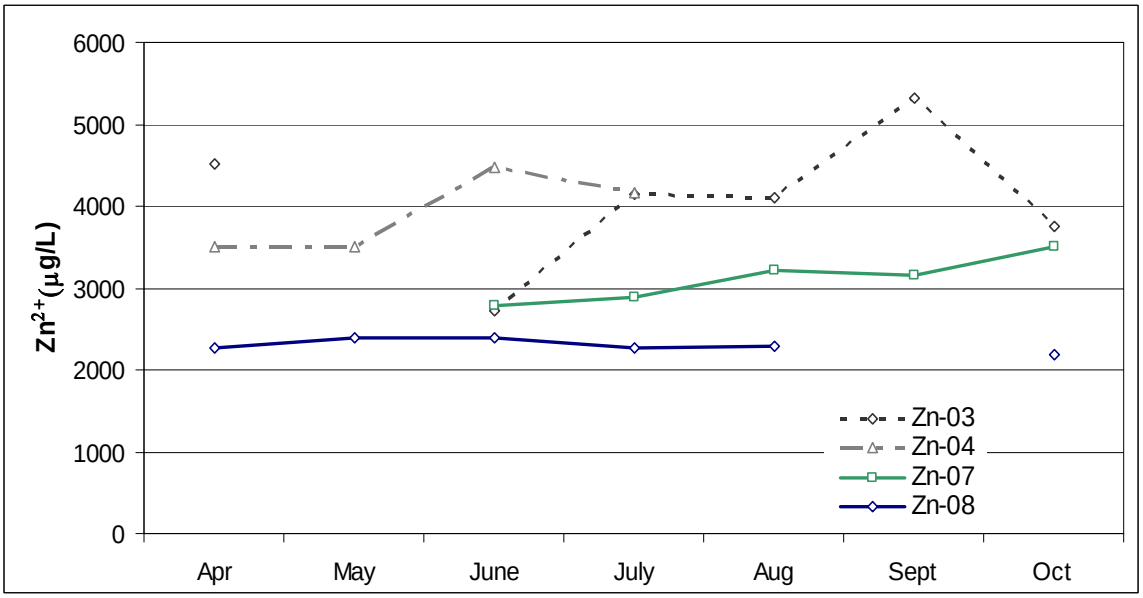

Figure 51: Summer Zinc Concentrations; 2003, 2004, 2007 and 2008

Table 20: p values: Zn^{2+} and Cu^{2+}

	Zn^{2+}	**Cu^{2+}**
2004 vs.		
2003	0.79	0.27
2007 vs.		
2003	*0.08*	0.50
2004	*0.09*	0.19
2008 vs.		
2003	**0.01**	**0.01**
2004	**0.01**	**0.00**
2007	**0.03**	**0.00**

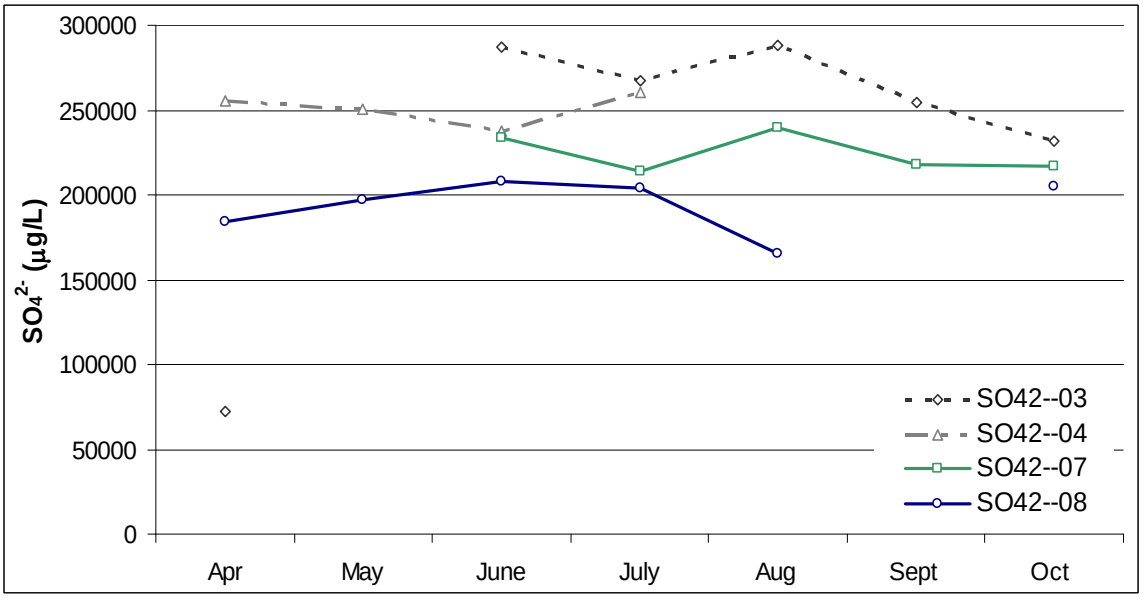

Figure 52: Summer Sulfate Concentrations 2003, 2004, 2007 and 2008

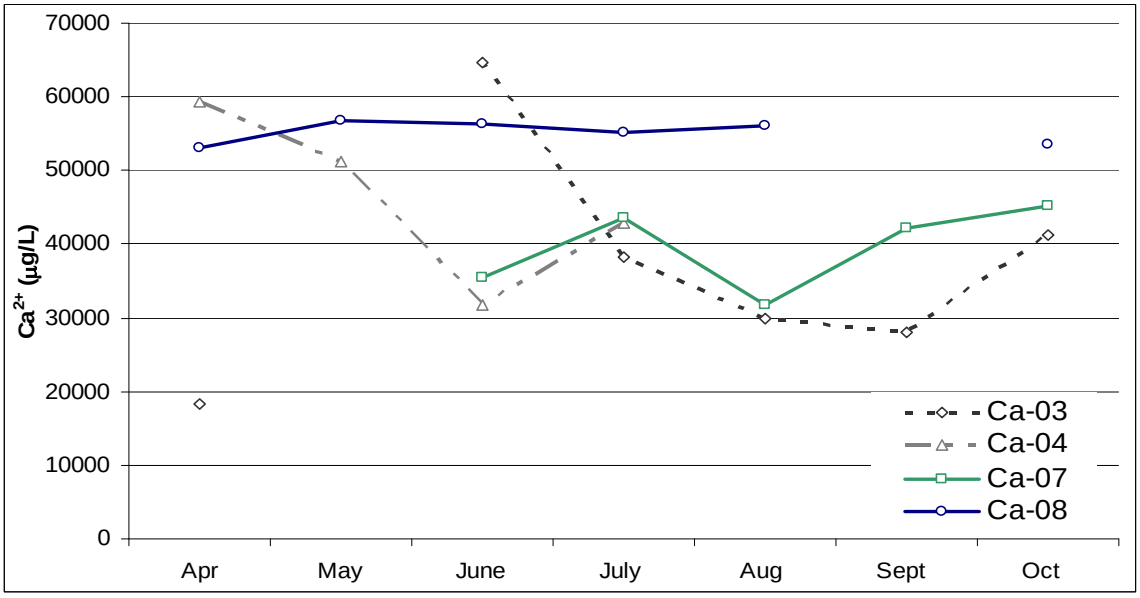

Figure 53: Summer Calcium Concentrations 2003, 2004, 2007, and 2008

Table 21: p values: Ca^{2+} and SO_4^{2-}

	Ca^{2+}	**SO_4^{2-}**
2004 vs.		
2003	0.86	0.61
2007 vs.		
2003	0.92	0.00
2004	0.40	0.45
2008 vs.		
2003	*0.09*	0.42
2004	0.25	**0.01**
2007	**0.02**	0.14

The composition of the shallow groundwater of the four summers compared (2003, 2004, 2007 and 2008) may be grouped by pH; lowest in 2003, intermediate in 2004 and 2007 and highest in 2008.

During the summer of 2003, low pH (~3) and high Fe^{tot} (up to ~10,000 μg/L) concentrations were recorded in the shallow groundwater. The differences in pH and Fe^{tot} between summer 2003 and summers 2004 and 2007 constitute a large natural variation in background levels of these species at the site. For this reason, comparisons of the values of Fe^{tot} and pH measured 2008 to those of summer 2003 are made with reservation that any differences do not necessarily result from limestone/organic carbon treatment. As would be expected, the high iron values recorded in the summer of 2003 are significantly different from other years. Though the concentrations of Zn^{2+}, Cu^{2+}, Al^{3+} and SO_4^{2-} are higher in 2003 than other years, they are not significantly so. The low pH, high Fe^{tot}, high SO_4^{2-} conditions observed in summer 2003 indicate that pyrite oxidation was particularly well-established that year.

Shallow groundwater sampled during summers of 2004 and 2007 was more moderately acidic and values of pH and ORP were similar between the two years. Shallow groundwater concentrations of Fe^{tot}, Al^{3+}, Cu^{2+}, Ca^{2+} and SO_4^{2-} measured during summers of 2004 and 2007 were also similar, though 2007 had less Zn^{2+}. Overall, these two summers present an appropriate baseline for which to compare the groundwater composition resulting from treatment in 2008.

Shallow groundwater taken during the summer of 2008 has the most consistent and highest pH on record for that monitoring well, with significantly less acidity than was found in 2007. Values of ORP decline (towards more reducing) in 2008 but are within the variance of previous years. Groundwater concentrations of Fe^{tot}, Al^{3+}, Cu^{2+} and Zn^{2+} values are all significantly lower than those measured in 2004 and 2007 (at p=0.00, 0.00, 0.01 and 0.00 for each metal vs. 2004 and at p=0.00, 0.02, 0.03 and 0.00 for each metal vs. 2007). The concentrations of SO_4^{2-} are also significantly lower than 2004 values and Ca^{2+} concentrations are also higher than

2007. The treated groundwater sampled during the summer of 2008 had demonstrably lower concentrations of trace metals than did similar periods in 2004 and 2007; a difference we believe is in response to calcite and organic carbon addition.

4.3.2 Process comparison with Surface water

Concentrations of dissolved species in the shallow groundwater and nearest surface water can differ naturally by an order of magnitude, responding appreciably to submeter variation in pH and redox conditions. Here, Fe^{tot} concentrations from the shallow groundwater (W8P3) and a surface water (Eff W) ~5m to its west (and within 1 vertical m piezometrically) are shown. Slightly more acidic and oxidizing conditions in the stream water translate to at times a 10x higher iron concentration than the nearest groundwater.

For this reason, comparisons with the surface water system are done more in terms of processes than concentrations.

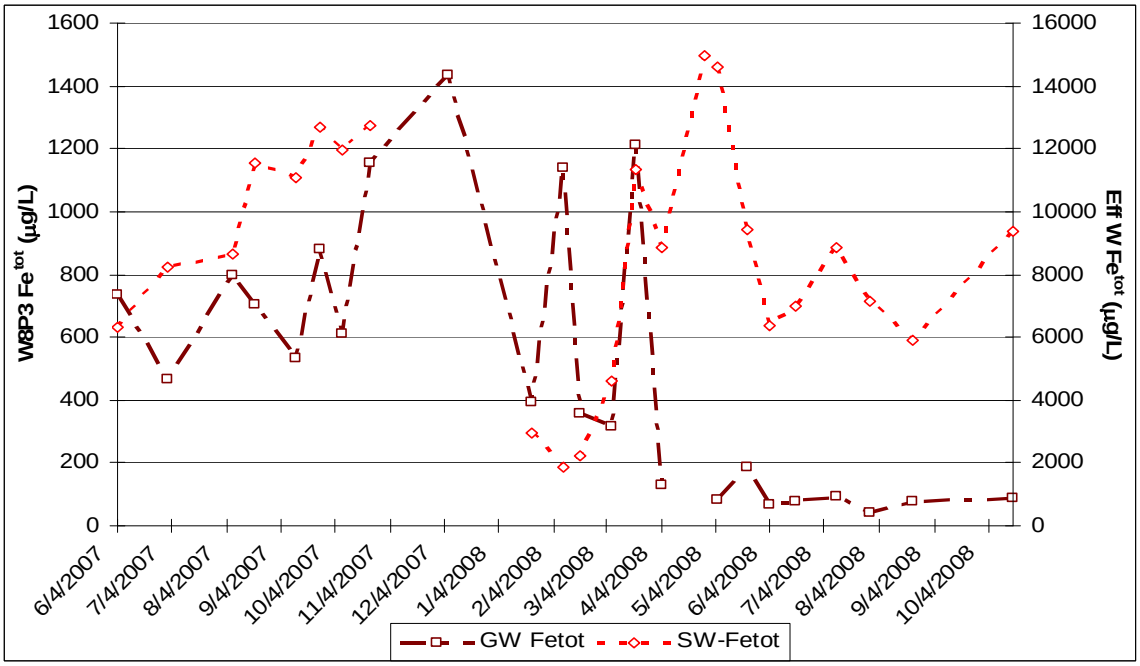

Figure 54: Shallow Groundwater and Surface water Fe^{tot}

The decreasing concentration in groundwater Fe^{tot}, as discussed previously, is likely occurring via hydrolysis and precipitation of solid phase iron. Trends in Fe^{tot} in the surface water

are not necessarily similar to those in groundwater, but both systems are influenced by the processes of iron oxidation and hydrolysis. Process level comparison will allow us to describe the untreated acidic and oxidizing surface water nearby.

A reasonable approach to group processes within the surface water system is to examine both conservative and more reactive elements. Within surface waters at acid mine drainage sites, major elements often reflect larger scale weathering processes whereas trace elements reflect in-stream processes (McKnight and Bencala, 1990). Surface water's Fe^{tot} profile may diverge from those of more conservative elements because it can be removed from solution to form the ochreous streambed lining, which in turn can dissolve and supply Fe^{tot} back to the stream if a flush of lower pH water passes through.

Stream water concentrations of Ca^{2+}, Si, Mn^{tot} and Fe^{tot} are shown in Figures 55 and 56 and their correlations in Tables 21 and 22. Calcium and Silicon are selected to display conservative behavior; change in response to dilution, and Mn^{tot} and Fe^{tot} to display reactive behavior; change in response to (or in control of) pH/redox changes. Stream water pH and ORP (shown in Figures 22 & 23) were quite acidic (~3.3) and oxidizing (~0.7V).

At the East branch of the effluent creek, Ca^{2+} and Si react similarly over the year ($r = 0.85$), whereas Fe^{tot} and Mn^{tot} do not ($r = -0.61$). It appears that Mn^{tot} is instead behaving as a conservative ion, as is suggested by the very good similarity to Ca^{2+} and Si (Mn^{tot} vs. Ca^{2+}, $r = 0.95$, Mn^{tot} vs. Si, $r = 0.91$).

Iron concentration here is generally low and anti-correlates with the conservative ions, suggesting continuous removal processes or disequilibrium with the iron hydroxide stream-bed. The iron oxide coating in the effluent's East branch is not well developed; stream bed sediments have visible ochreous coating but are not well cemented each to the other. It may be the Fe^{tot} is either being removed to form this coating or that relatively less coating is available to supply Fe^{tot} to the stream. During the spring melt dilution, Fe^{tot} increases in concentration. Although this

observation seems counter-intuitive, dissolved Fe^{tot} may also be contributed by solid phases in the streambed to the stream if the saturation state of these oxides is decreased.

At the West branch of the effluent creek, Ca^{2+} and Si again react similarly over time (r = 0.95), as does Mn^{tot} (Mn^{tot} vs. Ca^{2+}, r = 0.96, Mn^{tot} vs. Si, r = 0.90). Now surprisingly, Fe^{tot} now follows the conservative profile during the fall and winter of 2007, correlating loosely to Mn^{tot} (r = 0.57). If the Fe^{tot} profile resembles those of the conservative elements, it may be that dissolved Fe^{tot} is in equilibrium with the iron oxide streambed and is not being actively removed from solution. The spring melt corresponds to a peak in Fe^{tot} concentration at this sampling location as well.

pH and redox conditions between the two branches of the effluent stream are quite similar; the east branch has an average pH of 3.36 and ORP 484mV (0.69V) and the west branch has an average pH of 3.26 and an average ORP of 478mV (0.69V). The differences in bed properties may have an influence on the Fe^{tot} profile's from the two stream braids.

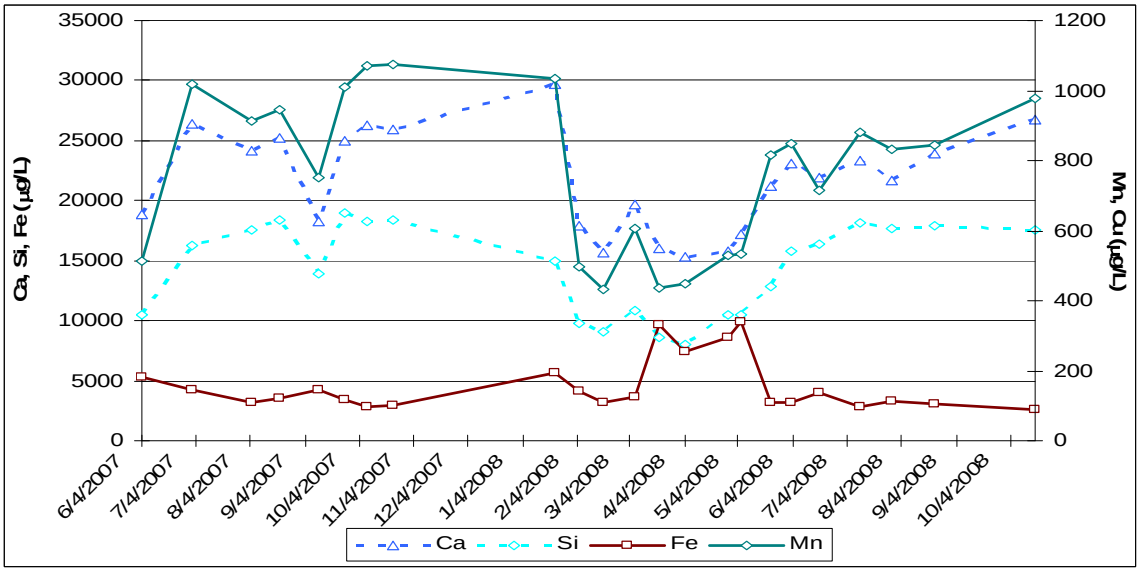

Figure 55: Effluent East: Ca^{2+}, Si, Mn^{tot} and Fe^{tot} Concentrations

Table 22: Effluent East: Ca^{2+}, Si, Mn^{tot} and Fe^{tot} Correlations

r	Ca	Si	Mn	Fe
Ca	1	0.85	0.95	-0.58
Si		1	0.91	-0.67
Mn			1	-0.61
Fe				1

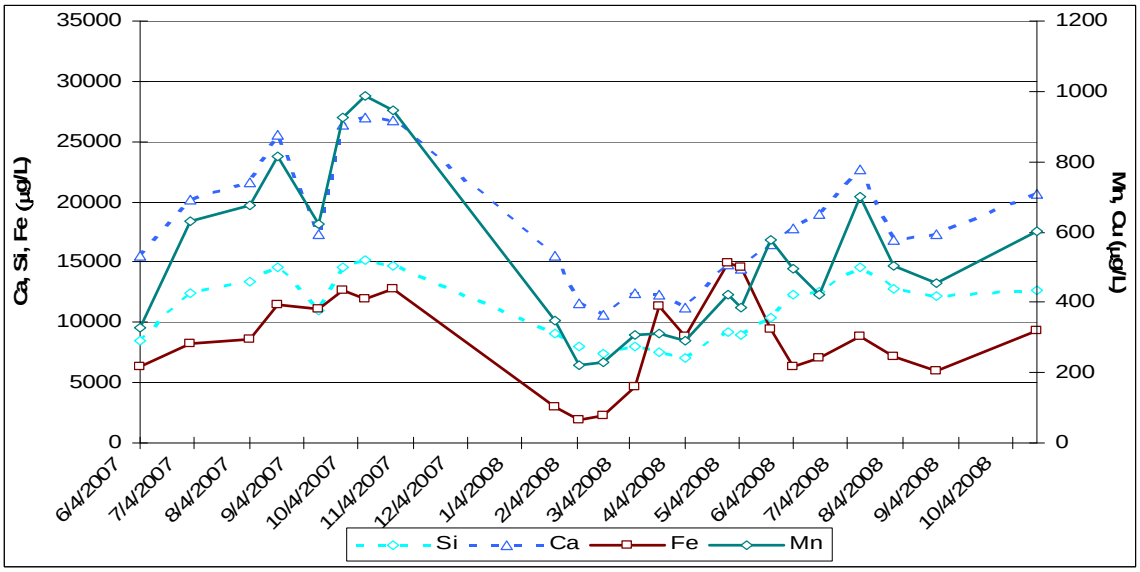

Figure 56: Effluent West: Ca^{2+}, Si, Mn^{tot} and Fe^{tot} Concentrations

Table 23: Effluent West: Ca^{2+}, Si, Mn^{tot} and Fe^{tot} Correlations

R	Ca	Si	Mn	Fe
Ca	1	0.95	0.96	0.48
Si		1	0.90	0.37
Mn			1	0.57
Fe				1

The dissolution and precipitation of iron oxides is likely to be controlling the dissolved concentration of Fe^{tot} within the effluent stream. The pH range of the stream is consistently close to the Fe^{3+} hydrolysis pH, meaning small changes can dissolve and precipitate the iron oxide lining of the stream-bed. It is likely that the increased volume at spring melt disrupted the processes responsible for maintaining low iron concentrations, and fairly consistent pH/redox conditions were maintained by internal iron-oxide buffering. The increasing volume at spring melt is inferred based on several previous years of discharge measurements, discharge at a nearby USGS gauge, the synchronous decreasing concentrations of several conservative ions, and the observational evidence of the snow-pack disappearance.

This increase in volume has a destabilizing effect on whatever in-stream processes control the dissolved iron concentration, since iron concentration increase 3-5 fold during the month of April.

Though pH and redox conditions vary between the stream water and groundwater systems, iron oxide formation and dissolution respond to, or buffer pH in each water.

Table 24: Comparison of Processes in Groundwater and Surface water

	Groundwater			**Surface water**			
Observation	Shallow	Intermediate	Bedrock	East	West	Seep	**Suggested Process**
Seasonal Variation In Major Cations	muted	muted	muted	clear	clear	clear	Conservative transport and dilution
Seasonal Variation In Sulfate	muted	muted	muted	clear	clear	clear	Conservative transport and dilution
Increasing Spring Iron Concentrations	---	----	----	clear	clear	-----	Iron hydroxide dissolution and precipitation
Decreasing Spring Iron Concentrations	clear	----	----	----	----	----	Iron hydroxide precipitation
Decreasing Spring Trace Metal Concentrations	clear	----	----	----	----	----	Sorption

4.4.2 Comparisons to other Organic Carbon and Limestone Permeable Reactive Barriers

The results of this study can be compared to findings from other comparable AMD studies (Table 24) in which a mixture of organic and inorganic carbon (limestone) was used to promote sulfidogenesis and sequester metals.

Data is listed from three major field installations of organic carbon permeable reactive barriers. Complementary laboratory studies (in the case of Waybrant *et al*., 1998 and Gibert *et al*., 2002) are also given, as well as a variant study by Rötting (2008).

The first major field trial of a sulfate-reducing PRB was installed at the Nickel Rim (ON, Canada) in 1995. Metal-laden, near-neutral mine drainage leaching from the mine-site impoundment was intercepted in the subsurface before reaching a neighboring water body; this was done so the large dissolved iron concentrations would not generate acidity upon surfacing via hydrolysis reactions. A trench 20m long by 3.5m deep by 4m wide was excavated and filled with the mixture of ~50% organic carbon and ~50% pea gravel. Pea gravel was added to improve permeability, and hydraulic conductivities were confirmed to be higher within the reactive fill than within the surrounding aquifer. Extensive monitoring at the site has measured decreased concentrations of Fe^{tot}, Zn^{2+}, Cu^{2+}, Al^{3+} and SO_4^{2-} in water exiting the PRB. The near complete removal of Al^{3+} suggests another mechanism in addition to BSR is involved. Bacterial sulfate reduction was determined to be responsible for the observed changes, as supported by; the generation of alkalinity, removal of SO_4^{2-} and parallel generation of S^{2-}, decreased redox potential, increasing bacterial cell counts, and the lowered concentrations of divalent metals. The authors additionally point out that barrier performance varies, with most volume passing through the “fast” flow path. (Benner *et al*., 1998, 1999, 2002).

The Nickel Rim site shares tailings mineralogy with Davis Mine (i.e. Fe-Cu-Zn sulfide) and the sites experience a similar temperate climate with winter snow-pack formation. The Nickel Rim study used a reactive fill containing 49% organic carbon from biodegraded sources

(compost and leaf mulch), an example followed in this study. In contrast, the input groundwater plume at Nickel Rim is mildly acidic to near-neutral before treatment and not strongly oxidizing, with the dissolved iron load present as Fe^{2+}. A large proportion of pea gravel (50%) was also used to encourage groundwater passage through the PRB, and PRB width was such that groundwater experienced a long residence time (60-164 days), considerations which were not addressed for this Davis Mine study. The more neutral and transitional redox condition of the untreated groundwater allowed for more ready establishment reducing conditions adequate for sulfate-reducing bacteria to utilize the carbon source.

Based on the success at Nickel Rim, another PRB was installed in a former ore-concentrating industrial site in Vancouver (BC, Canada) contaminated with Cu^{2+}, Cd^{2+}, Co^{2+}, Ni^{2+}, and Zn^{2+} (Ludwig *et al*., 2002). Based on physical constraints, a PRB placement was chosen mid-gradient in the contaminated plume, with effluent measurements representing a mixed signal of treated water and recharge of shallow groundwater containing fresh oxidation products. A trench 10m long by 2.5m wide by 6.5m deep was installed with the mixture of 15% organic carbon, 1% $CaCO_3$, and 84% pea gravel. Again, pea gravel was added to create a PRB more hydraulically conductive than the surrounding aquifer; and the relatively high proportion was chosen due to the high hydraulic conductivity of the tidal, deltaic deposits in which the PRB was placed. After 21 months of observation, decreased concentrations of the divalent metals (Cu^{2+}, Cd^{2+}, Co^{2+}, Ni^{2+}, and Zn^{2+}) were measured. Sulfate concentrations were not reported, although those of sulfide (S^{2-}) were. Also measured were a slightly increased pH, decreased redox potential, and the generation of S^{2-}, confirming metals sequestration via sulfidogenesis.

The Vancouver PRB was installed to treat metal-laden groundwater and similarly placed mid-gradient within an effluent plume. The Vancouver PRB used a relatively small proportion of organic carbon (15% leaf compost) so that enough coarse material could be included to encourage groundwater passage through it. Bacterial sulfate reduction was successfully stimulated with a lower proportion of organic carbon. Additionally, the estimated residence time (6 days) within

the PRB was much shorter than those at Nickel Rim and bacterial sulfate reduction was established. Again, initial conditions in the groundwater were circumneutral and less oxidizing, allowing for an easier transition to a reducing environment.

A third and more experimental PRB was placed in the valley of the Agrio river, which drains the Aznalcóllar mine-site (Sevilla, Spain) following a breach in the tailings impoundment dam (Carrera *et al*., 2001 and Bolzicco *et al*., 2004). Given the more severe acidity (pH <4), higher proportions of $CaCO_3$ were used (50-66%) along with an organic carbon source. The PRB consisted of three sections; Module 1 containing 50% $CaCO_3$, 30% municipal compost, and 20% sewage sludge, Module 2 containing 50% $CaCO_3$, 50% compost, and trace Fe^0 (to initiate Fe^{3+} reduction), and Module 3 containing 66% $CaCO_3$ and 33% compost. Sections were each 30m long by 1.40m wide by 3-7 m deep. Permeability in Module 1 was effectively too low and no data is reported. Interestingly, hydraulic conductivities in Modules 2 and 3 are lower than that of the aquifer, and the retardation of water is inferred by the increased hydraulic gradient within the PRB. After passing through the PRB, effluent water contained decreased concentrations of proton acidity, Al^{3+}, Zn^{2+}, and Cu^{2+} (Fe^{tot} not reported). The authors suggest that bacterial sulfate reduction does not take place in this barrier, based on the scant presence of sulfate-reducing bacteria cell counts and continued high concentration of sulfate. Instead, the formation of iron and aluminum (oxy)hydroxides during pH increase is cited as the more likely removal mechanism, and the authors note trace concentrations of Cu^{2+} and Zn^{2+} in these precipitates. They also suggest that sorption to the organic matter itself may remove some metals from solution.

The water treated by the permeable reactive barrier at the Rio Agrio was fairly acidic (pH ~4) shallow groundwater more similar to that found at Davis Mine study site. Although iron speciation or concentration was not reported, the inclusion of zero-valent iron in Module 3 indicates the authors anticipated some iron present as Fe^{3+}. Under initial conditions, both the groundwaters at Davis Mine and at the Rio Agrio site were more acidic and oxidizing than other

waters successfully treated by sulfidogenic organic-carbon based PRBs and in both cases a higher proportion of $CaCO_3$ (50 to 66%) was added in attempt to neutralize adequately in order for treatment to proceed through sulfidogenesis. The Rio Agrio's high flow, low-residence time conditions (2 days) may be similar to hydrogeologic conditions at Davis Mine. At the Rio Agrio site, the effective mechanism of treatment was suggested as Fe^{3+} and Al^{3+} hydrolysis for the decreased concentrations of Al^{3+}, H^{+}, Cu^{2+} and Zn^{2+}, as is also suggested in this thesis study.

In complementary column studies, Waybrant *et al.* (2002) were able to parallel the bacterial sulfate reduction observed in the field at Nickel Rim in the laboratory. pH, redox, and dissolved metal concentrations of the input water were all similar to field values, as was the residence time within the material. Metals removal was quite high, up to 98%. Again, bacterial sulfate reduction was confirmed by measuring decreased concentrations of sulfate, decreasing redox potential (E_H), and generation of S^{2-}. Similarly, in column studies done in support of the research at Aznalcóllar, Gibert *et al.* (2003) found that using their reactive mixture was capable of removing appreciable acidity, Fe^{tot}, Al^{3+}, Cu^{2+}, Zn^{2+}, and As. SEM/EDS examination of the brown/grey precipitates found them to be composed of Al^{3+}, Fe^{tot}, S and O with trace Cu^{2+}, Zn^{2+} and As. XRD analysis was precluded due to poor crystallinity. Under higher flow rates (>0.1m/d) and with more acidic (pH 3) input water, they found that the major mechanism of removal was in this case formation of Fe/Al (oxy)hydroxides and hydroxysulfates. Cation exchange experiments found Cu^{2+} and Zn^{2+} to be found mainly (~70-100%) in the exchangeable fraction, followed by the Fe/Mn (oxy)hydroxide fraction (10-20%). Via this secondary treatment mechanism, major removal of Fe^{tot} and Al^{3+} is accomplished by Fe/Al (oxy)hydroxide formation and minor removal of Cu^{2+} and Zn^{2+} mostly by co-precipitation / sorption to the hydroxide phases.

Lastly, in an attempt to better understand metals removal via (oxy)hydroxide formation, the column study by Rötting *et al.* (2008) input synthetic AMD under low pH, oxidizing conditions. Acid mine drainage is commonly treated via such alkalinity treatment systems as

anoxic limestone drains (ALD) and successive / reducing alkalinity producing systems (SAPs or RAPs), however some complications are encountered when the limestone grains' surfaces are passivated (coated) by Fe^{3+} hydroxides and gypsum, slowing dissolution. To lessen this problem, this experiment tried dispersing the limestone grains (25%) through an organic carbon substrate (wood chips, 75%) to lessen clogging. Since redox measurements stayed above +195 mV (E_H), the organic carbon substrate in this case was not used for its reducing equivalents. Their experiments resulted in pH increase and near complete removal of Al^{3+}, Fe^{3+}, Pb^{2+} and Cu^{2+}, with minor removal of Zn^{2+} and SO_4^{2+}. Scanning Electron Microscopy/Electron Dispersive Spectroscopy analyses found iron (oxy)hydroxides (with a composition between schwertmannite ($(Fe_8O_8(OH)_{5.5}(SO_4)_{1.25}$) and goethite ($\alpha$-FeOOH)) replacing the $CaCO_3$ grains at the column input, followed spatially by aluminum precipitates (with a composition between basalunite ($Al_4(SO_4)(OH)_{10}\bullet 5(H_2O)$)and aluminum hydroxide ($AlOH_3$) combined with gypsum ($CaSO_4\bullet 2H_2O$) coating the calcite grains. The authors hypothesize that limestone dissolution raises pH, inducing hydrolysis, which decreases pH, and then enhances $CaCO_3$ dissolution; a cycle which promotes more complete limestone dissolution.

The column studies are cited to clarify and support mechanistic explanations for permeable reactive barrier performance. The column-study by Gibert *et al.* was able confirm metals-removal via a Fe^{3+}/Al^{3+} hydrolysis mechanism (by detecting Al, Fe, S and O in precipitates), and because the input water was similarly acidic (pH 3), the retention time was short (11 hrs) and the removal of Fe^{tot}, Al^{3+}, Zn^{2+}, and Cu^{2+} similar to that measured at Davis Mine, this confirmation is supportive of the same process occurring at the Davis Mine study. Similarly, Cu^{2+} and Zn^{2+} were found to be easily displaced exchangers on the hydroxide solids, in agreement with the modeled part of this thesis study, where Cu^{2+} and Zn^{2+} were expected to fill iron oxide exchange sites at pH > 4. The column-study by Rötting *et al.* (2008) also confirmed formation of iron oxyhydroxides precipitates can occur at the input of their column under high flow, acidic, oxidizing conditions similar to those at Davis Mine. The decreased dissolved

concentrations of Fe^{3+}, Al^{3+}, Pb^{2+} and Cu^{2+} is again a removal profile similar to that of this study and suggestive that Fe^{3+} and Al^{3+} hydrolysis is responsible for the changing concentrations of trace metals measured in the shallow groundwater in this study.

Table 25: Summary of Limestone and Organic Carbon-based Acid Mine Drainage Treatment Systems							
Permeable Reactive Barriers	**Fill Material (by volume)**	**K (m/s) R_t (d)**	**pH influent**	**pH effluent**	**E_H influent**	**E_H effluent**	**Species Removed**
Nickel Rim, ON, Canada Benner *et al.*, 1999, 2002	20% municipal compost 20% leaf mulch 9% woodchips 1% $CaCO_3$ 50% pea gravel	$K_{prb} > K_{aq}$ 10^{-5} 10^{-6} R_t 60-164	~5	6.3	350 (mV)	200 (mV)	H^+ (minor) Fe, Ni, Zn, Al, (major) SO_4^{2-} (major)
Vancouver, BC, Canada Ludwig *et al.*, 2002	15% leaf compost 1% $CaCO_3$ 84% pea gravel	$K_{prb} > K_{aq}$ 10^{-2} 10^{-3} R_t ~6	6.39	6.86	430 (mV)	177 (mV)	H^+ (minor) Cu, Cd, Co, Ni, Zn (major) SO_4^{2-} (?)
Aznalcóllar, Sevilla, Spain Modules 2 and 3 Carrera *et al.*, 2001, Bolzicco *et al.*, 2004	2) 50% $CaCO_3$ 50% municipal compost 3) 66% $CaCO_3$ 33 % municipal compost trace Fe^0	$K_{prb} < K_{aq}$ 10^{-5} 10^{-3} R_t ~ 2	~4	~5	N.D.	N.D.	H^+, Al (50-90%) Zn, Cu, (60-90%) SO_4^{2-} (minor)
Column Studies	**Fill Material**	**Flow Data R_t (d)**	**pH influent**	**pH effluent**	**E_H influent**	**E_H effluent**	**Species Removed**
Waybrant *et al.*, 2002	(various: multiple organic carbon sources, $CaCO_3$, sediment, sand)	10^{-7} (as a.l.v.) ~46 d	5.5.-6.5	6.5 –7.5	~200 (mV)	~ -50 (mV)	H^+ (minor) Fe, Zn, Ni (major) SO_4^{2-} (major)
Gibert *et al.*, 2003 (column 1)	50% $CaCO_3$ 45% municipal compost 5% creek sediment	10^{-6} (as flux) R_t 11 hr	3	~6.5	N.D.	N.D.	H^+ (major) Fe, Al, Zn, Cu, As (major) SO_4^{2-} (minor)
Rötting *et al.*, 2008 (high flow column)	25% $CaCO_3$ 75% woodchips	varied: 10^{-1}-10^{-4} R_t 1-7 d	2.8	~6	12 (as pe) (oxidizing)	4 (as pe) (transitional)	H^+ (major) Fe, Al, Pb, Cu (major) SO_4^{2-} (minor) Other Me^{2+} (minor)

CHAPTER 5

CONCLUSIONS AND OUTLOOK

The installation of an organic carbon and limestone reactive fill at Davis Mine was performed to create a higher pH, more reducing environment suitable for stimulating the activity of the indigenous acid-tolerant sulfate reducing bacteria. In turn, these bacteria could then more effectively attenuate acidity by generating bicarbonate and sequestering metals via combination with biogenic sulfide. However, the material addition was insufficient to create the reducing environment necessary to support this biogeochemical process. While it is possible that bacterial sulfate reduction is occurring in favorable micro-environments within the reactive fill, the scale of groundwater sampling performed does not represent these locations and the overall changes in solution chemistry are not consistent with those expected to result from this process.

Instead, the groundwater chemistry seemed to respond less to the addition of organic carbon and more to the addition of limestone. Larger decreases in dissolved acid sensitive Fe^{tot} and Al^{3+} suggest the effective removal mechanism to be formation of solid hydroxide phases, a secondary mechanism observed in other AMD treatment studies. Although the pH increased overall in shallow groundwater, Fe^{3+} hydrolysis releases H^{+}, perhaps muting the pH signal from calcite dissolution. The formation of hydroxides seems to have had the larger influence on the groundwater composition, as supported by: measured pH and redox conditions, larger decreases in Fe^{tot} and Al^{3+}, minor decreases in Cu^{2+}, Zn^{2+} and SO_4^{2-}. Further support for this mechanism was found within models predicting adequate Fe^{3+} concentrations, super-saturation of Fe^{3+} and Al^{3+} secondary minerals, and confirming the affinity of trace metals Cu^{2+} and Zn^{2+} for sorption to oxide surfaces.

Iron hydroxide formation is used in AMD treatment with different strengths and weakness than bacterial sulfidogenesis, and it is possible for both processes to occur in the same system. Iron hydroxides should be regarded as temporary sinks, meaning the metals removed

from solution in this experiment will again be released to solution. In the near future, it is possible that any potential store of oxidized iron solids may be colonized by iron-reducing bacteria, whose activity will generate the benefit of increasing bicarbonate alkalinity at the cost of re-releasing iron and associated metals back to solution. If bacterial sulfate-reduction were to occur, it will most likely follow bacterial iron reduction if bacteria colonize the store of organic carbon which presently seems to be non-reactive or unavailable.

This thesis contributes to the body of studies which help to characterize the contributions of different mechanisms at work within chemical or biological treatment systems used for the remediation of acid mine drainage. In a broader sense, examples of mineral weathering, carbonate neutralization, secondary phase precipitation and trace metal sorption were found, in line with what processes are known to occur in and influence these biogeochemically complex aqueous environments.

APPENDIX A

WELL 8 BORING LOG

Well Location:	Tailings pile between two effluent streams			**Date:** 4/10/03-4/11/03 Thu/Fri	
Well Number:	**# 8**				
Geologists:	Jessica Bloom, Melinda Solomon, Klaus Nusslein, David Ahlfeld (Sample 26 only)				
	Richard Yuretich, Sarina Ergas, et al (Samples 25, 27, 29-31)				
Weather Conditions:	Sunny, 50 degrees F				
Sample #	**Picture #**	**Sample Recovery**	**Depth (ft)**	**Detailed Soil and Rock Description**	**Additional Notes**
		0	2'	Empty, no recovery	Blow counts: 1-2-2-3
26	7673 (K) and 7674 (K)	4"	4'	Ice, then sandy, yellow clay mud (1mm - 1cm grain sizes)	Blow counts: 2-1-1-2
25	100_020 (S)	6"	6'	Yellow-orange muddy tailings	Blow counts: 2-1-2-5
27	100_021 (S)	3"	8'	Yellow-gray, sandy, muddy tailings w/ noticable pyrite	Blow counts: 5-5-3-5
29	100_022 (S)	12"	10'	4" yellow pyritic muddy sand; transitions down through gray to black zone; black zone = 6" thick	Blow counts: 5-3-57
30	100_023 (S)	12"	12'	1" unconsolidated yellow slurry; followed by 6" black organic matter w/ roots; then 6" gray pyritic muddy mustard.	Blow counts: 5-12-28-77
31	100_024 (S)	5"	12'9"	Gravel pieces overlying orange-brown muddy sandy rock fragments	Blow counts: 33-60 (3")
		3'		Bedrock core	
					Total Well Depth = 15'3" **Port 1 = 3'** **Port 3 = 7'** **Port 5 = 12'** **Port 7 = 15'**

(Bloom 2005)

APPENDIX B

SITE PHOTOS

Well 8 Tailing-pile area

Figure B1: View from tailings-pile, facing south

Figure B2: Well 8 and sampling gear. Port 2 used in gradient measurements shown by circle.

Figure B3: Effluent West (author for scale)

Figure B4: Effluent West streambed (same stream bed ledge as B3)

Figure B5: Effluent East (when dry)

Figure B6: Effluent Seep (pen for scale)

Figure B7: Effluent South, facing North towards tailings-pile. Seep area outlined by box

APPENDIX C

REDOX CONVERSIONS

ORP/ E_H

Field measured Oxidation Reduction Potential (ORP) was converted to E_H so that comparisons with other studies could be made. E_H is the redox potential that would be measured by the Standard Hydrogen electrode. The Oxidation Reduction Potential measured by a Ag/AgCl electrode is related to E_H as:

$$E_H \text{ (in volts)} = \frac{(E'c + \text{ORP (in mVolts)})}{1000}$$

where E'c is an temperature dependent electrode-specific junction potential.

An Ag/AgCl reference electrode with a saturated KCl filling solution was used.

C4: E'c values

Temp °C	3*M* KCl [1]	3.5*M* KCl [2]	Saturated KCl [2]
10	0.220	0.215	0.214
15	0.216	0.212	0.209
20	0.213	0.208	0.204
25	0.209	0.205	0.199
30	0.205	0.201	0.194
35	0.202	0.197	0.189
40	0.198	0.193	0.184

from Nordstrom and Wilde (2005)

Here, the junction potential is linearly related to temperature as:

$E'c = (-0.001)(°C) + 0.204V$

This value added to the ORP converts it to an E_H.

E_H/pe

PHREEQCi's default unit for redox measurements is pe, the electron activity measurement analogous to pH. E_H relates to pe as:

$$pe = \frac{(E_H * F)}{2.303 * R * \text{Temp}}$$

where E_H is in Volts, F = Faraday's constant, R = Gas Constant, and temp is in K

$$pe = \frac{(E_H * 96420 \text{ J/Volt/gram equiv H})}{2.303 * 8.314 \text{ J/kmol} * (273.15 + °C)}$$

APPENDIX D

DATA TABLES

Table D1
Geochemistry of Davis Mine Samples

Date	Sample	Depth to Water	pH	Well ORP	Eh	pe	Temp.	Conduc tivity	H^+	DOC	Fe^{3+}	Fe^{2+}	Ave Total Fe	Mn^{2+}	Zn^{2+}	Cu^{2+}	Al^{3+}	Pb^{2+}	Na^{1+}	Mg^{2+}	K^{1+}	Ca^{2+}	Si^{4+}
		1/10 ft		mV	V		°C	µS/cm		mg/L	mol	mol	micrograms/Liter (µg/L)										
10/17/2008	W8P3	4.42	4.81	323.4	0.54	9.73	10.4	424.5	15.49	0.97	5.51E-07	1.06E-06	90.2	922	2188	247.3	1040	53.4	1606	11310	4866	53460	13480
10/17/2008	W8P5	4.50	4.84	274	0.49	8.83	10.4	518	14.45	0.65			6066.5	1559	2106	202.1	986	92.6	1751	14030	6140	73600	16870
10/17/2008	W8P7	4.17	4.73	302.8	0.52	9.36	10.3	440	18.62	1.15			1306.5	1235	2118	228.4	1105	62.6	1540	12650	5440	64750	13610
10/17/2008	Effluent East	NA	3.39	505.5	0.72	13.10	10.0	502	407.38	0.85			2602.5	979	3729	361.4	2470	11.02	1731	9730	4575	26720	17580
10/17/2008	Effluent West	NA	3.37	487.8	0.70	12.79	9.5	491.3	426.58	0.77			9370.5	601	3466	176.2	2112	3.873	2729	7570	3830	20680	12710
10/17/2008	Effluent Seep	NA	3.02	519.6	0.73	13.37	10.4	792	954.99	0.87			2556	593	2947	257.1	4331	19.94	2786	8530	3562	18860	21010
8/22/2008	W8P3	4.75	4.85	358.6	0.56	10.23	18.10	409.1	14.13	0.74	1.05E-06	3.20E-07	76.4	1012	2293	304.2	1197	32.95	1563	11760	5070	56110	14090
8/22/2008	W8P5	4.92	4.85	282.6	0.49	8.90	15.3	521	14.13	0.62			6204.5	1608	2160	211.3	1105	83.9	1815	13770	6280	75460	16480
8/22/2008	W8P7	4.58	4.82	303.5	0.51	9.28	15.3	482	15.14	1.01			1441.5	1279	2125	238.5	1202	69.2	1609	12930	5670	68350	13270
8/22/2008	Effluent East	NA	3.48	503.9	0.71	12.83	22.9	502	331.13	0.92			3071	844	3331	276.7	1874	32.95	1876	8510	4681	23970	17860
8/22/2008	Effluent West	NA	3.57	584	0.79	14.36	18.7	464.3	269.15	1.43			5919	453.5	2857	174.3	1657	32.95	2890	6250	3697	17370	12140
8/22/2008	Effluent Seep	NA	3.23	537.5	0.74	13.55	18.0	753	588.84	1.06			1838	517	2733	261.8	3626	32.95	2876	7780	3647	17620	21650
7/29/2008	W8P3	4.17	4.89	279.2	0.48	8.72	21.7	402.8	12.88	0.77	1.25E-07	6.26E-07	41.96	977	2154	243.8	1136	95.7	1512	11840	4821	57150	13700
7/29/2008	W8P5	4.33	4.81	264	0.47	8.52	17.6	535	15.49	0.63			6527	1614	2227	204.1	1191	153.6	1805	14350	6060	75080	16690
7/29/2008	W8P7	3.75	4.74	335.5	0.54	9.86	15.2	481.9	18.20	1.03			490.2	1175	2143	238.3	1234	173.3	1467	12110	5020	62770	12800
7/29/2008	Effluent East	NA	3.44	483.9	0.68	12.40	26.6	505	363.08	1.16			3333.5	834	3036	274.7	1931	31.13	1675	7810	4547	21700	17640
7/29/2008	Effluent West	NA	3.44	610.12	0.81	14.72	25.5	491.9	363.08	0.86			7167.5	504	2835	166.2	1836	31.13	2598	6260	3596	16890	12810
7/29/2008	Effluent Seep	NA	3.15	529.4	0.73	13.29	24.3	768	707.95	0.82			2289	649	3304	354.7	4280	56.7	2652	7840	3731	17960	22440
7/11/2008	W8P3	4.83	4.85	390.3	0.60	10.78	19	411.9	14.13	1.03	1.56E-06	1.28E-07	94.3	994	2370	284.1	1235	32.95	1320	10920	4294	53360	12410
7/11/2008	W8P5	4.83	5.03	300.2	0.51	9.21	15.3	540	9.33	0.77			5859	1654	2206	204	1159	65.4	1804	14910	6050	80450	15910
7/11/2008	W8P7	4.50	4.79	319.3	0.53	9.55	16.3	481.2	16.22	1.18			1478	1335	2213	255.2	1257	52.8	1647	12990	5220	69330	13000
7/11/2008	Effluent East	NA	3.00	498.5	0.70	12.74	23.6	521	1000.00	1.09			2793.5	879	3256	313	1834	32.95	1550	8230	4573	23370	18120
7/11/2008	Effluent West	NA	3.46	489.7	0.69	12.60	21.5	568	346.74	1.17			8841	701	3970	183	2020	32.95	2483	8040	4147	22650	14540
7/11/2008	Effluent Seep	NA	2.92	530.5	0.74	13.45	17.4	678	1202.26	0.86			1190.5	595	3429	300.3	3140	32.95	2481	7290	3243	17750	18670
6/18/2008	W8P3	4.17	4.85	522.1	0.73	13.20	17.5	492.9	14.13	1.22	1.35E-06	6.14E-10	75.25	1042	2404	276.6	1349	39.75	1583	11210	4508	53720	12690
6/18/2008	W8P5	4.17	4.95	311.1	0.52	9.48	11.8	541	11.22	1.04			6423	1631	2227	186.9	1251	13.57	1766	13580	5750	73670	15140
6/18/2008	W8P7	3.75	4.81	330.6	0.54	9.82	12.7	490.5	15.49	0.91			2774.5	1424	2235	232.4	1316	88.8	1621	12980	5190	68280	12270
6/18/2008	Effluent East	NA	3.44	486	0.69	12.53	21.8	230.1	363.08	1.29			4021.5	716	3381	374	2383	10.61	1548	7790	4364	21910	16330
6/18/2008	Effluent West	NA	3.53	468.6	0.67	12.24	20.2	489	295.12	1.27			6995	422.4	3464	361.4	2681	22.34	2426	6500	3505	18940	12520
6/18/2008	Effluent Seep	NA	3.01	542.6	0.75	13.68	16.4	677	977.24	1.07			1529.5	414.6	3377	500	3122	26.7	2791	5945	3751	15827	16289
6/3/2008	W8P3	4.33	4.84	443.2	0.65	11.79	16.5	414	14.45	3.56	1.21E-06	1.40E-08	68.25	1058	2367	277	1292	44.68	1378	12060	4476	59140	12560
6/3/2008	W8P5	4.17	4.82	325.7	0.54	9.71	13.5	544	15.14	1.58			6348.5	1643	2196	191.8	1191	77.4	1778	14180	5780	78310	14180
6/3/2008	W8P7	3.75	4.83	359.7	0.57	10.34	12.7	500	14.79	1.08			1151	1269	2151	238.2	1300	67	1536	13040	4995	67400	12050
6/3/2008	Effluent East	NA	3.4	483.6	0.68	12.41	26	514	436.52	1.13			3230	849	3447	331.8	1861	27.79	1590	7880	4025	23120	15810
6/3/2008	Effluent West	NA	3.5	469.7	0.67	12.27	19.8	466.6	309.03	0.75			6377	496.5	3349	245.5	2178	10.08	2624	6350	3195	17830	12300
6/3/2008	Effluent Seep	NA	2.9	511.7	0.72	13.15	15	621	1202.26	0.75			1818.5	439.3	3181	436.3	2971	27.88	2322	5770	2556	15220	14340
5/22/2008	W8P3	3.83	4.72	531.1	0.75	13.53	8.7	414.3	19.05	1.41	3.31E-06	2.06E-09	184.8	997	2367	291.2	1269	50.3	1565	12070	4587	57820	12430
5/22/2008	W8P5	4.00	4.82	431	0.65	11.73	7.6	546	15.14	1.01			6545.5	1586	2168	199.7	1144	64.9	1814	14530	5870	76750	14390
5/22/2008	W8P7	3.42	4.76	380.1	0.60	10.80	8.3	497.3	17.38	0.70			2423.5	1366	2123	245.3	1243	80	1657	13980	5480	72720	12600
5/22/2008	Effluent East	NA	3.94	477.4	0.69	12.54	11.2	297.3	114.82	0.93			3192.5	816	3183	334.6	1951	26.4	1817	7270	3457	21180	12800
5/22/2008	Effluent West	NA	3.52	480.1	0.69	12.64	9.4	460.9	302.00	0.79			9404	576	3497	203.2	2125	15.36	2619	5950	2617	16460	10340
5/22/2008	Effluent Seep	NA	3.16	522.6	0.74	13.45	8.5	549	691.83	0.75			1224	508	3159	398.2	2841	51.7	2212	5620	2309	14690	13310
5/5/2008	W8P3	3.50	4.70	554.2	0.77	13.92	10	426.6	19.95	1.47	1.53E-06	3.97E-10	85.4	1057	2427	279.2	1318	70.7	1445	11540	4397	55980	12060
5/5/2008	W8P5	3.58	4.75	335.5	0.55	9.98	9	544	17.78	0.95			6205.5	1616	2178	191.9	1194	60.9	1785	13370	5650	74020	13560
5/5/2008	W8P7	3.00	4.73	355.2	0.57	10.32	9.5	498.4	18.62	0.76			2523	1389	2225	243.2	1327	85.2	1591	12900	5130	68290	11730
5/5/2008	Effluent East	NA	3.21	480.7	0.69	12.60	13.4	493.4	616.60	1.32			9854	533	3782	526	2785	19.61	2067	6080	2661	17210	10470
5/5/2008	Effluent West	NA	2.96	478.2	0.69	12.63	9.6	485.7	1096.48	1.08			14612	384.7	3998	602	3201	17.15	2462	5550	2229	14500	9000
5/5/2008	Effluent Seep	NA	3.17	538.9	0.75	13.74	9.1	637	676.08	0.87			2265.5	348.9	3353	544	3118	22.3	2149	5080	2168	13390	11800

Geochemistry of Davis Mine Samples

Date	Sample	Cl^{1-}	SO_4^{2-}	NO_3^-	F^{1-}	PO_4^{3-}	Br^{1-}	H	Ave Total Fe	Mn	Zn	Cu	Al	Pb	Na	Mg	K	Ca	+ Charge Sum	Cl	SO_4	NO_3	F	PO_4	Br	- Charge Sum	Total Charge	Error
		micrograms/Liter (µg/L)								microequivalents/Liter (µequiv/L)										microequivalents/Liter (µequiv/L)								
10/17/2008	W8P3	2837	204825	162	47	0	36	15.49	4.85	33.57	66.92	7.78	115.63	0.52	69.86	930.67	124.46	2667.8	4037.537	-80.022	-4264.36	-2.61	-2.47	0	-0.451	-4349.92	-312.3854	-3.72%
10/17/2008	W8P5	3789	293208	35	50	0	51	14.45	325.88	56.75	64.41	6.36	109.63	0.89	76.16	1154.5	157.04	3672.8	5638.927	-106.87	-6104.46	-0.56	-2.63	0	-0.638	-6215.17	-576.2386	-4.86%
10/17/2008	W8P7	3285	260973	51	40	4	32	18.62	70.18	44.96	64.78	7.19	122.86	0.6	66.99	1040.9	139.14	3231.2	4807.459	-92.659	-5433.34	-0.82	-2.11	-0.13	-0.4	-5529.45	-721.9929	-6.98%
10/17/2008	Effluent East	4753	207842	66	122	16	0	407.38	139.80	35.64	114.05	11.37	274.63	0.11	75.29	800.66	117.01	1333.4	3309.355	-134.07	-4327.17	-1.06	-6.42	-0.51	0	-4469.23	-1159.878	-14.91%
10/17/2008	Effluent West	6373	86970	33	53	11	0	426.58	503.37	21.88	106.01	5.55	234.83	0.04	118.70	622.92	97.958	1032	3169.813	-179.76	-1810.68	-0.53	-2.79	-0.35	0	-1994.11	1175.7079	22.77%
10/17/2008	Effluent Seep	12518	261476	77	75	27	0	954.99	137.30	21.59	90.14	8.09	481.55	0.19	121.18	701.91	91.104	941.16	3549.223	-353.09	-5443.81	-1.24	-3.95	-0.85	0	-5802.94	-2253.72	-24.10%
8/22/2008	W8P3	2645	164930	85	80	60	200	14.13	4.10	36.84	70.13	9.57	133.09	0.32	67.99	967.7	129.67	2800	4233.589	-74.606	-3433.77	-1.37	-4.21	-1.9	-2.503	-3518.35	715.23565	9.23%
8/22/2008	W8P5	3705	237025	0	30	0	450	14.13	333.29	58.54	66.07	6.65	122.86	0.81	78.95	1133.1	160.62	3765.7	5740.672	-104.51	-4934.75	0	-1.58	0	-5.632	-5046.47	694.20405	6.44%
8/22/2008	W8P7	3065	204090	35	50	0	160	15.14	77.43	46.56	64.99	7.51	133.65	0.67	69.99	1064	145.02	3410.8	5035.782	-86.453	-4249.06	-0.56	-2.63	0	-2.002	-4340.71	695.07014	7.41%
8/22/2008	Effluent East	4670	113985	135	120	25	90	331.13	164.97	30.73	101.88	8.71	208.36	0.32	81.60	700.27	119.72	1196.2	2943.858	-131.72	-2373.12	-2.18	-6.32	-0.79	-1.126	-2515.25	428.60783	7.85%
8/22/2008	Effluent West	11065	88525	135	100	0	90	269.15	317.96	16.51	87.38	5.49	184.24	0.32	125.71	514.3	94.557	866.81	2482.417	-312.11	-1843.05	-2.18	-5.26	0	-1.126	-2163.72	318.69366	6.86%
8/22/2008	Effluent Seep	9710	142385	190	165	55	0	588.84	98.73	18.82	83.59	8.24	403.17	0.32	125.10	640.2	93.278	879.29	2939.572	-273.89	-2964.39	-3.07	-8.68	-1.74	0	-3251.76	-312.1916	-5.04%
7/29/2008	W8P3	1708	203526	124	66	0	0	12.88	2.25	35.57	65.88	7.67	126.31	0.92	65.77	974.29	123.3	2851.9	4266.788	-48.177	-4237.32	-2	-3.47	0	0	-4290.97	-24.18104	-0.28%
7/29/2008	W8P5	3226	291794	40	52	0	0	15.49	350.62	58.76	68.11	6.42	132.42	1.48	78.51	1180.8	154.99	3746.7	5794.337	-90.994	-6075.02	-0.65	-2.74	0	0	-6169.39	-375.0571	-3.13%
7/29/2008	W8P7	2608	240348	0	36	0	0	18.20	26.33	42.78	65.55	7.50	137.21	1.67	63.81	996.5	128.39	3132.4	4620.328	-73.563	-5003.93	0	-1.89	0	0	-5079.39	-459.0644	-4.73%
7/29/2008	Effluent East	5812	178968	0	74	0	0	363.08	179.07	30.36	92.86	8.65	214.70	0.3	72.86	642.67	116.3	1082.9	2803.726	-163.94	-3726.03	0	-3.9	0	0	-3893.86	-1090.138	-16.28%
7/29/2008	Effluent West	13832	194064	0	48	0	0	363.08	385.03	18.35	86.71	5.23	204.14	0.3	113.01	515.12	91.973	842.86	2625.79	-390.15	-4040.32	0	-2.53	0	0	-4433	-1807.214	-25.60%
7/29/2008	Effluent Seep	10278	308414	64	74	0	0	707.95	122.96	23.63	101.06	11.16	475.88	0.55	115.36	645.13	95.426	896.25	3195.35	-289.91	-6421.04	-1.03	-3.9	0	0	-6715.87	-3520.523	-35.52%
7/11/2008	W8P3	3171	192220	534	118	27	216	14.13	5.07	36.19	72.49	8.94	137.32	0.32	57.42	898.58	109.83	2662.8	4003.072	-89.443	-4001.93	-8.61	-6.21	-0.85	-2.703	-4109.76	-106.6849	-1.32%
7/11/2008	W8P5	5125	297193	2321	157	142	281	9.33	314.73	60.21	67.47	6.42	128.87	0.63	78.47	1226.9	154.74	4014.7	6062.458	-144.56	-6187.42	-37.4	-8.26	-4.49	-3.517	-6385.69	-323.231	-2.60%
7/11/2008	W8P7	4168	261357	53	107	645	290	16.22	79.40	48.60	67.69	8.03	139.76	0.51	71.64	1068.9	133.51	3459.8	5094.024	-117.57	-5441.33	-0.85	-5.63	-20.4	-3.629	-5589.39	-495.3651	-4.64%
7/11/2008	Effluent East	4706	195860	40	161	540	0	1000.00	150.06	32.00	99.59	9.85	203.92	0.32	67.42	677.23	116.96	1166.2	3523.571	-132.74	-4077.72	-0.65	-8.47	-17.1	0	-4236.63	-713.062	-9.19%
7/11/2008	Effluent West	13832	210413	207	131	791	0	346.74	474.92	25.52	121.43	5.76	224.60	0.32	108.00	661.59	106.07	1130.3	3205.239	-390.15	-4380.7	-3.34	-6.9	-25	0	-4806.08	-1600.838	-19.98%
7/11/2008	Effluent Seep	13265	213277	64	137	1150	0	1202.26	63.95	21.66	104.88	9.45	349.13	0.32	107.92	599.88	82.945	885.77	3428.164	-374.16	-4440.33	-1.03	-7.21	-36.3	0	-4859.06	-1430.896	-17.27%
6/18/2008	W8P3	3552	197160	14	22	108	0	14.13	4.04	37.93	73.53	8.71	149.99	0.38	68.86	922.44	115.3	2680.8	4076.082	-100.19	-4104.78	-0.23	-1.16	-3.41	0	-4209.77	-133.6834	-1.61%
6/18/2008	W8P5	4784	282464	136	16	38	0	11.22	345.03	59.38	68.11	5.88	139.10	0.13	76.82	1117.5	147.07	3676.3	5646.53	-134.94	-5880.77	-2.19	-0.84	-1.2	0	-6019.95	-373.4177	-3.20%
6/18/2008	W8P7	3994	259134	128	20	32	0	15.49	149.04	51.84	68.36	7.31	146.32	0.86	70.51	1068.1	132.74	3407.4	5117.923	-112.66	-5395.05	-2.06	-1.05	-1.01	0	-5511.84	-393.9132	-3.71%
6/18/2008	Effluent East	4310	180372	264	46	92	0	363.08	216.03	26.07	103.41	11.77	264.96	0.1	67.33	641.02	111.62	1093.4	2898.753	-121.57	-3755.26	-4.26	-2.42	-2.91	0	-3886.42	-987.6656	-14.56%
6/18/2008	Effluent West	11332	182568	124	46	46	66	295.12	375.76	15.38	105.95	11.37	298.09	0.22	105.53	534.87	89.646	945.16	2777.086	-319.64	-3800.98	-2	-2.42	-1.45	-0.826	-4127.32	-1350.233	-19.56%
6/18/2008	Effluent Seep	11632	235170	164	16	78	64	977.24	82.16	15.09	103.29	15.74	347.13	0.26	121.40	489.2	95.938	789.81	3037.251	-328.1	-4896.13	-2.65	-0.84	-2.46	-0.801	-5230.98	-2193.733	-26.53%
6/3/2008	W8P3	3076	219458	82	114	74	172	14.45	3.67	38.52	72.40	8.72	143.65	0.43	59.94	992.39	114.48	2951.2	4399.89	-86.763	-4569.01	-1.32	-6	-2.34	-2.153	-4667.59	-267.7013	-2.95%
6/3/2008	W8P5	4994	299494	34	108	34	144	15.14	341.03	59.81	67.17	6.04	132.42	0.75	77.34	1166.8	147.83	3907.9	5922.241	-140.86	-6235.33	-0.55	-5.68	-1.07	-1.802	-6385.3	-463.0592	-3.76%
6/3/2008	W8P7	4518	233750	4196	108	22	0	14.79	61.83	46.20	65.79	7.50	144.54	0.65	66.81	1073	127.75	3363.4	4972.334	-127.44	-4866.57	-67.7	-5.68	-0.69	0	-5068.07	-95.74041	-0.95%
6/3/2008	Effluent East	5750	199610	38	170	74	84	436.52	173.51	30.91	105.43	10.44	206.92	0.27	69.16	648.43	102.95	1153.8	2938.276	-162.19	-4155.79	-0.61	-8.95	-2.34	-1.051	-4330.93	-1392.65	-19.16%
6/3/2008	Effluent West	15632	174406	1354	70	50	52	309.03	342.56	18.07	102.43	7.73	242.17	0.1	114.14	522.53	81.717	889.76	2630.233	-440.93	-3631.05	-21.8	-3.68	-1.58	-0.651	-4099.74	-1469.503	-21.84%
6/3/2008	Effluent Seep	14454	205564	190	156	76	0	1202.26	97.69	15.99	97.29	13.73	330.34	0.27	101.00	474.8	65.374	759.52	3158.268	-407.7	-4279.75	-3.07	-8.21	-2.4	0	-4701.12	-1542.855	-19.63%
5/22/2008	W8P3	3980	209412	8	42	128	0	19.05	9.93	36.30	72.40	9.17	141.10	0.49	68.07	993.21	117.32	2885.4	4352.399	-112.26	-4359.86	-0.13	-2.21	-4.04	0	-4478.51	-126.108	-1.43%
5/22/2008	W8P5	5632	295162	8	50	40	0	15.14	351.61	57.74	66.31	6.29	127.20	0.63	78.90	1195.6	150.13	3830	5879.615	-158.86	-6145.14	-0.13	-2.63	-1.26	0	-6308.02	-428.4063	-3.52%
5/22/2008	W8P7	4946	269380	6	26	26	0	17.38	130.19	49.73	64.93	7.72	138.21	0.77	72.08	1150.4	140.16	3628.9	5400.464	-139.51	-5608.37	-0.1	-1.37	-0.82	0	-5750.16	-349.7004	-3.14%
5/22/2008	Effluent East	7934	189008	6	96	88	0	114.82	171.50	29.71	97.35	10.53	216.93	0.25	79.04	598.23	88.418	1056.9	2463.706	-223.79	-3935.06	-0.1	-5.05	-2.78	0	-4166.78	-1703.074	-25.69%
5/22/2008	Effluent West	16242	187648	146	74	60	0	302.00	505.17	20.97	106.96	6.40	236.27	0.15	113.92	489.61	66.934	821.4	2669.768	-458.13	-3906.75	-2.36	-3.9	-1.9	0	-4373.02	-1703.254	-24.18%
5/22/2008	Effluent Seep	14566	228666	88	66	76	0	691.83	65.75	18.49	96.62	12.53	315.88	0.5	96.22	462.46	59.056	733.07	2552.41	-410.86	-4760.72	-1.42	-3.47	-2.4	0	-5178.87	-2626.462	-33.97%
5/5/2008	W8P3	2550	185175	170	0	0	0	19.95	4.59	38.48	74.23	8.79	146.54	0.68	62.85	949.6	112.46	2793.6	4211.732	-71.927	-3855.26	-2.74	0	0	0	-3929.93	281.80392	3.46%
5/5/2008	W8P5	4205	245575	0	0	60	0	17.78	333.35	58.83	66.62	6.04	132.76	0.59	77.64	1100.2	144.51	3693.8	5632.095	-118.61	-5112.76	0	0	-1.9	0	-5233.26	398.83214	3.67%
5/5/2008	W8P7	3580	222050	0	0	55	0	18.62	135.53	50.57	68.05	7.65	147.55	0.82	69.20	1061.5	131.21	3407.9	5098.57	-100.98	-4622.98	0	0	-1.74	0	-4725.7	372.87451	3.80%
5/5/2008	Effluent East	7785	118430	175	0	45	725	616.60	529.34	19.40	115.68	16.55	309.66	0.19	89.91	500.31	68.059	858.83	3124.516	-219.59	-2465.66	-2.82	0	-1.42	-9.073	-2698.56	425.95185	7.31%
5/5/2008	Effluent West	9720	147480	275	0	15	1010	1096.48	784.93	14.00	122.28	18.95	355.91	0.17	107.09	456.7	57.01	723.59	3737.104	-274.17	-3070.47	-4.44	0	-0.47	-12.64	-3362.18	374.92006	5.28%
5/5/2008	Effluent Seep	6740	150560	160	0	35	820	676.08	121.70	12.70	102.55	17.12	346.68	0.22	93.48	418.02	55.45	668.2	2512.2	-190.11	-3134.59	-2.58	0	-1.11	-10.26	-3338.65	-826.4515	-14.13%

Geochemistry of Davis Mine Samples

Date	Sample	Depth to Water	pH	Well ORP	Eh	pe	Temp.	Conductivity	H^+	DOC	Fe^{3+}	Fe^{2+}	Ave Total Fe	Mn^{2+}	Zn^{2+}	Cu^{2+}	Al^{3+}	Pb^{2+}	Na^{1+}	Mg^{2+}	K^{1+}	Ca^{2+}	Si^{4+}
		1/10 ft		mV	V		°C	µS/cm		mg/L	mol	mol	micrograms/Liter (µg/L)										
4/28/2008	Effluent East	NA	3.42	482	0.70	12.73	6.9	493.2	380.19	1.32			8608.5	530	3454	442.4	2571	20.92	1753	5570	2662	15800	10470
4/28/2008	Effluent West	NA	3.39	474	0.69	12.56	8.3	497.8	407.38	1.08			14975.5	419.9	4167	547	3329	15.18	2304	5190	2486	14800	9190
4/28/2008	Effluent Seep	NA	2.44	534.5	0.75	13.76	5.6	641	3630.78	0.87			3290	375.4	3685	597	3542	18.15	1994	4762	2129	12920	11980
4/4/2008	W8P3	3.25	3.90	515.5	0.74	13.36	4.3	425.9	125.89	0.83	2.29E-06	5.02E-08	130.45	953	2265	292	1322	15.07	1489	10950	4345	53140	11790
4/4/2008	W8P5	3.33	4.04	325.3	0.54	9.88	5.6	548	91.20	0.71			6095.5	1602	2170	195.6	1228	15.07	1714	13470	5570	72790	14240
4/4/2008	W8P7	3.08	4.15	355.5	0.57	10.43	4.9	479.8	70.79	0.65			1044	1237	2145	248.8	1329	15.07	1483	12220	4796	63310	11560
4/4/2008	Effluent East	NA	3.26	464.1	0.68	12.40	7.6	393.2	549.54	0.80			7386	447.9	2654	267.1	2113	15.07	1711	5030	2206	15350	8000
4/4/2008	Effluent West	NA	3.29	460.5	0.68	12.40	3.9	360.8	512.86	0.84			8876	289.2	2407	232.8	2143	15.07	1882	3893	1757	11260	7060
4/4/2008	Effluent Seep	NA	1.86	520.1	0.74	13.54	4.5	555	13803.84	0.67			2200	293	2428	400.9	2416	20.32	1930	4267	1953	11860	9660
3/20/2008	W8P3	3.08	3.62	545.6	0.77	13.93	3.9	392.0	239.88	1.03	2.14E-05	2.51E-07	1209.5	838	2633	416.5	1832	18.27	1675	9300	3854	43570	11340
3/20/2008	W8P5	3.25	3.96	330.8	0.55	9.99	5.1	507	109.65	0.70			6146	1415	2454	246	1415	18.27	1838	12120	5270	61480	14440
3/20/2008	W8P7	2.75	4.05	549.4	0.77	13.96	5.1	516	89.13	0.56			2817	1328	2267	266.3	1389	19.98	1644	12130	5020	63940	12150
3/20/2008	Effluent East	NA	3.39	446.3	0.66	12.07	7.4	400.0	407.38	0.86			9688	438.3	2821	235.5	2216	18.27	1913	5150	2341	15990	8570
3/20/2008	Effluent West	NA	3.46	444.7	0.66	12.09	4.6	365.0	346.74	0.95			11355	312.9	2706	207.2	2220	18.27	1928	4301	1928	12350	7510
3/20/2008	Effluent Seep	NA	1.98	543.5	0.76	13.99	3.1	294.1	10471.29	0.81			2316	391.1	3252	486.9	2986	28.23	2085	5370	2280	14470	10940
3/7/2008	W8P3	3.17	3.55	588.2	0.81	14.68	5.4	385.4	281.84	0.83	5.61E-06	1.33E-08	313.75	766	2499	357.2	1765	19.77	1777	9240	3869	41550	11310
3/7/2008	W8P5	3.33	3.92	337.7	0.56	10.10	6.1	493.4	120.23	0.68			6273	1345	2612	254.9	1682	23.57	1940	11890	5260	60260	14960
3/7/2008	W8P7	NA	3.95	365.1	0.58	10.59	6.4	468.8	112.20	0.96			3003	1247	2343	248.8	1423	44.62	1678	11750	6340	60640	12430
3/7/2008	Effluent East	NA	3.20	446.2	0.66	12.06	8.1	446.2	630.96	0.78			3704	607	3128	293.6	2451	13.65	1832	6660	2934	19690	10850
3/7/2008	Effluent West	NA	3.32	485.7	0.70	12.82	6	356.1	478.63	0.69			4609	306.4	2595	207.3	2097	15.92	2050	4401	2150	12370	8030
3/7/2008	Effluent Seep		1.83	538	0.76	13.89	3.7	538	14791.08	0.68			1969.5	308	2630	384.5	2345	16.36	2064	4671	2208	12620	9880
2/18/2008	W8P3	3.33	4.12	624.2	0.85	15.40	0.4	365.8	75.86	0.74	6.41E-06	7.11E-10	358.15	762	2276	337.1	1373	13.65	1597	9300	4238	42290	11360
2/18/2008	W8P5	3.25	4.35	340	0.56	10.17	3.6	535	44.67	0.71			5169.5	1578	2229	185.1	1277	16.01	1691	13590	5300	72760	14910
2/18/2008	W8P7	2.83	4.37	347.8	0.57	10.34	1.7	470.6	42.66	0.82			766	1268	2317	251.1	1500	17.2	1583	12750	4879	65880	12690
2/18/2008	Effluent East	NA	3.58	496	0.71	12.98	6.9	382.8	263.03	0.86			3148.5	430.9	2675	338.6	2152	15.21	1855	5380	2270	15620	9020
2/18/2008	Effluent West	NA	3.64	492.4	0.71	13.00	2.1	311.9	229.09	0.76			2213.5	227.8	2160	303.2	1812	23	1934	3781	1685	10620	7380
2/18/2008	Effluent Seep	NA	2.12	553.1	0.78	14.20	1.1	592	7585.78	1.84			3074.5	247.1	2386	527	2107	26.09	1989	4233	2909	11700	9430
2/8/2008	W8P3	3.33	4.23	480.8	0.70	12.75		367.8	58.88	1.15	1.97E-05	6.84E-07	1137.5	815	2290	306.1	1357	13.65	1577	10130	4036	46050	11690
2/8/2008	W8P5	3.17	4.42	308.1	0.53	9.57		538	38.02	0.78			3929.5	1592	2284	195.4	1285	19.59	1810	13790	5480	74140	15420
2/8/2008	W8P7	2.67	4.46	334.8	0.55	10.05		438.9	34.67	0.95			810	1317	2247	237	1308	13.65	1618	12850	5120	67160	12780
2/8/2008	Effluent East	NA	3.58	509.2	0.73	13.27		383.1	263.03	0.92			4086	497.1	3015	440.2	2151	13.65	1886	6020	2610	17890	9790
2/8/2008	Effluent West	NA	3.40	486.3	0.71	12.87		311	398.11	0.81			1874	221.9	2471	458.8	1625	28.88	2135	4194	1917	11610	8060
2/8/2008	Effluent Seep	NA	2.40	567.6	0.79	14.43		692	3981.07	0.82			7125.5	283.2	2517	593	2355	20.08	2144	4874	2166	13470	10330
1/22/2008	W8P3	3.50	3.78	468.7	0.69	12.55	2.7	354.6	165.96	1.72	5.81E-06	1.20E-06	391.25	690	2467	361.9	1548	24.01	1899	9250	3779	38630	11450
1/22/2008	W8P5	3.58	5.43	234.6	0.45	8.22	3.9	502	3.72	0.87			5618.5	1427	2371	237.8	1369	13.65	1874	12990	5430	66010	16290
1/22/2008	W8P7	3.08	5.19	314.1	0.53	9.64	5.5	481.7	6.46	0.70			2734.5	1296	2206	238.1	1218	13.65	1681	12690	5170	63720	13010
1/22/2008	Effluent East	NA	3.56	527	0.75	13.64	1.6	527	275.42	1.24			5668	1034	4326	514	3516	13.65	1832	10270	4115	29710	14910
1/22/2008	Effluent West	NA	3.03	462.3	0.69	12.50	0.7	343.5	933.25	0.78			2945	346.7	2586	222.1	1963	20.96	2536	5690	2571	15480	9070
1/22/2008	Effluent Seep	NA	2.64	481.9	0.70	12.86	1.4	568	2290.87	0.80			1774.5	361	2514	348	2046	19.95	2486	5800	2496	16550	9830
12/6/2007	W8P3	NA	3.39	453.3	0.67	12.28	3.2	494.1	407.38	5.11			1645	856	3531	624	3514	1663	2076	9310	5450	35530	13030
12/6/2007	W8P5	NA	4.32	325.6	0.54	9.86	6.3	515	47.86	1.56			1148.5	1463	3253	459.4	2629	265	2042	11900	5140	55770	17610
12/6/2007	W8P7	NA	3.36	285.7	0.50	9.17	6	474.1	436.52	0.94			232.2	1417	2503	395.7	1785	2080	1612	12040	5180	63460	13200
12/6/2007	Effluent East	NA	NA	NA					NA	NA													
12/6/2007	Effluent West	NA	NA	NA					NA	NA													
12/6/2007	Effluent Seep	NA	2.66	524.4	0.75	13.61	2.8	1064	2187.76	1.12			11535	799	4361	895	5090	1365	2449	8310	2901	23910	14540

Geochemistry of Davis Mine Samples

Date	Sample	Cl^{1-}	SO_4^{2-}	NO_3^-	F^{1-}	PO_4^{3-}	Br^{1-}	H	Ave Total Fe	Mn	Zn	Cu	Al	Pb	Na	Mg	K	Ca	+ Charge Sum	Cl	SO_4	NO_3	F	PO_4	Br	- Charge Sum	Total Charge	Error
		micrograms/Liter (µg/L)								microequivalents/Liter (µequiv/L)										microequivalents/Liter (µequiv/L)								
4/28/2008	Effluent East	5465	99175	120	0	45	0	380.19	462.43	19.29	105.64	13.92	285.86	0.2	76.25	458.34	68.085	788.46	2658.689	-154.15	-2064.78	-1.94	0	-1.42	0	-2222.28	436.40438	8.94%
4/28/2008	Effluent West	11395	145385	120	0	35	0	407.38	804.46	15.29	127.45	17.22	370.14	0.15	100.22	427.07	63.583	738.56	3071.513	-321.41	-3026.85	-1.94	0	-1.11	0	-3351.3	-279.7914	-4.36%
4/28/2008	Effluent Seep	6730	149805	115	0	50	0	3630.78	176.73	13.67	112.71	18.79	393.83	0.18	86.73	391.85	54.452	644.74	5524.461	-189.83	-3118.87	-1.86	0	-1.58	0	-3312.14	2212.3249	25.04%
4/4/2008	W8P3	2935	184415	0	25	0	0	125.89	7.01	34.69	69.28	9.19	146.99	0.15	64.77	901.05	111.13	2651.8	4121.972	-82.786	-3839.44	0	-1.32	0	0	-3923.54	198.43395	2.47%
4/4/2008	W8P5	4265	268195	0	30	0	360	91.20	327.44	58.32	66.37	6.16	136.54	0.15	74.55	1108.4	142.46	3632.4	5644.018	-120.3	-5583.7	0	-1.58	0	-4.505	-5710.08	-66.06406	-0.58%
4/4/2008	W8P7	2630	203180	0	20	0	310	70.79	56.08	45.03	65.61	7.83	147.77	0.15	64.51	1005.6	122.67	3159.3	4745.325	-74.183	-4230.11	0	-1.05	0	-3.88	-4309.23	436.09505	4.82%
4/4/2008	Effluent East	6745	97045	0	15	0	590	549.54	396.76	16.31	81.17	8.41	234.94	0.15	74.42	413.91	56.422	766.01	2598.033	-190.25	-2020.43	0	-0.79	0	-7.384	-2218.86	379.17423	7.87%
4/4/2008	Effluent West	7875	73305	155	10	0	615	512.86	476.80	10.53	73.62	7.33	238.27	0.15	81.86	320.35	44.938	561.9	2328.609	-222.13	-1526.18	-2.5	-0.53	0	-7.697	-1759.03	569.58233	13.93%
4/4/2008	Effluent Seep	7730	104505	190	260	0	700	13803.84	118.18	10.67	74.26	12.62	268.63	0.2	83.95	351.12	49.951	591.85	15365.26	-218.04	-2175.75	-3.07	-13.7	0	-8.761	-2419.29	12945.968	72.79%
3/20/2008	W8P3	5020	155545	0	3070	0	405	239.88	64.97	30.51	80.53	13.11	203.70	0.18	72.86	765.27	98.572	2174.3	3743.84	-141.6	-3238.38	0	-162	0	-5.069	-3546.63	197.20647	2.70%
3/20/2008	W8P5	4700	224380	0	2800	0	380	109.65	330.15	51.51	75.06	7.74	157.33	0.18	79.95	997.33	134.79	3068	5011.699	-132.57	-4671.49	0	-147	0	-4.756	-4956.2	55.502574	0.56%
3/20/2008	W8P7	4165	221050	50	30	0	325	89.13	151.32	48.35	69.34	8.38	154.44	0.19	71.51	998.15	128.39	3190.8	4909.977	-117.48	-4602.16	-0.81	-1.58	0	-4.067	-4726.09	183.88369	1.91%
3/20/2008	Effluent East	7025	91755	0	15	0	650	407.38	520.42	15.96	86.28	7.41	246.39	0.18	83.21	423.78	59.875	797.94	2648.831	-198.15	-1910.3	0	-0.79	0	-8.135	-2117.37	531.45807	11.15%
3/20/2008	Effluent West	7915	85595	0	230	0	690	346.74	609.97	11.39	82.76	6.52	246.84	0.18	83.86	353.92	49.312	616.3	2407.788	-223.26	-1782.05	0	-12.1	0	-8.635	-2026.05	381.74296	8.61%
3/20/2008	Effluent Seep	8080	123645	175	230	0	625	10471.29	124.41	14.24	99.46	15.32	332.01	0.27	90.69	441.88	58.315	722.09	12369.98	-227.91	-2574.23	-2.82	-12.1	0	-7.822	-2824.89	9545.0921	62.82%
3/7/2008	W8P3	5158	159148	158	368	0	0	281.84	16.85	27.89	76.43	11.24	196.25	0.19	77.30	760.34	98.956	2073.5	3620.736	-145.49	-3313.39	-2.55	-19.4	0	0	-3480.8	139.93897	1.97%
3/7/2008	W8P5	5062	243336	234	378	8	0	120.23	336.97	48.96	79.89	8.02	187.02	0.23	84.39	978.4	134.53	3007.1	4985.775	-142.78	-5066.14	-3.77	-19.9	-0.25	0	-5232.85	-247.074	-2.42%
3/7/2008	W8P7	5756	237616	114	326	10	0	112.20	161.32	45.40	71.66	7.83	158.22	0.43	72.99	966.88	162.16	3026.1	4785.18	-162.36	-4947.06	-1.84	-17.2	-0.32	0	-5128.73	-343.5474	-3.47%
3/7/2008	Effluent East	7746	164798	226	388	24	0	630.96	198.97	22.10	95.67	9.24	272.52	0.13	79.69	548.04	75.042	982.58	2914.94	-218.49	-3431.02	-3.65	-20.4	-0.76	0	-3674.33	-759.3935	-11.52%
3/7/2008	Effluent West	11238	123264	282	36	18	0	478.63	247.59	11.15	79.37	6.52	233.16	0.15	89.17	362.15	54.99	617.3	2180.183	-316.99	-2566.3	-4.55	-1.89	-0.57	0	-2890.3	-710.1153	-14.00%
3/7/2008	Effluent Seep	11576	167530	276	280	26	0	14791.08	105.80	11.21	80.44	12.10	260.73	0.16	89.78	384.37	56.473	629.77	16421.92	-326.52	-3487.9	-4.45	-14.7	-0.82	0	-3834.43	12587.489	62.14%
2/18/2008	W8P3	4560	157794	176	34	0	0	75.86	19.24	27.74	69.61	10.61	152.66	0.13	69.47	765.27	108.39	2110.4	3409.37	-128.62	-3285.2	-2.84	-1.79	0	0	-3418.45	-9.079123	-0.13%
2/18/2008	W8P5	3938	273350	82	144	0	0	44.67	277.70	57.45	68.18	5.83	141.99	0.15	73.55	1118.3	135.56	3630.9	5554.271	-111.08	-5691.02	-1.32	-7.58	0	0	-5811	-256.73	-2.26%
2/18/2008	W8P7	3370	250774	86	118	0	0	42.66	41.15	46.16	70.87	7.90	166.78	0.17	68.86	1049.2	124.79	3287.6	4906.085	-95.056	-5221	-1.39	-6.21	0	0	-5323.65	-417.5691	-4.08%
2/18/2008	Effluent East	8368	132980	338	30	28	0	263.03	169.13	15.69	81.82	10.66	239.28	0.15	80.69	442.71	58.059	779.48	2140.675	-236.03	-2768.58	-5.45	-1.58	-0.88	0	-3012.53	-871.8566	-16.92%
2/18/2008	Effluent West	9184	113656	298	72	16	0	229.09	118.91	8.29	66.07	9.54	201.47	0.22	84.12	311.13	43.097	529.97	1601.903	-259.05	-2366.27	-4.81	-3.79	-0.51	0	-2634.42	-1032.515	-24.37%
2/18/2008	Effluent Seep	11092	223032	246	84	24	0	7585.78	165.16	9.00	72.98	16.59	234.27	0.25	86.52	348.32	74.402	583.86	9177.119	-312.87	-4643.42	-3.97	-4.42	-0.76	0	-4965.44	4211.6797	29.78%
2/8/2008	W8P3	3664	164508	118	42	36	0	58.88	61.10	29.67	70.04	9.63	150.88	0.13	68.60	833.57	103.23	2298	3683.762	-103.35	-3424.98	-1.9	-2.21	-1.14	0	-3533.58	150.18024	2.08%
2/8/2008	W8P5	4592	270088	100	64	0	0	38.02	211.09	57.96	69.86	6.15	142.88	0.19	78.73	1134.7	140.16	3699.8	5579.555	-129.52	-5623.11	-1.61	-3.37	0	0	-5757.61	-178.0599	-1.57%
2/8/2008	W8P7	4250	252622	116	76	0	0	34.67	43.51	47.94	68.73	7.46	145.43	0.13	70.38	1057.4	130.95	3351.5	4958.072	-119.88	-5259.47	-1.87	-4	0	0	-5385.22	-427.152	-4.13%
2/8/2008	Effluent East	8834	157154	238	140	48	0	263.03	219.49	18.10	92.22	13.85	239.16	0.13	82.04	495.37	66.755	892.76	2382.904	-249.18	-3271.87	-3.84	-7.37	-1.52	0	-3533.78	-1150.872	-19.45%
2/8/2008	Effluent West	9748	113642	336	610	30	0	398.11	100.67	8.08	75.58	14.44	180.68	0.28	92.87	345.11	49.03	579.37	1844.211	-274.96	-2365.97	-5.42	-32.1	-0.95	0	-2679.41	-835.1975	-18.46%
2/8/2008	Effluent Seep	10570	254568	246	262	34	0	3981.07	382.77	10.31	76.98	18.66	261.85	0.19	93.26	401.07	55.399	672.19	5953.755	-298.14	-5299.99	-3.97	-13.8	-1.07	0	-5616.97	336.78926	2.91%
1/22/2008	W8P3	5080	145638	88	618	68	0	165.96	21.02	25.12	75.45	11.39	172.12	0.23	82.60	761.16	96.654	1927.7	3339.447	-143.29	-3032.12	-1.42	-32.5	-2.15	0	-3211.5	127.9444	1.95%
1/22/2008	W8P5	4144	255356	86	192	0	0	3.72	301.82	51.95	72.52	7.48	152.22	0.13	81.51	1068.9	138.88	3294.1	5173.218	-116.89	-5316.39	-1.39	-10.1	0	0	-5444.78	-271.5579	-2.56%
1/22/2008	W8P7	3584	241850	104	12	0	0	6.46	146.89	47.18	67.47	7.49	135.43	0.13	73.12	1044.2	132.23	3179.8	4840.432	-101.09	-5035.21	-1.68	-0.63	0	0	-5138.61	-298.1753	-2.99%
1/22/2008	Effluent East	6780	224708	92	178	0	0	275.42	304.47	37.64	132.31	16.18	390.93	0.13	79.69	845.09	105.25	1482.6	3669.735	-191.24	-4678.32	-1.48	-9.37	0	0	-4880.41	-1210.676	-14.16%
1/22/2008	Effluent West	13228	122582	160	648	28	0	933.25	158.20	12.62	79.09	6.99	218.26	0.2	110.31	468.22	65.757	772.49	2825.401	-373.12	-2552.1	-2.58	-34.1	-0.88	0	-2962.79	-137.3906	-2.37%
1/22/2008	Effluent Seep	13964	184048	188	394	32	0	2290.87	95.32	13.14	76.89	10.95	227.49	0.19	108.13	477.27	63.839	825.89	4189.991	-393.88	-3831.79	-3.03	-20.7	-1.01	0	-4250.45	-60.4627	-0.72%
12/6/2007	W8P3	9296	252810	748	0	0	0	407.38	88.37	31.16	108.00	19.64	390.71	16.1	90.30	766.1	139.39	1773	3830.144	-262.21	-5263.39	-12.1	0	0	0	-5537.66	-1707.519	-18.23%
12/6/2007	W8P5	5708	254698	410	28	0	0	47.86	61.70	53.26	99.50	14.46	292.31	2.56	88.82	979.22	131.46	2783.1	4554.223	-161	-5302.7	-6.61	-1.47	0	0	-5471.79	-917.5637	-9.15%
12/6/2007	W8P7	3464	243476	302	0	0	0	436.52	12.47	51.59	76.56	12.45	198.47	20.1	70.12	990.74	132.49	3166.8	5168.303	-97.708	-5069.06	-4.87	0	0	0	-5171.64	-3.334772	-0.03%
12/6/2007	Effluent East																											
12/6/2007	Effluent West																											
12/6/2007	Effluent Seep	11286	436562	80	8	0	0	2187.76	619.64	29.09	133.38	28.17	565.94	13.2	106.53	683.81	74.198	1193.2	5634.867	-318.34	-9089.02	-1.29	-0.42	0	0	-9409.07	-3774.205	-25.09%

Geochemistry of Davis Mine Samples

Date	Sample	Depth to Water	pH	Well ORP	Eh	pe	Temp.	Conductivity	H^+	DOC	Fe^{3+}	Fe^{2+}	Ave Total Fe	Mn^{2+}	Zn^{2+}	Cu^{2+}	Al^{3+}	Pb^{2+}	Na^{1+}	Mg^{2+}	K^{1+}	Ca^{2+}	Si^{4+}
		1/10 ft		mV	V		°C	µS/cm		mg/L	mol	mol	micrograms/Liter (µg/L)										
10/23/2007	W8P3	4.33	3.70	473.3	0.68	12.44	13.6	436.3	199.53	0.57	1.66E-05	4.10E-06	1155	1049	3439	474.2	3058	108.1	1792	10980	4749	44330	15970
10/23/2007	W8P5	4.50	4.37	360.3	0.57	10.37	12.6	521	42.66	0.54			6835	1731	2448	226.2	1414	108.1	1776	12960	5830	69360	17660
10/23/2007	W8P7	4.08	4.38	367	0.58	10.50	12.3	482.8	41.69	0.46			1887.5	1421	2240	248.7	1331	255	1554	12430	5530	66210	13450
10/23/2007	Effluent East	NA	3.09	504.9	0.71	12.99	16.2	528	812.83	5.86			2987.5	1076	3787	413.6	3262	108.1	1693	9230	4591	25900	18440
10/23/2007	Effluent West	NA	3.09	507.9	0.72	13.09	13.8	671	812.83	1.13			12755	948	4975	217	3003	108.1	2342	9350	4646	26790	14680
10/23/2007	Effluent Seep	NA	2.79	496.3	0.71	12.89	14	921	1621.81	2.29			2886.5	1028	4868	470.1	6460	108.1	2522	10670	4127	27960	21400
10/8/2007	W8P3	4.50	4.42	469.6	0.68	12.31	14.8	436.8	38.02	1.59	1.07E-05	2.68E-07	613	1092	3572	532	2867	108.1	1972	11730	5190	46200	17080
10/8/2007	W8P5	4.58	5.14	356.7	0.57	10.27	13.2	530.1	7.24	0.56			7175	1698	2499	252.7	1329	108.1	1825	13540	5940	67670	18310
10/8/2007	W8P7	4.00	5.05	364.1	0.57	10.40	13.7	478	8.91	0.54			2064	1456	2150	257.3	1256	108.1	1508	12720	5580	66310	13420
10/8/2007	Effluent East	NA	3.70	504.7	0.71	12.93	17.8	555	199.53	0.76			2846	1069	3429	371.2	2603	108.1	1676	9380	4783	26260	18310
10/8/2007	Effluent West	NA	3.54	501.8	0.71	12.91	16.7	680	288.40	1.07			11975	988	4805	210.6	2630	108.1	2446	9150	6200	27030	15220
10/8/2007	Effluent Seep	NA	3.62	504.1	0.71	12.96	15.7	816	239.88	11.75			2011	1012	4778	262.2	5210	108.1	2652	10670	6520	26280	21900
9/25/2007	W8P3	4.92	3.84	450.5	0.66	11.99	15.1	453.1	144.54	0.75	1.10E-05	4.75E-06	880.5	1019	3484	416.2	3095	187.4	2036	10060	5160	41480	16620
9/25/2007	W8P5	4.83	4.63	348.9	0.56	10.15	13.1	516	23.44	0.54			6750	1651	2291	263.9	1308	271.6	1825	11900	6180	68540	17620
9/25/2007	W8P7		4.65	336.8	0.55	9.93	13	480.6	22.39	0.56			2499	1420	2284	298	1510	86.7	1638	11830	6010	65110	14070
9/25/2007	Effluent East	NA	3.50	493	0.70	12.74	17.1	528	316.23	0.70			3433	1011	3445	410.1	2780	126.2	1745	8350	5170	25040	19030
9/25/2007	Effluent West	NA	3.39	486.8	0.69	12.65	15.9	670	407.38	0.72			12680	925	4810	233.1	2844	86.7	2467	8770	5040	26350	14570
9/25/2007	Effluent Seep	NA	3.17	488.8	0.70	12.71	15.4	811	676.08	2.90			1734	928	4461	362	5290	86.7	2861	9920	6430	25740	21520
9/11/2007	W8P3	4.00	4.16	409.1	0.62	11.24	14.4	410.3	69.18	0.65	5.42E-06	4.13E-06	533.5	1005	2806	439.1	2083	86.7	1756	9520	4924	43090	14230
9/11/2007	W8P5	4.50	4.51	347.1	0.56	10.14	12	553	30.90	0.51			6330	1667	2200	251.6	1232	151.9	1767	12320	6380	67530	16260
9/11/2007	W8P7	4.58	4.54	359.4	0.57	10.36	12.3	450	28.84	0.49			640.5	1126	2079	266.6	1188	86.7	1490	10570	5700	54960	12450
9/11/2007	Effluent East	NA	3.29	460.8	0.67	12.19	15.4	508	512.86	0.78			4239.5	753	2752	298.4	1929	103.7	1432	6420	4470	18220	13870
9/11/2007	Effluent West	NA	3.25	465.1	0.67	12.29	14.7	557	562.34	1.19			11080	624	3203	172.1	1936	119.6	1826	5830	4302	17300	11030
9/11/2007	Effluent Seep	NA	3.14	465.7	0.67	12.27	16.3	766	724.44	2.06			1229.5	854	4124	255.5	4151	86.7	2598	8610	4236	22850	20100
8/20/2007	W8P3	5.50	3.44	400.1	0.61	11.07	16.1	460.7	363.08	0.96	1.35E-06	1.13E-05	706.5	836	3372	452.7	3125	30.96	2135	9100	6324	31770	16100
8/20/2007	W8P5	4.92	4.44	348	0.56	10.15	12.5	518	36.31	0.46			5122	1581	2194	219.9	1275	30.96	1615	12260	7930	67660	16090
8/20/2007	W8P7	4.50	4.43	338.9	0.55	9.97	13.1	458.9	37.15	0.55			877	1230	2135	255.8	1346	30.96	1384	11020	7037	58790	13650
8/20/2007	Effluent East	NA	3.27	461.6	0.67	12.16	18.3	553	537.03	0.64			3518	947	3230	332.7	2346	30.96	1750	8540	6005	25220	18330
8/20/2007	Effluent West	NA	3.12	465.6	0.67	12.28	16	627	758.58	0.79			11527	815	4192	183.4	2683	30.96	2528	8270	6409	25540	14620
8/20/2007	Effluent Seep	NA	3.03	449.2	0.66	11.98	15.9	714	933.25	2.45			1094	710	3465	247	3739	32.06	2782	8380	5118	21280	20530
8/4/2007	W8P3	NA	3.39	451.6	0.66	11.97	18.3	467.5	407.38	12.46	6.29E-06	8.03E-06	799.5	749	3053	484.7	2768	150.6	2236	9580	6910	31720	15650
8/4/2007	W8P5	NA	4.43	325.8	0.54	9.72	14.1	526	37.15	1.04			380.95	1571	2215	231.4	1215	30.96	1607	14050	5740	71200	14120
8/4/2007	W8P7	NA	4.50	306.3	0.52	9.36	14.5	440.8	31.62	0.62			47.91	1115	2151	296.2	1240	30.96	1344	12070	4692	58370	11170
8/4/2007	Effluent East	NA	3.15	486.9	0.68	12.44	28.4	547	707.95	0.78			3131	912	3185	294.2	1882	30.96	1526	8700	5120	24140	17520
8/4/2007	Effluent West	NA	3.12	470.8	0.67	12.21	24.8	586	758.58	0.83			8648.5	675	3671	172.8	2249	30.96	2487	8040	4101	21630	13320
8/4/2007	Effluent Seep	NA	2.97	485.7	0.71	12.94		572	1071.52	2.30			840	545	2895	253	2940	30.96	2041	6480	2993	15400	14880
7/2/2007	W8P3	NA	3.71	462.3	0.67	12.21	15.1	370.8	194.98	1.68	6.00E-06	2.34E-06	465.6	902	2886	538	1978	86.2	1794	10260	3897	43510	13600
7/2/2007	W8P5	NA	3.99	314	0.53	9.58	10.8	538	102.33	0.59			4694	1711	2349	283	1374	54.4	1686	14610	5600	75120	13940
7/2/2007	W8P7	NA	4.30	382	0.59	10.79	11.3	476.5	50.12	0.57			1352.5	1389	2343	311.3	1380	52.8	1446	13320	4988	68730	11500
7/2/2007	Effluent East	NA	3.20	495.5	0.70	12.76	19.2	503	630.96	0.76			4192	1017	3615	494.1	2394	155.8	1589	9040	4355	26390	16220
7/2/2007	Effluent West	NA	2.93	468.8	0.68	12.36	15.1	461.3	1174.90	0.64			8230	629	3622	272.3	2409	168.9	2442	7530	3434	20200	12370
7/2/2007	Effluent Seep	NA	3.05	492.1	0.70	12.77	15.6	572	891.25	5.44			1156	531	3337	438.4	3106	115.6	2747	6970	3439	17330	14880
6/4/2007	W8P3	3.77	4.23	404	0.61	11.08	17.5	434.4	58.88	1.53	7.82E-06	5.33E-06	734	626	2779	573	2191	79	2277	8740	4224	35350	13200
6/4/2007	W8P5	3.44	4.34	317.3	0.53	9.61	12	601	45.71	1.11			4372.5	1516	2165	241.7	1286	49.51	1817	14860	6470	79460	13770
6/4/2007	W8P7	2.62	3.76	336.7	0.55	9.99	11.2	488.1	173.78	0.80			2004	1412	2223	275	1347	135.9	1800	15030	6540	81700	11880
6/4/2007	Effluent East	NA	3.97	492	0.70	12.75	14.3	498	107.15	1.15			5303.5	515	2850	380.7	1440	48.24	2300	6440	3273	18860	10530
6/4/2007	Effluent West	NA	4.13	505.9	0.72	13.04	11.8	443	74.13	0.99			6328	327.9	2714	377.9	1564	13.16	2946	5590	2694	15530	8430
6/4/2007	Effluent Seep	NA	3.23	560.4	0.77	14.06	12.8	784	588.84	72.98			2618.5	422.4	3277	665	3535	408.6	2585	5840	3040	15890	15200

Geochemistry of Davis Mine Samples

Date	Sample	Cl^{1-}	SO_4^{2-}	NO_3^-	F^{1-}	PO_4^{3-}	Br^{1-}	H	Ave Total Fe	Mn	Zn	Cu	Al	Pb	Na	Mg	K	Ca	+ Charge Sum	Cl	SO_4	NO_3	F	PO_4	Br	- Charge Sum	Total Charge	Error
		micrograms/Liter (µg/L)								microequivalents/Liter (µequiv/L)										microequivalents/Liter (µequiv/L)								
10/23/2007	W8P3	4508	213096	166	64	80	0	199.53	62.04	38.19	105.18	14.92	340.01	1.04	77.95	903.52	121.46	2212.2	4076.037	-127.16	-4436.56	-2.68	-3.37	-2.53	0	-4572.29	-496.2527	-5.74%
10/23/2007	W8P5	3326	292732	60	6	0	0	42.66	367.16	63.02	74.87	7.12	157.22	1.04	77.25	1066.4	149.11	3461.3	5467.154	-93.815	-6094.55	-0.97	-0.32	0	0	-6189.64	-722.4901	-6.20%
10/23/2007	W8P7	2998	263596	64	0	0	0	41.69	101.39	51.73	68.51	7.83	147.99	2.46	67.60	1022.8	141.44	3304.1	4957.528	-84.563	-5487.95	-1.03	0	0	0	-5573.54	-616.0158	-5.85%
10/23/2007	Effluent East	4844	262134	48	166	0	0	812.83	160.48	39.17	115.83	13.02	362.69	1.04	73.64	759.51	117.42	1292.5	3748.124	-136.63	-5457.51	-0.77	-8.74	0	0	-5603.65	-1855.53	-19.84%
10/23/2007	Effluent West	13724	363810	38	24	0	0	812.83	685.18	34.51	152.16	6.83	333.90	1.04	101.87	769.39	118.83	1336.9	4353.432	-387.11	-7574.36	-0.61	-1.26	0	0	-7963.34	-3609.908	-29.31%
10/23/2007	Effluent Seep	10802	452310	134	38	0	0	1621.81	155.06	37.42	148.89	14.80	718.27	1.04	109.70	878.01	105.55	1395.3	5185.835	-304.69	-9416.89	-2.16	-2	0	0	-9725.74	-4539.901	-30.45%
10/8/2007	W8P3	5540	216416	248	192	0	0	38.02	32.93	39.75	109.25	16.74	318.77	1.04	85.78	965.23	132.74	2305.5	4045.773	-156.26	-4505.68	-4	-10.1	0	0	-4676.05	-630.2803	-7.23%
10/8/2007	W8P5	3404	268802	36	106	0	0	7.24	385.43	61.82	76.43	7.95	147.77	1.04	79.38	1114.2	151.92	3376.9	5410.083	-96.015	-5596.33	-0.58	-5.58	0	0	-5698.51	-288.4268	-2.60%
10/8/2007	W8P7	2700	253470	48	68	0	0	8.91	110.87	53.01	65.76	8.10	139.65	1.04	65.59	1046.7	142.72	3309	4951.401	-76.158	-5277.13	-0.77	-3.58	0	0	-5357.64	-406.2391	-3.94%
10/8/2007	Effluent East	5044	275152	40	172	0	0	199.53	152.88	38.92	104.88	11.68	289.42	1.04	72.90	771.86	122.33	1310.4	3075.887	-142.27	-5728.54	-0.65	-9.05	0	0	-5880.51	-2804.624	-31.31%
10/8/2007	Effluent West	13724	366018	36	116	0	0	288.40	643.28	35.97	146.96	6.63	292.42	1.04	106.40	752.93	158.57	1348.9	3781.476	-387.11	-7620.33	-0.58	-6.11	0	0	-8014.12	-4232.645	-35.88%
10/8/2007	Effluent Seep	15258	409584	142	170	0	0	239.88	108.03	36.84	146.14	8.25	579.29	1.04	115.36	878.01	166.76	1311.4	3591.038	-430.38	-8527.35	-2.29	-8.95	0	0	-8968.97	-5377.928	-42.82%
9/25/2007	W8P3	6496	236276	84	272	90	0	144.54	47.30	37.10	106.56	13.10	344.12	1.81	88.56	827.81	131.98	2070	3812.845	-183.23	-4919.16	-1.36	-14.3	-2.84	0	-5120.9	-1308.057	-14.64%
9/25/2007	W8P5	3374	256510	30	138	0	0	23.44	362.60	60.10	70.07	8.31	145.43	2.62	79.38	979.22	158.06	3420.3	5309.575	-95.169	-5340.42	-0.48	-7.26	0	0	-5443.34	-133.7617	-1.24%
9/25/2007	W8P7	2914	221036	40	96	0	0	22.39	134.24	51.69	69.86	9.38	167.89	0.84	71.25	973.46	153.72	3249.2	4903.881	-82.194	-4601.87	-0.65	-5.05	0	0	-4689.76	214.12032	2.23%
9/25/2007	Effluent East	4384	256192	26	198	0	0	316.23	184.41	36.81	105.37	12.91	309.10	1.22	75.90	687.1	132.23	1249.6	3110.84	-123.66	-5333.8	-0.42	-10.4	0	0	-5468.3	-2357.459	-27.48%
9/25/2007	Effluent West	13438	361842	26	170	0	0	407.38	681.15	33.67	147.12	7.34	316.22	0.84	107.31	721.66	128.91	1314.9	3866.521	-379.04	-7533.38	-0.42	-8.95	0	0	-7921.79	-4055.271	-34.40%
9/25/2007	Effluent Seep	12416	398106	134	166	0	0	676.08	93.15	33.78	136.44	11.39	588.18	0.84	124.45	816.29	164.46	1284.5	3929.56	-350.21	-8288.38	-2.16	-8.74	0	0	-8649.5	-4719.937	-37.52%
9/11/2007	W8P3	4127	199540	613	132	0	0	69.18	28.66	36.59	85.82	13.82	231.60	0.84	76.38	783.38	125.94	2150.3	3602.517	-116.41	-4154.33	-9.89	-6.95	0	0	-4287.58	-685.0592	-8.68%
9/11/2007	W8P5	3640	283647	69	122	0	0	30.90	340.04	60.69	67.29	7.92	136.98	1.47	76.86	1013.8	163.18	3369.9	5269.032	-102.67	-5905.4	-1.11	-6.42	0	0	-6015.61	-746.5745	-6.62%
9/11/2007	W8P7	2333	219881	63	84	0	0	28.84	34.41	40.99	63.59	8.39	132.09	0.84	64.81	869.78	145.79	2742.7	4132.174	-65.806	-4577.82	-1.02	-4.42	0	0	-4649.07	-516.8913	-5.89%
9/11/2007	Effluent East	4282	225045	31	103	0	0	512.86	227.74	27.41	84.17	9.39	214.48	1	62.29	528.29	114.33	909.23	2691.186	-120.78	-4685.33	-0.5	-5.42	0	0	-4812.04	-2120.849	-28.27%
9/11/2007	Effluent West	8993	250880	199	78	0	0	562.34	595.20	22.72	97.97	5.42	215.26	1.15	79.43	479.74	110.03	863.32	3032.561	-253.66	-5223.21	-3.21	-4.11	0	0	-5484.18	-2451.623	-28.79%
9/11/2007	Effluent Seep	12280	305023	366	100	0	0	724.44	66.05	31.09	126.14	8.04	461.54	0.84	113.01	708.5	108.34	1140.3	3488.246	-346.38	-6350.44	-5.9	-5.26	0	0	-6707.98	-3219.738	-31.58%
8/20/2007	W8P3	9477	256827	96	221	0	0	363.08	37.95	30.43	103.14	14.25	347.46	0.3	92.87	748.82	161.75	1585.4	3485.445	-267.31	-5347.02	-1.55	-11.6	0	0	-5627.52	-2142.07	-23.51%
8/20/2007	W8P5	4127	301211	154	143	0	0	36.31	275.14	57.56	67.11	6.92	141.76	0.3	70.25	1008.8	202.82	3376.4	5243.429	-116.41	-6271.07	-2.48	-7.53	0	0	-6397.49	-1154.065	-9.91%
8/20/2007	W8P7	3063	245836	96	98	0	0	37.15	47.11	44.78	65.30	8.05	149.66	0.3	60.20	906.81	179.98	2933.8	4433.122	-86.397	-5118.19	-1.55	-5.16	0	0	-5211.3	-778.1746	-8.07%
8/20/2007	Effluent East	5117	279518	102	137	0	0	537.03	188.98	34.48	98.79	10.47	260.85	0.3	76.12	702.74	153.59	1258.5	3321.885	-144.33	-5819.44	-1.65	-7.21	0	0	-5972.63	-2650.741	-28.52%
8/20/2007	Effluent West	14470	317777	109	100	0	0	758.58	619.21	29.67	128.22	5.77	298.32	0.3	109.96	680.52	163.92	1274.5	4068.974	-408.15	-6615.97	-1.76	-5.26	0	0	-7031.14	-2962.169	-26.69%
8/20/2007	Effluent Seep	13726	323146	163	91	0	0	933.25	58.77	25.85	105.98	7.77	415.73	0.31	121.01	689.57	130.9	1061.9	3551.072	-387.16	-6727.75	-2.63	-4.79	0	0	-7122.33	-3571.263	-33.46%
8/4/2007	W8P3	12979	239244	126	108	0	0	407.38	42.95	27.27	93.38	15.26	307.77	1.45	97.26	788.32	176.73	1582.9	3540.671	-366.09	-4980.95	-2.03	-5.68	0	0	-5354.76	-1814.089	-20.39%
8/4/2007	W8P5	3946	303816	60	142	0	0	37.15	20.46	57.19	67.75	7.28	135.09	0.3	69.90	1156.1	146.81	3553.1	5251.153	-111.3	-6325.31	-0.97	-7.47	0	0	-6445.05	-1193.902	-10.21%
8/4/2007	W8P7	2277	240591	52	112	0	0	31.62	2.57	40.59	65.79	9.32	137.87	0.3	58.46	993.21	120.01	2912.8	4372.568	-64.226	-5008.99	-0.84	-5.9	0	0	-5079.95	-707.3864	-7.48%
8/4/2007	Effluent East	6213	267200	49	249	0	0	707.95	168.19	33.20	97.42	9.26	209.25	0.3	66.38	715.9	130.95	1204.7	3343.449	-175.25	-5562.98	-0.79	-13.1	0	0	-5752.13	-2408.677	-26.48%
8/4/2007	Effluent West	14239	283226	131	91	0	0	758.58	464.58	24.57	112.28	5.44	250.06	0.3	108.18	661.59	104.89	1079.4	3569.866	-401.63	-5896.64	-2.11	-4.79	0	0	-6305.17	-2735.306	-27.70%
8/4/2007	Effluent Seep	11354	259360	78	101	0	0	1071.52	45.12	19.84	88.55	7.96	326.89	0.3	88.78	533.22	76.551	768.5	3027.235	-320.26	-5399.76	-1.26	-5.32	0	0	-5726.59	-2699.353	-30.84%
7/2/2007	W8P3	6362	213451	106	118	0	0	194.98	25.01	32.84	88.27	16.93	219.93	0.83	78.03	844.27	99.672	2171.3	3772.039	-179.45	-4443.95	-1.71	-6.21	0	0	-4631.32	-859.2837	-10.23%
7/2/2007	W8P5	4345	341037	58	142	0	0	102.33	252.15	62.29	71.85	8.91	152.77	0.53	73.34	1202.2	143.23	3748.7	5818.298	-122.56	-7100.23	-0.94	-7.47	0	0	-7231.2	-1412.904	-10.83%
7/2/2007	W8P7	3428	291550	62	102	0	13	50.12	72.65	50.57	71.66	9.80	153.44	0.51	62.90	1096.1	127.58	3429.8	5125.103	-96.692	-6069.94	-1	-5.37	0	-0.163	-6173.16	-1048.058	-9.28%
7/2/2007	Effluent East	4847	328740	69	121	0	0	630.96	225.19	37.02	110.57	15.55	266.18	1.5	69.12	743.88	111.39	1316.9	3528.287	-136.72	-6844.22	-1.11	-6.37	0	0	-6988.42	-3460.128	-32.90%
7/2/2007	Effluent West	13527	310409	51	90	0	0	1174.90	442.10	22.90	110.78	8.57	267.85	1.63	106.22	619.63	87.83	1008	3850.44	-381.55	-6462.57	-0.82	-4.74	0	0	-6849.68	-2999.243	-28.03%
7/2/2007	Effluent Seep	14682	322624	153	92	0	110	891.25	62.10	19.33	102.06	13.80	345.35	1.12	119.49	573.54	87.958	864.81	3080.81	-414.13	-6716.88	-2.47	-4.84	0	-1.377	-7139.7	-4058.89	-39.71%
6/4/2007	W8P3	8229	233288	132	285	0	0	58.88	39.43	22.79	85.00	18.03	243.61	0.76	99.04	719.19	108.04	1764.1	3158.842	-232.11	-4856.95	-2.13	-15	0	0	-5106.19	-1947.35	-23.56%
6/4/2007	W8P5	4554	302096	44	342	0	0	45.71	234.88	55.19	66.22	7.61	142.99	0.48	79.04	1222.8	165.48	3965.3	5985.648	-128.45	-6289.5	-0.71	-18	0	0	-6436.66	-451.0162	-3.63%
6/4/2007	W8P7	3861	298422	113	340	0	0	173.78	107.65	51.40	67.99	8.66	149.77	1.31	78.30	1236.8	167.27	4077	6119.962	-108.91	-6213.01	-1.82	-17.9	0	0	-6341.63	-221.6721	-1.78%
6/4/2007	Effluent East	10324	255379	158	81	0	0	107.15	284.89	18.75	87.17	11.98	160.11	0.47	100.04	529.93	83.712	941.16	2325.375	-291.2	-5316.87	-2.55	-4.26	0	0	-5614.89	-3289.516	-41.43%
6/4/2007	Effluent West	14527	237542	233	77	0	0	74.13	339.93	11.94	83.01	11.89	173.90	0.13	128.14	459.99	68.903	774.99	2126.948	-409.76	-4945.52	-3.76	-4.05	0	0	-5363.08	-3236.137	-43.21%
6/4/2007	Effluent Seep	11850	320780	132	679	0	0	588.84	140.66	15.38	100.23	20.93	393.05	3.94	112.44	480.56	77.753	792.95	2726.74	-334.25	-6678.49	-2.13	-35.7	0	0	-7050.61	-4323.87	-44.22%

Table D2. Hydrous Ferric Oxide Surface Reactions - Modelling Inputs, Conditions and Outputs

Whole Year 2004	PHREEQC Input Solution for Hydrous Ferric Oxide Surface Reactions: Whole Year 2004 Average (May-May, n=6)						
	pH	ORP (mV)	(^{o}C)	pe	Fe^{tot}	Mn^{2+} (260)	Zn^{2+} (213)
	3.09	406.50	8.92	11.93	1031.17	852.50	3817.33
µg/L	Cu^{2+}	Al^{3+} (167)	Na^{1+}	Mg^{2+}	K^{1+}	Ca^{2+}	Si^{4+}
	535.23	2898.83	1955.50	10411.67	17901.67	41410.00	13416.67
	Cl^{-}	SO_4^{2-}	NO_3^{-}	F^{-}	PO_4^{3-}	Br^{-}	
	9851.83	257543.33	70.67	149.50	0.00	61.17	

Summer 2007	PHREEQC Input Solution for Hydrous Ferric Oxide Surface Reactions: Summer 2007 Average (June-October, n=8)						
	pH	ORP (mV)	(^{o}C)	pe	Fe^{tot}	Mn^{2+} (260)	Zn^{2+} (213)
	3.73	440.06	15.6	11.66	735.95	909.75	3173.88
µg/L	Cu^{2+}	Al^{3+} (167)	Na^{1+}	Mg^{2+}	K^{1+}	Ca^{2+}	Si^{4+}
	488.74	2645.63	1999.75	9996.25	5172.25	39681.25	15306.25
	Cl^{-}	SO_4^{2-}					
	7214.75	226017.25					

Summer 2008	PHREEQC Input Solution for Hydrous Ferric Oxide Surface Reactions: Summer 2008 Average (May-October, n=8)						
	pH	ORP (mV)	(^{o}C)	pe	Fe^{tot}	Mn^{2+} (260)	Zn^{2+} (213)
	4.81	425.26	15.2	11.44	89.57	1007.38	2321.25
µg/L	Cu^{2+}	Al^{3+} (167)	Na^{1+}	Mg^{2+}	K^{1+}	Ca^{2+}	Si^{4+}
	275.43	1229.50	1496.50	11588.75	4627.38	55842.50	12927.50
	Cl^{-}	SO_4^{2-}					
	2939.88	197088.25					

Table D2. Hydrous Ferric Oxide Surface Reactions - Modelling Inputs, Conditions and Outputs

Conditions for Hydrous Ferric Oxide Surface in PHREEQCi

Dzombak and Morel Diffuse Double Layer	
Hfo_strong site	5.00E-06 # Sites (moles)
Hfo_weak site	4.00E-04 # Sites (moles)
Surface area	600 (m^2/g)
Mass	0.9 (g)

Table D2. Hydrous Ferric Oxide Surface Reactions - Modelling Inputs, Conditions and Outputs

Whole Year 2004

----------Surface composition----------

Hfo

8.903e-005 Surface charge, eq
1.591e-002 sigma, C/m**2
6.001e-002 psi, V
"=-2.468 -F*psi/RT"
8.472e-002 exp(-F*psi/RT)
6.000e+002 specific area, m**2/g
5.400e+002 m**2 for 9.000e-001 g

Hfo_s

5.000e-006 moles

Species	Moles	Mole Fraction	Molality	Log Molality
Hfo_sOH2+	4.987e-006	0.997	4.986e-006	-5.302
Hfo_sOH	6.267e-009	0.001	6.267e-009	-8.203
Hfo_sOCu+	4.272e-009	0.001	4.272e-009	-8.369
Hfo_sOHCa+2	2.585e-009	0.001	2.585e-009	-8.587
Hfo_sOZn+	3.613e-010	0.000	3.613e-010	-9.442
Hfo_sOMn+	4.236e-012	0.000	4.236e-012	-11.373
Hfo_sOFe+	9.613e-013	0.000	9.613e-013	-12.017
Hfo_sO-	1.804e-013	0.000	1.804e-013	-12.744

Hfo_w

4.000e-004 moles

Species	Moles	Mole Fraction	Molality	Log Molality
Hfo_wOH2+	2.421e-004	0.605	2.421e-004	-3.616
Hfo_wSO4-	1.572e-004	0.393	1.572e-004	-3.803
Hfo_wOHSO4-2	3.942e-007	0.001	3.942e-007	-6.404
Hfo_wOH	3.042e-007	0.001	3.042e-007	-6.517
Hfo_wOCu+	1.064e-009	0.000	1.064e-009	-8.973
Hfo_wOZn+	1.836e-011	0.000	1.836e-011	-10.736
Hfo_wO-	8.758e-012	0.000	8.758e-012	-11.058
Hfo_wOFe+	4.355e-013	0.000	4.355e-013	-12.361
Hfo_wOMg+	3.506e-013	0.000	3.506e-013	-12.455
Hfo_wOMn+	1.633e-013	0.000	1.633e-013	-12.787
Hfo_wOCa+	4.655e-014	0.000	4.655e-014	-13.332
Hfo_wOFeOH	2.872e-017	0.000	2.872e-017	-16.542
Hfo_wOFeOH	5.513e-018	0.000	5.513e-018	-17.259

Table D2. Hydrous Ferric Oxide Surface Reactions - Modelling Inputs, Conditions and Outputs

Summer 2007

----------Surface composition----------

Hfo

8.657e-005 Surface charge, eq
1.547e-002 sigma, C/m**2
6.194e-002 psi, V
"=-2.494 -F*psi/RT"
8.254e-002 exp(-F*psi/RT)
6.000e+002 specific area, m**2/g
5.400e+002 m**2 for 9.000e-001 g

Hfo_s

5.000e-006 moles

Species	Moles	Mole Fraction	Molality	Log Molality
Hfo_sOH2+	4.949e-006	0.990	4.949e-006	-5.305
Hfo_sOCu+	2.621e-008	0.005	2.621e-008	-7.582
Hfo_sOH	1.651e-008	0.003	1.651e-008	-7.782
Hfo_sOHCa+2	6.254e-009	0.001	6.254e-009	-8.204
Hfo_sOZn+	2.017e-009	0.000	2.017e-009	-8.695
Hfo_sOMn+	3.007e-011	0.000	3.007e-011	-10.522
Hfo_sOFe+	2.056e-012	0.000	2.056e-012	-11.687
Hfo_sO-	1.262e-012	0.000	1.262e-012	-11.899

Hfo_w

4.000e-004 moles

Species	Moles	Mole Fraction	Molality	Log Molality
Hfo_wOH2+	2.409e-004	0.602	2.409e-004	-3.618
Hfo_wSO4-	1.572e-004	0.393	1.572e-004	-3.803
Hfo_wOHSO4-2	1.047e-006	0.003	1.047e-006	-5.980
Hfo_wOH	8.039e-007	0.002	8.039e-007	-6.095
Hfo_wOCu+	6.544e-009	0.000	6.544e-009	-8.184
Hfo_wOZn+	1.028e-010	0.000	1.028e-010	-9.988
Hfo_wO-	6.145e-011	0.000	6.145e-011	-10.211
Hfo_wOMg+	2.226e-012	0.000	2.226e-012	-11.652
Hfo_wOMn+	1.163e-012	0.000	1.163e-012	-11.935
Hfo_wOFe+	9.340e-013	0.000	9.340e-013	-12.030
Hfo_wOCa+	2.998e-013	0.000	2.998e-013	-12.523
Hfo_wOFeOH	1.636e-016	0.000	1.636e-016	-15.786

Table D2. Hydrous Ferric Oxide Surface Reactions - Modelling Inputs, Conditions and Outputs

Summer 2008

----------Surface composition----------

Hfo

8.689e-005 Surface charge, eq
1.553e-002 sigma, C/m**2
6.205e-002 psi, V
"=-2.499 -F*psi/RT"
8.215e-002 exp(-F*psi/RT)
6.000e+002 specific area, m**2/g
5.400e+002 m**2 for 9.000e-001 g

Hfo_s

5.000e-006 moles

Species	Moles	Mole Fraction	Molality	Log Molality
Hfo_sOH2+	3.230e-006	0.646	3.230e-006	-5.491
Hfo_sOCu+	1.424e-006	0.285	1.424e-006	-5.847
Hfo_sOZn+	1.427e-007	0.029	1.427e-007	-6.846
Hfo_sOH	1.302e-007	0.026	1.302e-007	-6.885
Hfo_sOHCa+2	7.020e-008	0.014	7.020e-008	-7.154
Hfo_sOMn+	3.197e-009	0.001	3.197e-009	-8.495
Hfo_sO-	1.202e-010	0.000	1.202e-010	-9.920
Hfo_sOFe+	2.068e-012	0.000	2.068e-012	-11.684

Hfo_w

4.000e-004 moles

Species	Moles	Mole Fraction	Molality	Log Molality
Hfo_wOH2+	2.411e-004	0.603	2.411e-004	-3.618
Hfo_wSO4-	1.376e-004	0.344	1.376e-004	-3.861
Hfo_wOHSO4-2	1.106e-005	0.028	1.106e-005	-4.956
Hfo_wOH	9.718e-006	0.024	9.718e-006	-5.012
Hfo_wOCu+	5.450e-007	0.001	5.450e-007	-6.264
Hfo_wOZn+	1.115e-008	0.000	1.115e-008	-7.953
Hfo_wO-	8.973e-009	0.000	8.973e-009	-8.047
Hfo_wOMg+	3.812e-010	0.000	3.812e-010	-9.419
Hfo_wOMn+	1.896e-010	0.000	1.896e-010	-9.722
Hfo_wOCa+	6.233e-011	0.000	6.233e-011	-10.205
Hfo_wOFe+	1.441e-012	0.000	1.441e-012	-11.841
Hfo_wOFeOH	3.047e-015	0.000	3.047e-015	-14.516

Table D3: Well 8 Port 3: Saturation Indices for Select Minerals

	Sulfates		Clays					Iron Species		Aluminum Species		Si Species	
	K-Jarosite	Alunite	MontMoril	K-Mica	Kaolinite	Illite	Chlorite	$Fe(OH)_3$ a	Goethite	$Al(OH)_3$ an	Gibbsite	Quartz	SiO_2
6/4/2007	0.81	0.85	-3.19	-1.5	0.04	-6.45	-42.71	0.06	5.68	-3.61	-0.85	0.44	-0.88
7/2/2007	-0.35	-2.25	-6.87	-6.67	-3.08	-10.52	-51.3	-0.75	4.77	-5.2	-2.42	0.49	-0.85
8/7/2007	-0.93	-3.86	-9.09	-9.47	-4.94	-12.78	-55.58	-1.49	4.15	-6.12	-3.36	0.5	-0.82
8/20/2007	-3.01	-3.48	-8.53	-9.09	-4.48	-12.4	-55.47	-2.04	3.53	-5.95	-3.18	0.54	-0.78
9/11/2007	0.5	0.32	-3.78	-2.36	-0.57	-7.07	-44.69	-0.07	5.43	-3.98	-1.19	0.52	-0.82
9/25/2007	1.13	-0.086	-5.53	-4.88	-2.06	-9.04	-49.14	-0.3	5.22	-4.78	-1.99	0.57	-0.76
10/8/2007	1.84	2.51	-1.29	0.88	1.4	-4.4	-39.61	0.54	6.05	-3.07	-0.28	0.59	-0.75
10/23/2007	1.21	-1.78	-6.57	-6.33	-2.89	-10.19	-51.59	-0.32	5.15	-5.21	-2.41	0.58	-0.77
12/6/2007	0.05	-4.71	-10.25	-11.2	-5.85	-14.11	-61.4	-0.79	4.26	-6.86	-3.95	0.66	-0.76
1/22/2008	-0.12	-3.9	-8.39	-8.66	-4.3	-12.06	-56.02	-0.28	4.76	-6.04	-3.13	0.62	-0.81
2/8/2008	2.58	-1.14	-5.07	-4.13	-1.6	-8.43	-48.65	1.04	6.08	-4.7	-1.79	0.63	-0.8
2/18/2008	0.96	-2.05	-6.12	-5.52	-2.45	-9.55	-51.52	0.47	5.41	-5.17	-2.23	0.65	-0.79
3/7/2008	-0.95	-4.9	-9.76	-10.49	-5.41	-13.56	-58.56	-0.86	4.29	-6.52	-3.64	0.56	-0.84
3/20/2008	-0.89	-3.7	-7.95	-7.99	-4	-11.5	-53.68	-0.51	4.58	-5.86	-2.97	0.6	-0.81
4/4/2008	1.02	-4.78	-9.47	-10.12	-5.19	-13.25	-58.11	-0.08	5	-6.45	-3.55	0.59	-0.82
5/5/2008	-0.4	2.59	-1.01	1.49	1.72	-3.98	-38.13	0.22	5.55	-2.87	-0.03	0.52	-0.85
5/22/2008	0.64	2.11	-1.25	1.16	1.49	-4.19	-38.43	0.64	5.92	-3.03	-0.18	0.55	-0.83
6/3/2008	-1	3.65	0.32	3.37	2.8	-2.51	-33.58	-0.01	5.57	-2.19	0.58	0.43	-0.9
6/18/2008	-0.97	4.35	0.95	4.21	3.34	-1.86	-32.75	0.01	5.63	-1.9	0.86	0.42	-0.9
7/11/2008	-0.91	3.67	0.45	3.58	2.92	-2.37	-32.78	0.01	5.68	-2.07	0.67	0.39	-0.92
7/29/2008	-4.3	4.71	1.51	4.99	3.77	-1.24	-30.53	-1.16	4.61	-1.63	1.09	0.39	-0.9
8/22/2008	-1.22	3.93	0.71	3.88	3.08	-2.07	-32.72	-0.13	5.51	-2.07	0.69	0.46	-0.86
10/17/2008	-1.99	1.67	-1.02	1.51	1.62	-3.87	-36.84	-0.11	5.24	-2.96	-0.13	0.56	-0.81
Average	*-0.27*	*-0.27*	*-4.40*	*-3.19*	*-1.07*	*-7.71*	*-45.82*	*-0.26*	*5.13*	*-4.27*	*-1.45*	*0.53*	*-0.83*

BIBLIOGRAPHY

Adams, R., Ahlfeld, D., and Sengupta, A., 2007a. Investigating the Potential for Ongoing Pollution from an Abandoned Pyrite Mine. *Mine Water and the Environment* 26, 2-13.

Adams, L.K., Harrison, J.M., Lloyd, J.R., Langley, S., and Fortin, D., 2007b. Activity and Diversity of Fe(III)-Reducing Bacteria in a 3000-Year-Old Acid Mine Drainage Site Analogue. *Geomicrobiology Journal* 24, 295-305.

Ball, J.W. and Nordstrom, D.K., 1991, WATEQ4F--User's manual with revised thermodynamic data base and test cases for calculating speciation of major, trace and redox elements in natural waters: U.S. Geological Survey Open-File Report 90-129, 185 p.

Baker, J. P., Van Sickle J., Gagen C. J., DeWalle D. R., Sharpe W. E., Carline R. F., Baldigo B. P., Murdoch P. S., Bath D. W., Krester W. A.., Simonin H. A., and Wigington P. J., Jr., 1996. Episodic Acidification of Small Streams in the Northeastern United States: Effects on Fish Populations. *Ecological Applications*, 6, 422-437.

Becerra, C.A., López-Luna, E.L., Ergas, S.J., Nüsslein, K., 2009. Microcosm-based Study of an Acid Mine Drainage-Impacted Site through Biological Sulfate and Iron Reduction. *Geomicrobiology Journal*, 26: 9-20.

Benner, S.G., Blowes, D.W., Gould, W.D., Herbert Jr, R.B., Ptacek, C.J., 1999. Geochemistry of a permeable reactive barrier for metals and acid mine drainage. *Environmental Science and Technology* 33, 2793–2799.

Benner, S.G., Gould, W.D., and Blowes, D.W., 2000. Microbial populations associated with the generation and treatment of acid mine drainage. *Chemical Geology* 169:435-448.

Benner, S.G., Blowes, D.W., Ptacek, C.J., Mayer, K.U., 2002. Rates of sulfate reduction and metal sulfide precipitation in a permeable reactive barrier. *Applied Geochemistry* 17: 301-320.

Berner, R.A. and Morse, J.W., 1974. Dissolution Kinetics of Calcium Carbonate in Sea Water IV. Theory of Calcite Dissolution. *American Journal of Science* 274: 108-134.

Bigham, J.M., Schwertmann, U., Traina, S.J., Winland, R.L., and Wolf, M., 1996. Schwertmannite and the chemical modeling of iron in acid sulfate waters. *Geochimica et Cosmochimica Acta* 60: 2111-2121.

Bloom, J.E., 2005, Natural Attenuation of Acid Mine Drainage in Groundwater and Streamwater at the Davis Pyrite Mine in Rowe, MA. M.S. Thesis, Univ. of Massachusetts-Amherst. 205p.

Bloom, J.E., Yuretich, R.F., and Gál, N.E, 2007. Environmental Consequences of Acid Mine-Drainage from Davis Pyrite Mine, Rowe, Massachusetts. *Northeastern Geology and Environmental Sciences,* 29:107-120.

Blowes, D.W., Ptacek, C.J., and Jurjovec, J., 2003. "Mill Tailings: Hydrogeology and Geochemistry", chapter in Environmental Aspects of Mine Wastes, Mineralogical Association of Canada, Short Course Series Volume 31, Vancouver, Jambor, J.L., Blowes, D.W., and Ritchie, A.I.M, (Eds) 95-116.

Blowes, D.W., Ptacek, C.J., Jambor, J.L., Weisener, C.G., 2005. The Geochemistry of Acid Mine Drainage, chapter 9 in Treatise on Geochemistry; *Environmental Geochemistry*, Elsevier, Holland. 149-201.

Bolzicco, J., Carrera, J., and Ayora, C., 2004. Eficiencia de la Barrera Permeable Reactiva de Aznalcóllar (Sevilla; España) como remedio de Aguas Ácidas de Mina. *Revista Latino-Americano de Hidrogeología*, 4:27-34.

Bond P.L., Druschel, G.K., and Banfield, J. F., 2000. Comparison of Acid Mine Drainage Microbial Communities in Physically and Geochemically Distinct Ecosystems. *Applied and Environmental Microbiology,* 66: 4962-4971.

Caraballo, M.A., Rötting, T. S., Macías, F., Nieto, J.M, Ayora, C., 2009. Field multi-step limestone and MgO passive system to treat acid mine drainage with high metal concentrations. *Applied Geochemistry*. 2301-2311.

Carrera, J., Alcolea, A., Bolzicco, J., Bernet, O., Knudby, C., Manzano, M., Saaltink, M., Ayora, C., Domenech, C., de Pablo, J., Cortina, J.L., Coscera, G., Gibert, O., Galache, J., Silgado, A., Mantecon. R., 2001. An Experimental Geochemical Barrier at Aznalcollar, in Thornton S. and Oswald, S. (Eds) Proceeding of the 3rd International Conference on Groundwater Quality, 18-21 June 2001, Sheffield, UK. 407-409.:

Catalan L. J. J. and Yin G, 2003. Comparison of Calcite to Quicklime for Amending Partially Oxidized Sulfidic Mine Tailings before Flooding. *Environmental Science and Technology* 37: 1409-1413.

Cerato, A.B., 2003. Mineralogical Study of Davis Mine, Rowe, Massachusetts. M.S. Project Report. Department of Geosciences. University of Massachusetts-Amherst, 140p.

Doshi, S.M., 2006. Bioremediation of Acid Mine Drainage Using Sulfate-Reducing Bacteria. US-EPA. Office of Solid Waste and Emergency Response and Office of Superfund Remediation and Technology Innovation. 72p.

Field, S.W., 1985. Mineralogy and Petrology of the Davis Mine, Rowe, Massachusetts. M.S. Thesis, Department of Geosciences, University of Massachusetts-Amherst. 305p.

Fortin, D., Rioux, J.-P., Roy, M., 2002. Geochemistry of Iron and Sulfur in the Zone of Microbial Sulfate Reduction in Mine Tailings. *Water, Air and Soil Pollution: Focus,* 2, 37-56.

Gál, N.E., 2000, The Impact of Acid-Mine Drainage on Groundwater Quality, Davis Pyrite Mine, Massachusetts, Ph.D. Dissertation, Department of Geosciences, University of Massachusetts-Amherst, 153p.

Garcia Sanchez, A., Alvarez Ayuso, E., and Jimenez de Blas, O. 1999. Sorption of heavy metals from industrial waste water by low-cost mineral silicates. *Clay Minerals,* 34: 469-477.

Gibert, O., de Pablo, J., Cortina, J.L., and Ayora, C., 2002. Treatment of acid mine drainage by sulphate-reducing bacteria using permeable reactive barriers: A review from laboratory to full-scale experiments. *Re/Views in Environmental Science and Bio/*Technology 1: 327-333.

Gibert, O., de Pablo, J., Cortina, J.L., and Ayora, C., 2003. Evaluation of municipal compost/limestone/iron mixtures as filling material for permeable reactive barriers for in situ acid mine drainage treatment. *Journal of Chemical Technology and Biotechnology*, 78: 489-496.

Gibert, O., de Pablo, J., Cortina, J.L., and Ayora, C., 2005. Municipal compost-based mixture for acid mine drainage bioremediation: Metal retention mechanisms. *Applied Geochemistry* 20: 1648-1657.

Hammarstrom, J.M., Seal, R.R. II., Meier, A.L., Kornfield, J.M., 2005. Secondary sulfate minerals associated with acid drainage in the eastern US: recycling of metals and acidity in surficial environments. *Chemical Geology* 215, 407-431.

Harrison, J.M., 2005. Ferric Iron and Sulfate Reduction in the Attenuation of Acid Mine Drainage: A Microcosm study. M.S. Thesis, Department of Civil and Environmental Engineering, University of Massachusetts-Amherst. 144p.

Hatch, N.L and Hartshorn, J.H., 1968. Geologic Map of the Heath Quadrangle, Massachusetts-Vermont. U.S. Geological Survey Geologic Quadrangle Map # CQ-735.

Helm, K.R., 1982. The Geology and Geochemistry of the Davis Mine and the Surrounding Hawley Formation, Northwest Massachusetts. M.S. Project Report, State University of New York at Binghampton, Binghampton, N.Y., 144p.

Jambor J.L., Dutrizac, J.E., Groat, L.A., and Raudsepp, M., 2002. Static tests of neutralization potentials of silicate and aluminosilicate minerals. *Environmental Geology* 43, 1-17.

Johnson, C. A. 1986. The regulation of trace element concentrations in river and estuarine waters contaminated with acid mine drainage: The adsorption of Cu and Zn on amorphous Fe oxyhydroxides. *Geochimica et Cosmochimica Acta* 50: 2433-2438.

Johnson, D.B. and Hallberg, K.B., 2005. Acid mine drainage remediation options: a review. *Science of the Total Environment* 338, 3-14.

Johnson, D.B., Sen, A.M, Kimura, S., Rowe, O.F., and Hallberg, K.B., 2006. Novel biosulfidogenic system for selective recovery of metals from acidic leach liquors and waste streams. *Mineral Processing and Extractive Metallurgy* 115: 19-24.

Keddie, M., 2007. Trace Elements in the Sediments of Acidic Drainage from Davis Mine, Rowe, MA. Undergraduate Honors Thesis. Department of Geosciences. 30p.

Kleinmann, R.L.P., Crerar, D.A., Pacelli, R.R., 1981. Biogeochemistry of Acid Mine Drainage and a Method to Control Acid Formation. *Mining Engineering*, 300-306.

Klöppel, H., Fliedner, A., Kordel, W. 1997. Behaviour and ecotoxicology of aluminum in soils and waters—a review of the scientific literature. *Chemosphere* 35: 353-363.

Lee, G., Bigham, J.M., Faure, G., 2002. Removal of trace metals by coprecipitation with Fe, Al and Mn from natural waters contaminated with acid mine drainage in the Ducktown Mining District, Tennessee. *Applied Geochemistry* 17:569-581.

López-Luna, E., 2008. Contributions of Fe(III) and Sulfate-Reducing Bacteria to Attenuation of An Acid Mine Drainage Site: Linking Microcosm Studies and Geochemistry. PhD. Dissertation, Environmental and Civil Engineering, University of Massachusetts-Amherst. 194p.

Ludwig R.D., McGregor, R.G., Blowes, D.W., Benner, S.G., and Mountjoy, K., 2002. McCarthy, 1977. A Permeable Reactive Barrier for Treatment of Heavy Metals. *GROUND WATER*, 40: 59-66.

McKnight, D.M. and Bencala, K.E., 1990. The Chemistry of Iron, Aluminum, and Dissolved Organic Material in Three Acidic, Metal-Enriched, Mountain Streams, as Controlled by Watershed and in-Stream Processes. *Water Resources Research* 26: 3087-3100.

Monserrate, M., 2004. Field and Column Studies of Sulfate Reducing Bacteria in Acid Mine Drainage. M.S. Thesis. Department of Civil and Environmental Engineering. University of Massachusetts-Amherst. 100p.

Morse, J.W. and Arvidson, R.S., 2002. The dissolution kinetics of major sedimentary carbonate minerals. Earth-Science Reviews 58: 51-84.

Neculita, C-M., Zagury, G.Z., and Bussiere, B., 2007. Passive Treatment of Acid Mine Drainage in Bioreactors using Sulfate-Reducing Bacteria: Critical Review and Research Needs. *Journal of Environmental Quality* 36: 1-16.

Nordstrom, D.K., Plummer, L.N., Langmuir, Donald, Busenberg, Eurybiades, May, H.M., Jones, B.F., and Parkhurst, D.L., 1990, Revised chemical equilibrium data for major water-mineral reactions and their limitations, *in* Bassett, R.L. and Melchior, D. eds., Chemical modeling in aqueous systems II: Washington D.C., American Chemical Society Symposium Series 416, Chapter 31, p. 398-413.

Parkhurst, D.L., Thorstenson, D.C., and Plummer, L.N., 1980, PHREEQE--A computer program for geochemical calculations: U.S. Geological Survey Water-Resources Investigations Report 80-96, 195 p. (Revised and reprinted August, 1990.)

Parkhurst, D.L. and Appelo, C.A.J., 1999, User's guide to PHREEQC (Version 2)—A computer program for speciation, batch-reaction, one-dimensional transport, and inverse geochemical calculations: U.S. Geological Survey Water-Resources Investigations Report 99-4259, 310 p.

Pfaff, J.D., 1993. US-EPA Method 300.0, Determination of Inorganic Anions by Ion Chromatography. Revision 2.1. EMSL, Office of Research and Development, US-EPA, Cincinnati, OH. accessed 12/2009 online at: www.epa.gov/waterscience/methods/method/files/300_0.pdf

Praharaj, T. and Fortin, D., 2004. Indicators of Microbial Sulfate Reduction in Acidic Sulfide-Rich Mine Tailings. *Geomicrobiology Journal* 21: 457-467.

Rötting, T.S., Thomas, R.C., Ayora, C., and Carrera, J., 2008. Passive Treatment of Acid Mine Drainage with High Metal Concentration Using Dispersed Alkaline Substrate. *Journal of Environmental Quality 37*: 1741-1751.

Rowe, F.R., Sánchez España, J., Hallberg, K.B., and Johnson, D.B., 2007. Microbial communities and geochemical dynamics in an extremely acidic, metal-rich stream at an abandoned sulfide mine (Huelva, Spain) underpinned by two functional primary production systems. *Environmental Microbiology* 9:1761-1771.

Russell, M., 2003. Sequential Extraction of Trace Metals from Rock Coatings at Davis Mine; Rowe, MA. Undergraduate Independent Study, Geosciences. 27p.

Sánchez España, J., Lopez Pamo, E., Santofimia, E., Aduvire, O., Reyes, and Barettino, D., 2005. Acid mine drainage in the Iberian Pyrite Belt (Odiel river watershed, Huelva, SW Spain): Geochemistry, mineralogy and environmental implications. *Applied Geochemistry* 20: 1320-1356.

Schwertmann, U., 1991. Solubility and dissolution of iron oxides. *Plant and Soil*, 130: 1-25.

Sillén, L.G. and Martell, A.E., 1964. Stability Constants of Metal-Ion Complexes. London Chemical Society 17.

Singer, P.C., and Stumm, W., 1970. Acid mine drainage: the Rate Determining Step. *Science* 167: 1121-1123.

Sparks, D.L., 1995. Chemistry of Acid Soils, *chapter in* Environmental Soil Chemistry. San Diego, Academic Press. 267p.

Stumm, M., and Morgan, J.J., 1996. Aquatic Chemistry: Chemical Equilibria and Rates in Natural Waters. John Wiley and Sons, New York, New York. 1022p.

Tuttle J.H., Dugan, P.R., Macmillan, C.B., Randles, C.I., 1969. Microbial dissimilatory sulfur cycle in acid mine water. *Journal of Bacteriology* 97: 594-602.

US-EPA Drinking Water Contaminants Secondary Standards, accessed 1/2010 at http://www.epa.gov/safewater/contaminants/index.html

Waybrant, K.R., Blowes, D.W., Ptacek, C.J., 1998. Selection of Reactive Mixtures for Use in Permeable Reactive Walls for Treatment of Mine Drainage. *Environmental Science and Technology* 32:1972-1979.

Waybrant, K.R., Ptacek, C.L., and Blowes, D.W., 2002. Treatment of mine drainage using permeable reactive barriers: Column experiments. *Environmental Science and Technology* 36:1349-1356.

Weber, K.A., Achenbach, L.A., and Coates, J.D., 2006. Microorganisms pumping iron: anaerobic microbial iron oxidation and reduction. *Nature Reviews: Microbiology* 4:752-764

Wilde, F.D., ed., 2005. Field measurements: U.S. Geological Survey Techniques of Water-Resources Investigations, book 9, chapter A6.5, accessed 12/2009 at http://pubs.water.usgs.gov/twri9A6/